



Incorporation of Foundation Deformations in *AASHTO LRFD* Bridge Design Process

First Edition

A product of the SHRP2 solution, Service Limit State Design
for Bridges

February 08, 2016

The second Strategic Highway Research Program (SHRP2) is a national partnership of key transportation organizations: the Federal Highway Administration (FHWA), American Association of State Highway and Transportation Officials (AASHTO), and Transportation Research Board (TRB). Together, these partners are deploying products that will help the transportation community enhance the productivity, boost the efficiency, increase the safety, and improve the reliability of the nation's highway system.

This report is a work product of the SHRP2 Solution, *Service Limit State Design for Bridges* (R19B). The product leads are Matthew DeMarco at FHWA, Matthew.Demarco@dot.gov, and Patricia Bush at AASHTO, pbush@aaashto.org. This report was co-authored by the subject matter experts, Dr. Naresh C. Samtani of NCS GeoResources, LLC, and Dr. John M. Kulicki of Modjeski and Masters, Inc., in consultation with Kelley Severns, National Bridge Project Manager, CH2M HILL.

All rights reserved.

Contents

Chapter	Page
Definitions.....	vii
Chapter 1. Introduction.....	1
Chapter 2. Bridge Foundation Types and Deformations	3
Chapter 3. Consideration of Foundation Deformations in AASHTO Bridge Design Specifications.....	5
3.1 <i>AASHTO LRFD</i>	5
3.2 <i>AASHTO Standard Specifications for Highway Bridges (AASHTO, 2002)</i>	9
3.3 General Observations	10
Chapter 4. Effect of Foundation Deformations on Bridge Structures and Uncertainty	11
Chapter 5. Tolerable Foundation Deformation Criteria	15
5.1 Tolerable Vertical Deformation Criteria	15
5.2 Tolerable Horizontal Deformation Criteria.....	18
5.3 Perspective on Tolerable Deformations	18
Chapter 6. Construction-Point Concept.....	21
6.1 Vertical Deformation (Settlement).....	21
6.2 Horizontal Deformations	23
Chapter 7. Reliability of Predicted Foundation Deformations	25
Chapter 8. Calibration Procedures	27
8.1 Relevant <i>AASHTO LRFD</i> Articles for Foundation Deformations	27
8.2 Overarching Characteristics to Be Considered	28
8.2.1 Load-Driven versus Non-Load-Driven Limit States	28
8.2.2 Reversible versus Irreversible Limit States	28
8.2.3 Consequences of Exceeding Deformation-Related Limit States and Target Reliability Indices.....	29
8.3 Calculation Models	29
8.3.1 Incorporation of Load-deformation ($Q-\delta$) Characteristics in <i>AASHTO LRFD</i> Framework.....	30
8.3.2 Consideration of Bias Factor in Calibration of Deformations.....	33
8.3.3 Application of $Q-\delta$ Curves in the <i>AASHTO LRFD</i> Framework.....	34
8.3.4 Deterioration of Foundations and Wall Elements	36

8.3.5	Determination of Load Factor for Deformations.....	36
Chapter 9.	Calibration Implementation.....	39
9.1	General.....	39
9.2	Steps for Calibration	41
9.2.1	Step 1: Formulate the Limit State Functions and Identify Basic Variables.....	41
9.2.2	Step 2: Identify and Select Representative Structural Types and Design Cases	41
9.2.3	Step 3: Determine Load and Resistance Parameters for the Selected Design Cases.....	41
9.2.4	Step 4: Develop Statistical Models for Load and Resistance.....	41
9.2.5	Step 5: Apply the Reliability Analysis Procedure	58
9.2.6	Step 6: Review the Results and Selection of Load Factor for Settlement, γ_{SE}	62
9.2.7	Step 7: Select Value of γ_{SE}	63
Chapter 10.	Meaning and Effect of γ_{SE} in Bridge Design Process	65
Chapter 11.	Incorporating Values of γ_{SE} in <i>AASHTO LRFD</i>	67
Chapter 12.	The “$S_f=0$” Concept	69
12.1	Foundations Proportioned for Equal Settlement	73
Chapter 13.	Flow Chart to Consider Foundation Deformations in Bridge Design Process ...	75
Chapter 14.	Proposed Modifications to <i>AASHTO LRFD</i> Bridge Design Specifications	79
Chapter 15.	Application of Calibration Procedures.....	81
Chapter 16.	Summary	83
Chapter 17.	References.....	85
Appendices		
A	Conventions	
B	Application of γ_{SE} Load Factor	
C	Examples (Developed by AECOM)	
D	Proposed Modifications to Section 3 of <i>AASHTO LRFD</i> Bridge Design Specifications	
E	Proposed Modifications to Section 10 of <i>AASHTO LRFD</i> Bridge Design Specifications	

List of Tables

- 5-1 Tolerable Movement Criteria for Highway Bridges (*AASHTO LRFD*)
- 5-2 Tolerable Movement Criteria for Highway Bridges (WSDOT, 2012)
- 8-1 Summary of *AASHTO LRFD* Articles for Estimation of Vertical and Horizontal Deformation of Structural Foundations
- 9-1 Basic Framework for Calibration of Deformations
- 9-2 Data for Measured and Predicted (Calculated) Settlements Shown in Figure 9-1 Based on Gifford, et al. (1987)
- 9-3 Accuracy ($X=S_P/S_M$) Values Based on Data Shown in Table 9-2
- 9-4 Statistics of Accuracy, X , Values Based on Data Shown in Table 9-3
- 9-5 Correlated Statistics of Accuracy (X) for Lognormal PDFs
- 9-6 Lognormal of Accuracy Values [$\ln(X)$] Based on Data Shown in Table 9-3
- 9-7 Statistics of $\ln(X)$, Values Based on Data Shown in Table 9-6
- 9-8 Values of β and Corresponding P_e Based on Normally Distributed Data
- 9-9 Computed Values of γ_{SE} for Various Methods to Estimate Immediate Settlement of Spread Footings on Cohesionless Soils
- 9-10 Proposed Values of γ_{SE} for Various Methods to Estimate Immediate Settlement of Spread Footings on Cohesionless Soils
- 9-11 Target Reliability Index γ_{SE} for Various Structural Limit States (Kulicki, et al., 2015)
- 11-1 Load Factors for *SE* Loads

List of Figures

- 2-1 Illustration of major components of a bridge structure (Nielson, 2005)
- 2-2 Geometry of a typical shallow foundation
- 2-3 Common configurations of deep foundations, (a) group configuration, (b) single element configuration
- 3-1 Table 3.4.1-1 of *AASHTO LRFD* - Load Combinations and Load Factors
- 3-2 Table 3.4.1-2 of *AASHTO LRFD* - Load Factors for Permanent Load, γ_P
- 3-3 Table 3.4.1-3 of *AASHTO LRFD* - Load Factors for Permanent Loads Due to Superimposed Deformations, γ_P
- 3-4 Key to *AASHTO LRFD* Loads and Load Designations
- 4-1 Idealized Vertical Deformation (Settlement) Patterns and Terminology
- 4-2 Concept of total settlement, S , differential settlement, Δ_d , and angular distortion, A_d , in bridges

- 6-1 Construction-point concept for a bridge pier
- 6-2 Factored Angular distortion in bridges based on construction-point concept

- 8-1 Basic *AASHTO LRFD* framework for loads and resistances
- 8-2 Incorporation of Q - δ mechanism into the basic *AASHTO LRFD* framework
- 8-3 Significant points of interest on the mean Q - δ curve
- 8-4 Range and distribution along a Q - δ curve
- 8-5 Relationship of measured mean with theoretical prediction
- 8-6 Relationship of deterministic value of tolerable deformation, δ_T , and a probability distribution function for predicted deformation, δ_P
- 8-7 PEC for evaluation of load factor for a target probability of exceedance (P_{eT}) at the applicable SLS combination

- 9-1 Comparison of measured and calculated (predicted) settlements based on service load data in Table 9-2
- 9-2 Schmertmann method: (a) histograms for accuracy (X), and (b) plot of standard normal variable (z) as a function of the X
- 9-3 Hough method: (a) histograms for accuracy (X), and (b) plot of standard normal variable (z) as a function of the X
- 9-4 D'Appolonia method: (a) histograms for accuracy (X), and (b) plot of standard normal variable (z) as a function of the X
- 9-5 Peck and Bazarra method: (a) histograms for accuracy (X), and (b) plot of standard normal variable (z) as a function of the X
- 9-6 Burland and Burbridge method: (a) histograms for accuracy (X), and (b) plot of standard normal variable (z) as a function of the X
- 9-7 Cumulative Distribution Functions (CDFs) for various analytical methods for estimation of immediate settlement of spread footings
- 9-8 PEC for Schmertmann method
- 9-9 PEC for Hough method
- 9-10 PEC for D'Appolonia method
- 9-11 PEC for Peck and Bazarra method
- 9-12 PEC for Burland and Burbridge method
- 9-13 Relationship between β and P_e for the case of a single load and single resistance
- 9-14 Evaluation of γ_{SE} based on current and target reliability indices

- 12-1 Estimation of maximum factored angular distortion in bridges – Mode 1 and Mode 2
- 12-2 Factored Angular distortion in bridges based on construction-point concept

- 13-1 Consideration of foundation deformation in bridge design process

Definitions

A_d	Angular Distortion
$A_{d1}, A_{d2}, A_{d3}, A_{d4}$	Angular distortions for a four-span bridge
A_{df}	Factored Angular Distortion
$A_{df1-1}, A_{df2-1}, A_{df3-1}, A_{df4-1}$	Mode 1 factored angular distortions for a four-span bridge
$A_{df1-2}, A_{df2-2}, A_{df3-2}, A_{df4-2}$	Mode 2 factored angular distortions for a four-span bridge
AASHTO	American Association of State Highway and Transportation Officials
ASD	Allowable Stress Design
B_f	Least lateral plan dimension (width) of spread footing
CDF	Cumulative Distribution Function
CV	Coefficient of Variation
D_f	Depth to bottom of spread footing measured from finished grade
DL	Dead Load
E	Elastic Modulus
f	Frequency
F	Point on Q - δ curve representing strength limit state
FHWA	Federal Highway Administration
g	Limit state function
I	Moment of Inertia
IAP	Implementation Assistance Program
in.	inch
LFD	Load Factor Design
L_s	Span Length
$L_{S1}, L_{S2}, L_{S3}, L_{S4}$	Span lengths for a four-span bridge
L_f	Longer lateral plan dimension (length) of spread footing
LL	Live Load
ln (or LN)	Natural logarithm
ln(X)	Natural logarithm of Accuracy, X , values
LRFD	Load and Resistance Factor Design
MC	Monte Carlo
mm	Millimeter
MSE	Mechanically Stabilized Earth
M_{Δ}	Bending moment induced by a differential settlement, Δ_d
N	Point on Q - δ curve representing nominal resistance level

NCHRP	National Cooperative Highway Research Program
PDF	Probability Distribution Function
P	Lateral soil reaction on a deep foundation
P_e	Probability of Exceedance
PEC	Probability Exceedance Chart
P_{eT}	Target Probability of Exceedance
Q	Load (or force effect)
Q_{mean}	Mean load
Q_n	Nominal load
R	Resistance
R_{mean}	Mean resistance
R_n	Nominal resistance
S	Foundation settlement (vertical deformation); also refers to point on Q - δ curve representing service limit state
$S_{A1}, S_{P1}, S_{P2}, S_{P2}, S_{A2}$	Support settlements for a four-span bridge
SE	Force effect due to settlement
S_f	Factored total relevant settlement
$S_{f-A1}, S_{f-P1}, S_{f-P2}, S_{f-P2}, S_{f-A2}$	Factored support settlements for a four-span bridge
S_M	Measured Settlement
S_P	Predicted (calculated) Settlement
S_t	Unfactored predicted settlement
S_T	Tolerable Settlement
S_{tr}	Unfactored total relevant settlement
S_W, S_X, S_Y, S_Z	Settlements corresponding to vertical loads W, X, Y and Z
SCOBS	AASHTO Subcommittee on Bridges and Structures
SHRP2	Second Strategic Highway Research Program
SLS	Service Limit State
SWM	Strain Wedge Method
TRB	Transportation Research Board
y	Lateral deflection of pile
W	Vertical load due to foundation
X	Accuracy ($X = \delta_P / \delta_T$ or $X = S_P / S_M$); or vertical load of substructure
Y	Vertical load due to superstructure
z	Standard normal variable (variate)
Z	Vertical load due to wearing surface
β	Reliability Index
β_T	Target Reliability Index

γ	Load factor
γ_{SE}	Load factor for <i>SE</i> load; Deformation Load Factor
δ	Deformation
δ_f	Factored Deformation
δ_S	Deformation at nominal force effect, Q_n
δ_F	Deformation at factored force effect, $Q_F = \gamma(Q_n)$
δ_N	Deformation at load corresponding to nominal resistance, R_n
δ_P	Predicted deformation (force effect)
δ_T	Tolerable deformation (resistance)
$\delta_{T1}, \delta_{T2}, \delta_{T3}$	Various tolerable deformations
Δ_d	Differential settlement
$\Delta_{d1}, \Delta_{d2}, \Delta_{d3}, \Delta_{d4}$	Differential settlements for a four-span bridge
$\Delta_{d100'}$	Differential settlement over 100 ft with pier or abutments and differential settlement between piers
Δ_f	Factored Differential settlement
$\Delta_{f1-1}, \Delta_{f2-1}, \Delta_{f3-1}, \Delta_{f4-1}$	Mode 1 factored differential settlements for a four-span bridge
$\Delta_{f2-1}, \Delta_{f2-2}, \Delta_{f3-2}, \Delta_{f4-2}$	Mode 2 factored differential settlements for a four-span bridge
λ_Q	Bias factor for load
λ_R	Bias factor for resistance
μ	Mean
μ_{LNA}	Arithmetic mean of $\ln(X)$ values
μ_{LNC}	Correlated mean value
σ	Standard deviation
σ_{LNA}	Arithmetic standard deviation of $\ln(X)$ values
σ_{LNC}	Correlated standard deviation
ϕ	Resistance factor

Chapter 1. Introduction

The second Strategic Highway Research Program (SHRP2) is being advanced into practice primarily through the Implementation Assistance Program (IAP) sponsored by the Federal Highway Administration (FHWA) and the American Association of State Highway and Transportation Officials (AASHTO). The IAP provides technical and financial support to transportation agencies to encourage widespread adoption and use of research initially conducted through the Transportation Research Board (TRB).

Service Limit State Design for Bridges (R19B) is a SHRP2 Solution whose objectives include the development of design and detailing guidance and calibrated service limit states (SLSs) to provide 100-year bridge life and a framework for further development of calibrated SLSs. The *Service Limit* team developed a set of possible SLSs on the basis of a survey of owners and a literature review that included other national and international bridge design specifications. Those SLSs were reviewed to determine what could be calibrated using reliability theory. Calibrated, reliability-based load factors or resistance factors, or both, were developed for:

- Foundation deformations
- Cracking of reinforced concrete components
- Live-load deflections
- Permanent deformations
- Cracking of prestressed concrete components
- Fatigue of steel and reinforced concrete components

The details of these topics are provided in Kulicki, et al. (2015). Portions of the work were presented at several meetings of AASHTO Subcommittee on Bridges and Structures (SCOBS). The consideration of foundation deformations in the bridge design process can lead to the use of cost-effective structures with more efficient foundation systems. The proposed approach and modifications will help avoid overly conservative criteria that can lead to (a) foundations that are larger than needed, or (b) a choice of less economical foundation type (such as, using a deep foundation at a location where a shallow foundation would be adequate). The work pertaining to foundation deformations was presented at the annual AASHTO SCOBS meetings in 2012 (New Orleans, LA), 2014 (Columbus, OH), and 2015 (Saratoga Springs, NY), as well as at a joint T-5 and T-15 committee mid-year meeting in 2015 (Chicago, IL). These presentations generated considerable discussion and valuable comments.

This report was developed as part of the technical assistance provided through the IAP and concentrates on the work related to foundation deformations developed as part of SHRP2's *Service Limit State Design for Bridges*. The goal of the report is to explain the implementation

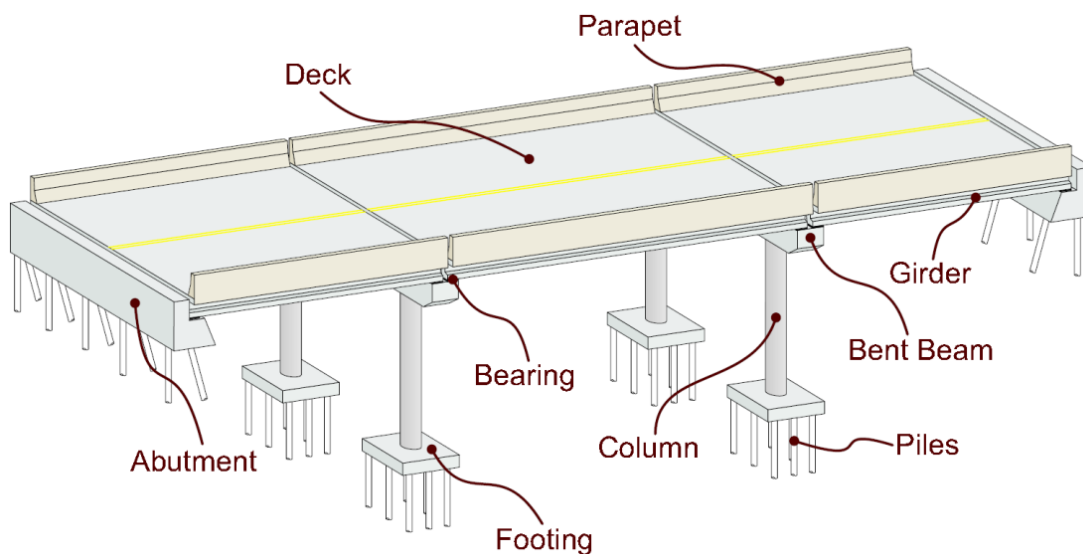
of calibrations for foundation deformations into the bridge design process. The scope of this report is to identify and consolidate the relevant content of the R19B report (Kulicki, et al., 2015) and additional materials developed since the issuance of the R19B report (for example, flow charts and examples based on the comments received as part of the various presentations previously noted). This information will provide background and rationale that can be used to support decisions regarding changes to the *AASHTO LRFD* bridge design specifications.

Documents from various sources such as AASHTO, FHWA, and SHRP2 are referenced in this report. Each reference document has its own style and organization, which often creates confusion during cross-referencing of documents. Appendix A provides the conventions used in this report vis-à-vis conventions in other publications.

Chapter 2. Bridge Foundation Types and Deformations

Figure 2-1 illustrates major components of a common bridge structure. In broad terms, bearings and all components above the bearing level are part of the bridge superstructure, while all components below the bearing level are part of a bridge substructure. The foundation is defined as the component of the substructure that is below the ground level. In Figure 2-1, the foundation is shown as footing supported by piles.

Figure 2-1: Illustration of major components of a bridge structure (Nielson, 2005)



The two major alternate foundation types are the “shallow” and “deep” foundations. The geometry of a typical shallow foundation or spread footing is shown in Figure 2-2. Shallow foundations are those wherein the depth to the bottom of the footing, D_f , is small compared to the cross-sectional size (width, B_f , or length, L_f). This is in contrast to deep foundations, such as driven piles and drilled shafts, whose depth of embedment is considerably larger than the cross-section dimension (diameter) as shown in Figure 2-3.

Foundation design and construction involves assessment of factors related to engineering and economics. The selection of the most feasible foundation system requires consideration of both shallow and deep foundation types in relation to the characteristics and constraints of the project and site conditions. In general, the presence of unsuitable soil layers in the subsurface profile, adverse hydraulic conditions, or relatively small tolerable movements of the structure dictate the use of deep foundations because they are designed to transfer load through less suitable subsurface layers to more suitable bearing strata.

Figure 2-2: Geometry of a typical shallow foundation

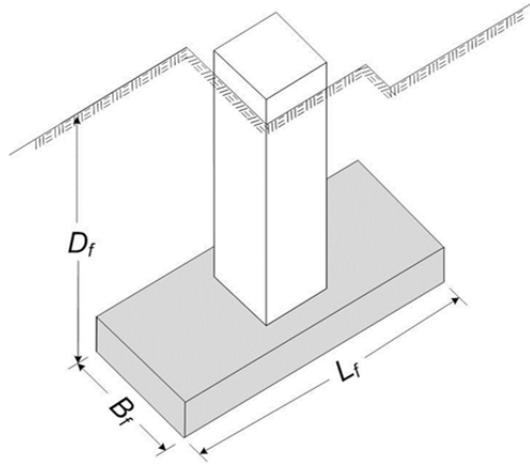
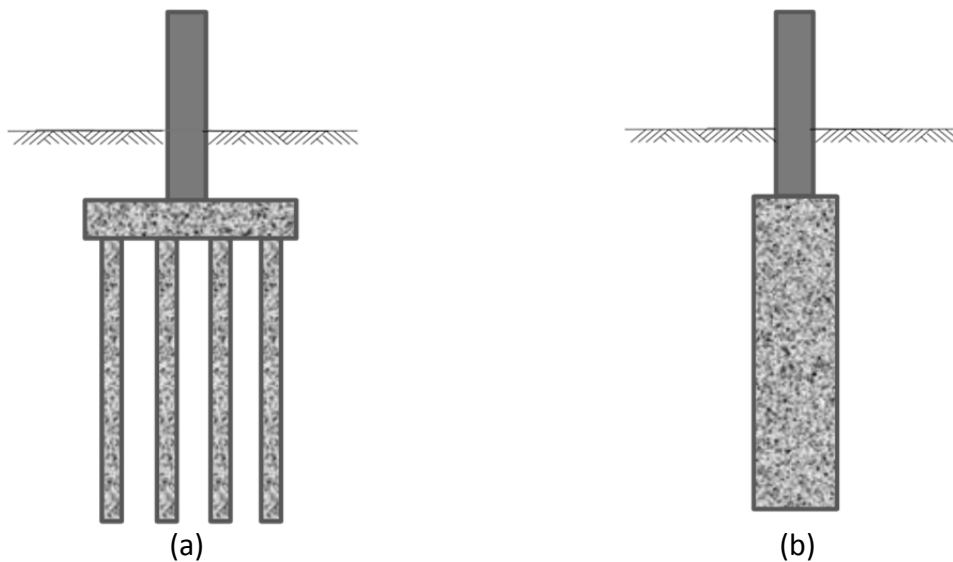


Figure 2-3: Common configurations of deep foundations, (a) group configuration, (b) single element configuration



Regardless of the type of foundation, the key point of interest is the effect of the estimated foundations deformation on the various elements of the bridge substructure and superstructure components above the foundations. The foundation deformations can have multiple degrees of freedom, but for the purpose of analyses the foundations deformations can be broadly categorized as vertical (settlement) and lateral. Rotational deformations can be manifested due to the combined effects of vertical and lateral deformations. Torsional deformations may also be possible under certain specific loading conditions (for example, dynamic). Bridge foundations and other geotechnical features, such as approach embankments, should be designed so that their deformations (settlements and/or lateral movements) will not cause damage to the bridge structure.

Chapter 3. Consideration of Foundation Deformations in AASHTO Bridge Design Specifications

3.1 AASHTO LRFD

Figures 3-1, 3-2 and 3-3 present Tables 3.4.1-1, 3.4.1-2 and 3.4.1-3, respectively from *AASHTO LRFD*. These tables present load factors for various loads to develop design load combinations. Two-letter abbreviations are used for load designations in Figures 3-1, 3-2, and 3-3. Figure 3-4 provides definitions for the two-letter abbreviations for load designations in accordance with Article 3.3.2 of *AASHTO LRFD*.

Figure 3-1: Table 3.4.1-1 of *AASHTO LRFD* - Load Combinations and Load Factors

Load Combination Limit State	DC DD DW EH EV ES EL PS CR SH	LL IM CE BR PL LS	WA	WS	WL	FR	TU	TG	SE	Use One of These at a Time				
										EQ	BL	IC	CT	CV
Strength I (unless noted)	γ_P	1.75	1.00	—	—	1.00	0.50/1.20	γ_{TG}	γ_{SE}	—	—	—	—	—
Strength II	γ_P	1.35	1.00	—	—	1.00	0.50/1.20	γ_{TG}	γ_{SE}	—	—	—	—	—
Strength III	γ_P	—	1.00	1.40	—	1.00	0.50/1.20	γ_{TG}	γ_{SE}	—	—	—	—	—
Strength IV	γ_P	—	1.00	—	—	1.00	0.50/1.20	—	—	—	—	—	—	—
Strength V	γ_P	1.35	1.00	0.40	1.0	1.00	0.50/1.20	γ_{TG}	γ_{SE}	—	—	—	—	—
Extreme Event I	γ_P	γ_{EO}	1.00	—	—	1.00	—	—	—	1.00	—	—	—	—
Extreme Event II	γ_P	0.50	1.00	—	—	1.00	—	—	—	—	1.00	1.00	1.00	1.00
Service I	1.00	1.00	1.00	0.30	1.0	1.00	1.00/1.20	γ_{TG}	γ_{SE}	—	—	—	—	—
Service II	1.00	1.30	1.00	—	—	1.00	1.00/1.20	—	—	—	—	—	—	—
Service III	1.00	0.80	1.00	—	—	1.00	1.00/1.20	γ_{TG}	γ_{SE}	—	—	—	—	—
Service IV	1.00	—	1.00	0.70	—	1.00	1.00/1.20	—	1.0	—	—	—	—	—
Fatigue I—LL, IM & CE only	—	1.50	—	—	—	—	—	—	—	—	—	—	—	—
Fatigue II—LL, IM & CE only	—	0.75	—	—	—	—	—	—	—	—	—	—	—	—

Figure 3-2: Table 3.4.1-2 of AASHTO LRFD - Load Factors for Permanent Load, γ_P

Type of Load, Foundation Type, and Method Used to Calculate Downdrag		Load Factor	
		Maximum	Minimum
<i>DC</i> : Component and Attachments		1.25	0.90
<i>DC</i> : Strength IV only		1.50	0.90
<i>DD</i> : Downdrag	Piles, α Tomlinson Method	1.4	0.25
	Piles, λ Method	1.05	0.30
	Drilled shafts, O'Neill and Reese (1999) Method	1.25	0.35
<i>DW</i> : Wearing Surfaces and Utilities		1.50	0.65
<i>EH</i> : Horizontal Earth Pressure			
• Active		1.50	0.90
• At-Rest		1.35	0.90
• <i>AEP</i> for anchored walls		1.35	N/A
<i>EL</i> : Locked-in Construction Stresses		1.00	1.00
<i>EV</i> : Vertical Earth Pressure			
• Overall Stability		1.00	N/A
• Retaining Walls and Abutments		1.35	1.00
• Rigid Buried Structure		1.30	0.90
• Rigid Frames		1.35	0.90
• Flexible Buried Structures			
○ Metal Box Culverts, Structural Plate Culverts with Deep Corrugations, and Fiberglass Culverts		1.5	0.9
○ Thermoplastic Culverts		1.3	0.9
○ All others		1.95	0.9
<i>ES</i> : Earth Surcharge		1.50	0.75

Figure 3-3: Table 3.4.1-3 of AASHTO LRFD - Load Factors for Permanent Loads Due to Superimposed Deformations, γ_P

Bridge Component	<i>PS</i>	<i>CR, SH</i>
Superstructures—Segmental Concrete Substructures supporting Segmental Superstructures (see 3.12.4, 3.12.5)	1.0	See γ_P for <i>DC</i> , Table 3.4.1-2
Concrete Superstructures—non-segmental	1.0	1.0
Substructures supporting non-segmental Superstructures		
• using I_g	0.5	0.5
• using $I_{effective}$	1.0	1.0
Steel Substructures	1.0	1.0

Figure 3-4: Key to AASHTO LRFD Loads and Load Designations

Permanent Loads	Transient Loads
<i>CR</i> = force effects due to creep	<i>BL</i> = blast loading
<i>DD</i> = downdrag force	<i>BR</i> = vehicular braking force
<i>DC</i> = dead load of structural components and nonstructural attachments	<i>CE</i> = vehicular centrifugal force
<i>DW</i> = dead load of wearing surfaces and utilities	<i>CT</i> = vehicular collision force
<i>EH</i> = horizontal earth pressure load	<i>CV</i> = vessel collision force
<i>EL</i> = miscellaneous locked-in force effects resulting from the construction process, including jacking apart of cantilevers in segmental construction	<i>EQ</i> = earthquake load
<i>ES</i> = earth surcharge load	<i>FR</i> = friction load
<i>EV</i> = vertical pressure from dead load of earth fill	<i>IC</i> = ice load
<i>PS</i> = secondary forces from post-tensioning for strength limit states; total prestress forces for service limit states	<i>IM</i> = vehicular dynamic load allowance
<i>SH</i> = force effects due to shrinkage	<i>LL</i> = vehicular live load
	<i>LS</i> = live load surcharge
	<i>PL</i> = pedestrian live load
	<i>SE</i> = force effect due to settlement
	<i>TG</i> = force effect due to temperature gradient
	<i>TU</i> = force effect due to uniform temperature
	<i>WA</i> = water load and stream pressure
	<i>WL</i> = wind on live load
	<i>WS</i> = wind load on structure

Article 3.4.1 of AASHTO LRFD states the following:

“All relevant subsets of the load combinations shall be investigated. For each load combination, every load that is indicated to be taken into account and that is germane to the component being designed, including all significant effects due to distortion, shall be multiplied by the appropriate load factor.....”

“The factors shall be selected to produce the total extreme factored force effect. For each load combination, both positive and negative extremes shall be investigated.

In load combinations where one force effect decreases another effect, the minimum value shall be applied to the load reducing the force effect. For permanent force effects, the load factor that produces the more critical combination shall be selected from Table 3.4.1-2. Where the permanent load increases the stability or load-carrying capacity of a component or bridge, the minimum value of the load factor for that permanent load shall also be investigated.”

As per Article 3.3.2 of AASHTO LRFD, the *SE* load type is categorized as transient and represents “force effect due to settlement.” The force effects can be manifested in a variety of forms, such as additional (secondary) moments and change in roadway grades. Thus, even though *SE* load is

considered as a transient load, the force effects because of *SE* load type may induce irreversible (permanent) effects in the bridge superstructure unless the induced force effects are made reversible through intervention with respect to the bridge superstructure. As per Article 3.12 of *AASHTO LRFD*, the *SE* load type is considered to be similar to load types *TU*, *TG*, *SH*, *CR*, and *PS*, in that it generates force effects because of superimposed deformations. While *AASHTO LRFD* uses the word “settlement,” the broader meaning of *SE* load type applies to foundation movements or deformations, whether it is settlement (vertical deformation) or lateral deformation or rotation. Article 3.12.1 of *AASHTO LRFD* used the word “support movements” as follows:

“Force effects resulting from resisting component deformation, displacement of points of load application, and support movements shall be included in the analysis.”

Any reference to *SE* load type should, in general, be considered a reference to foundation deformation, whether it is vertical deformation (settlement) or lateral deformation or rotation. Based on these discussions, it is clear that *AASHTO LRFD* incorporates the force effects of foundation deformations in the bridge design process through the concept of force effects generated by superimposed deformations¹. Furthermore, by including the load factor γ_{SE} for foundation deformations in both the strength and service limit states, *AASHTO LRFD* is clearly acknowledging that foundation deformations can affect the long-term load carrying capacity and functionality of the bridge structure. Note that this load factor is shown in 4 out of the 5 strength limit states and 3 out of the 4 service limit states with an explicit factor of 1.0 for Service IV limit state. The other superimposed deformation load factors for *CR*, *SH*, *PS*, *TU* and *TG* are defined in *AASHTO LRFD* but *SE* does not have a value of load factor clearly defined except for Service Limit IV, for which a value of 1.0 is provided. Article 3.4.1 of *AASHTO LRFD* states the following for selection of a value of γ_{SE} :

“The load factor for settlement, γ_{SE} , should be considered on a project-specific basis. In lieu of project-specific information to the contrary, γ_{SE} , may be taken as 1.0. Load combinations which include settlement shall also be applied without settlement.”

This specification provision indicates that γ_{SE} can take a value of 1.0 when settlement is considered and a value of 0.0 when settlement is not considered. Use of a load factor of 1.0 implies that the loads are taken at nominal value. For foundation deformation, the nominal value of induced force effect, such as moments, is directly proportional to the value of the

¹ Conceptually the treatment of *SE* load type is similar to that of the *DD* load type that represents downdrag force (or drag load) due to a settlement based mechanism. Drag load is categorized as a permanent load type and in the *AASHTO LRFD* framework a geotechnical phenomenon of settlement is considered in terms of additional permanent load that is induced. The *DD* load type is considered in both strength and service limit state evaluations.

foundation deformation (for example, settlement). When a value of $\gamma_{SE} = 1.0$ is used, the implication is that that computed value of foundation deformation has no uncertainty. However, the provision does state that “In lieu of project-specific information to the contrary,” which means that other values of γ_{SE} may be used but no recommendations are provided for the selection of an appropriate value.

Article 3.12.6 of *AASHTO LRFD* further indicates the following regarding *SE* load type:

“Force effects due to extreme values of differential settlement among substructures and within individual substructure units shall be considered.”

The commentary portion (Article C3.12.6 of *AASHTO LRFD*) states the following:

“Force effects due to settlement may be reduced by considering creep. Analysis for the load combinations in Tables 3.4.1-1 and 3.1.4-2 which include settlement should be repeated for settlement of each possible substructure unit settling individually, as well as combinations of substructure units settling, that could create critical force effects in the structure.”

Based on these discussions, it is clear that *AASHTO LRFD* makes explicit consideration of foundation deformations in the bridge design process.

3.2 AASHTO Standard Specifications for Highway Bridges (AASHTO, 2002)

AASHTO (2002) represented the 17th and last edition of the *Standard Specifications for Highway Bridges* that was based on the Allowable Stress Design (ASD) (also referred to as Service Load Design) and LFD platform. It is worth noting that settlement is handled more explicitly in Table 3.4.1-1 of *AASHTO LRFD*, than it was in corresponding Table 3.22.1A AASHTO (2002) wherein the settlement was not included. It may appear that the *AASHTO LRFD*-based specifications are a departure from past practice as exemplified by AASHTO (2002), in that settlement does not appear in the load combinations in AASHTO (2002) but this is not the case. Settlement is mentioned in Article 3.22.1 of AASHTO (2002), which states “If differential settlement is anticipated in a structure, consideration should be given to stresses resulting from this settlement.” The parent article is 3.3 DEAD LOAD, implying that settlement effects should be considered wherever dead load appears in the ASD or LFD load combinations. The consideration of foundation deformations in the bridge design process has been mandated by AASHTO in the past and is not a new requirement in *AASHTO LRFD* specifications.

3.3 General Observations

Based on the discussions described in Section 3.2, the following general observations are made:

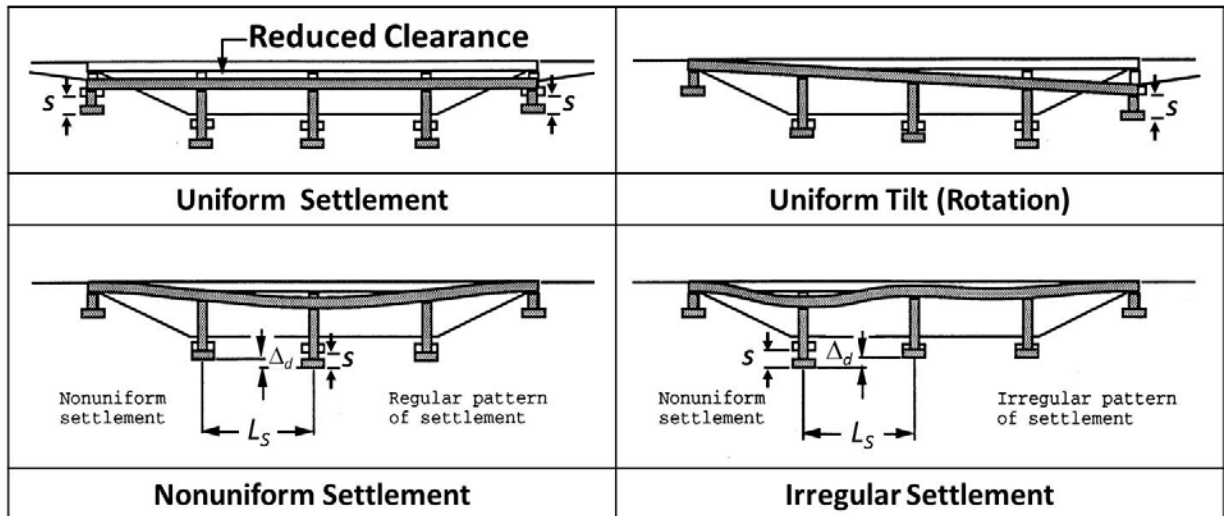
- Although the *AASHTO LRFD* refers to settlement, it should be considered in the broader context of foundation deformations since a foundation can have multiple degrees of freedom.
- Evaluation of differential deformation has been mandated by AASHTO bridge design specification regardless of design platform (ASD, LFD, or LRFD). It is not a new requirement.
- In *AASHTO LRFD* platform, foundation deformations are included in the category of superimposed deformation and the γ_{SE} load factor appears in both strength and service limit state load combinations.
- The choice of $\gamma_{SE} = 1.0$ implies that there is no uncertainty in the estimated value of foundation deformations. This value was calibrated by TRB's SHRP2 Project R19B (Kulicki, et al., 2015) to incorporate uncertainty based on the type of method used to estimate the foundation deformations.
- Although the issue of foundation deformations may appear to belong to *AASHTO LRFD*, Section 10 (Foundations), it is the induced force effects of foundation deformations that need to be incorporated in the design of the bridge structure. Therefore, the effect of foundation deformations has been included in *SE* load type in *AASHTO LRFD*, Section 3 (Loads and Load Factors), Table 3.4.1-1 (Load Combination and Load Factors).

Chapter 4. Effect of Foundation Deformations on Bridge Structures and Uncertainty

The bridge superstructure and substructure deformations can be caused by a variety of reasons, including foundation deformations. The foundation deformations need to be evaluated in the context of span lengths and various construction steps to understand their effect on the bridge superstructures.

Figure 4-1 presents idealized vertical deformation (settlement) patterns that serve to illustrate the effect of a bridge structure within the framework of AASHTO bridge design specifications.

Figure 4-1: Idealized Vertical Deformation (Settlement) Patterns and Terminology



Sources: Barker et al., 1991 and Samtani and Nowatzki, 2006

S = Total Settlement; Δ_d = Differential Settlement; L_s = Span Length

Vertical deformation (settlement) can be subdivided into the following three components, which are illustrated in Figure 4-1:

1. Uniform settlement

In this case, all bridge support elements settle equally. Even though the bridge support elements settle equally, they can cause differential settlement with respect to the approach embankment and associated features such as approach slabs and utilities that are commonly located in or across the end-spans of bridges. Such differential settlement can create problems. For example, it can reduce the clearance of the overpass, create a bump at the end of the bridge, change grades at the end of the bridge causing drainage problems, misaligned joints, and distorted underground utilities at the interfaces of the bridge and approaches.

Although uniform settlements may be computed theoretically, from a practical viewpoint it is not possible for the bridge structure to experience truly uniform settlement because of a combination of many factors including the variability of loads and soil properties.

2. Tilt or rotation

Tilt or rotation occurs mostly in single-span bridges with stiff superstructures. Tilt or rotation may not cause distortion of the superstructure and associated damage, but because of its differential movement with respect to the facilities associated with approach embankments, tilt or rotation can create problems similar to those of uniform settlement, discussed previously. Examples include a bump at the end of the bridge, drainage problems, and damage to underground utilities.

3. Differential settlement, Δ_d

Differential settlement, Δ_d , defined as the difference in settlement between adjacent supports, directly results in deformation of the bridge superstructure. As shown in Figure 4-1, two different patterns of differential settlement can occur. These are:

- a) Regular pattern: The settlement increases progressively from the abutments towards the center of the bridge.
- b) Irregular (uneven) pattern: The settlement at each support location varies along the length of the bridge.

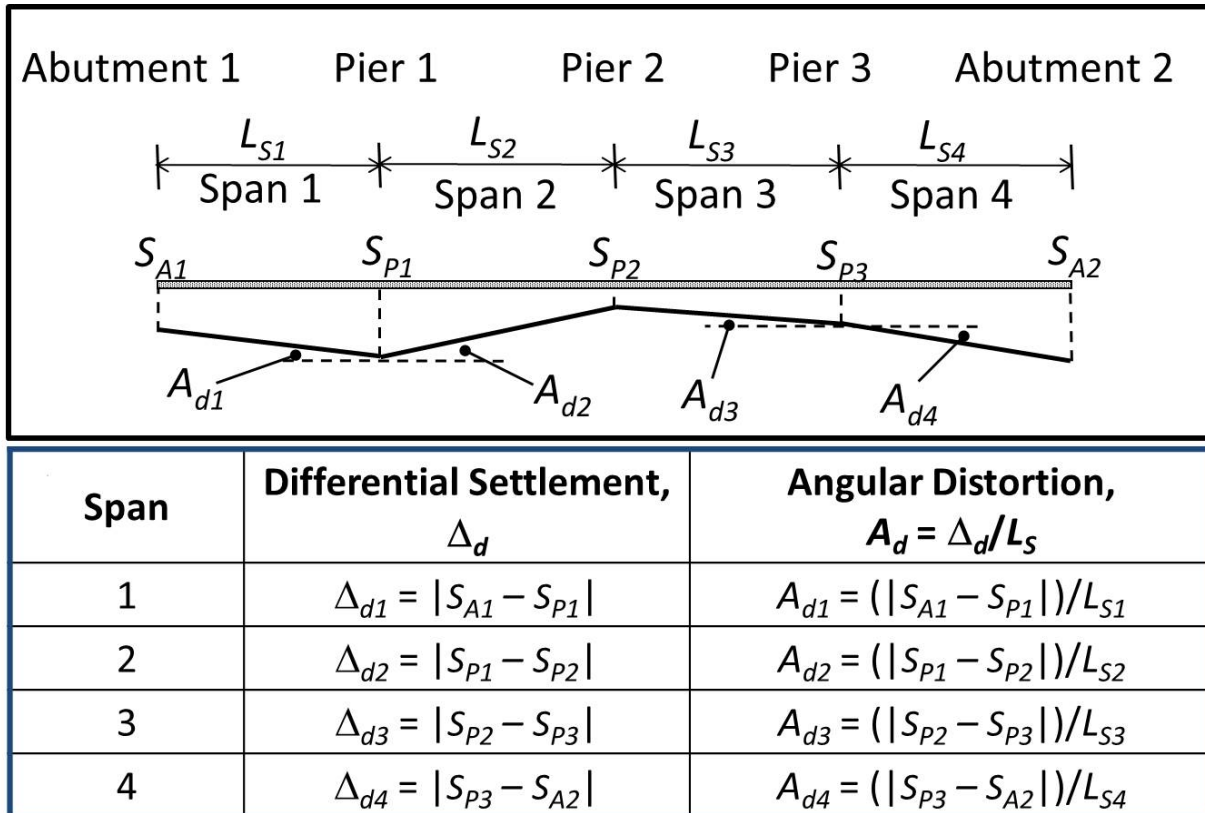
Both of these patterns of settlement lead to angular distortion, A_d , which is defined as the ratio of the difference in settlement between two points divided by the distance between the two points. For bridge structures, the two points to evaluate the differential settlement, Δ_d , are commonly selected as the distance between adjacent support elements, L_s , as shown in Figure 4-1. Thus, angular distortion $A_d = \Delta_d/L_s$. Stated another way, angular distortion is a normalized measure of differential settlement that includes the distance over which the differential settlement occurs. A number of studies (for example, Skempton and MacDonald (1956) and Grant et al. (1974)), have determined that the severity of differential settlement on structures is roughly proportional to the angular distortion.

Because of the inherent variability of geomaterials, the vertical deformations at the support elements of a given bridge (that is, piers and abutments) will generally be different. This is true regardless of whether deep foundations or spread footings are used. Therefore, differential settlement and associated angular distortion is the most common and is detailed herein.

Figure 4-2 shows the hypothetical case of a four-span bridge structure with five support elements (two abutments and three piers), wherein the calculated settlement, S , at each support is different. The settlements at Abutment 1, Pier 1, Pier 2, Pier 3 and Abutment 2 are

S_{A1} , S_{P1} , S_{P2} , S_{P3} and S_{A2} , respectively. In this hypothetical case, it is assumed that the substructure units between foundations and bridge superstructure are rigid (that is, all the deformations experienced by the superstructure are equal to the foundation deformations). Differential settlements, Δ_d , are defined as noted in the second column of the table in Figure 4-2. The angular distortion, A_d , term for each span is shown in the third column of the table in Figure 4-2. Angular distortion is a dimensionless quantity that is expressed as an angle in radians. Theoretically, the ratio Δ_d/L_s represents the tangent of the angle of distortion, but for small values of the tangent, the angles are also very small. Therefore, the tangents (that is, angular distortion, A_d) are shown as angles in Figure 4-2.

Figure 4-2: Concept of total settlement, S , differential settlement, Δ_d , and angular distortion, A_d , in bridges



Differential settlements induce bending moments and shear in the bridge superstructure when spans are continuous over supports and potentially cause structural damage. For a continuous-span beam, the bending moment, M_{Δ} , induced by a differential settlement, Δ_d , can be computed by using Equation 4-1.

$$M_{\Delta} = \frac{6EI\Delta_d}{L_S^2} \quad (4-1)$$

where, E is the elastic modulus and I is moment of inertia of a prismatic beam with a span length, L_S . Equation 4-1 can be re-written as follows:

$$M_{\Delta} = 6 \left(\frac{EI}{L_S} \right) \frac{\Delta_d}{L_S} \quad (4-2)$$

Most equations for moments in beams can be re-arranged in a format similar to that shown in Equation 4-2. Equation 4-3 shows a generalized format of a moment equation for beams.

$$M_{\Delta} = func \left(\frac{EI}{L_S}, \frac{\Delta_d}{L_S} \right) \quad (4-3)$$

The term EI/L_S is a representation of the stiffness of the superstructure over the span length L_S , while the term Δ_d/L_S is the angular distortion as discussed earlier.

Depending on factors such as the type of superstructure, the connections between the superstructure and substructure units, and the span lengths and widths, the magnitudes of differential settlement that can cause damage to the bridge structure can vary significantly. For example, the damage to the bridge structure because of a differential settlement of 2 inches (in.) over a 50-foot span is likely to be more severe than the same amount of differential settlement over a 150-foot span. Because the induced force effect (for example, moment) is a direct function of EI/L_S for all bridges, stiffness should be appropriate to the considered limit state. Similarly, the effects of continuity with the substructure should be considered. In assessing the structural implications of foundation deformations of concrete bridges, the determination of the stiffness of the bridge components should consider the effects of cracking, creep, and other inelastic responses. To a lesser extent, differential settlements can also cause damage to a simple-span bridge. However, the major concern with simple-span bridges is the quality of the riding surface, adverse deck drainage, and aesthetics. Because of a lack of continuity over the supports, the changes in slope of the riding surface near the supports of a simple-span bridge induced by differential settlements may be more severe than those in a continuous-span bridge.

Chapter 5. Tolerable Foundation Deformation Criteria

5.1 Tolerable Vertical Deformation Criteria

As discussed in chapter 4, uneven displacements of bridge abutments and pier foundations can affect the ride quality, functioning of deck drainage, and the safety of the traveling public as well as the structural integrity and aesthetics of the bridge. Such movements often lead to costly maintenance and repair measures. In contrast, overly conservative criteria can be wasteful by leading to (a) foundations that are larger than needed, or (b) choice of a less economical foundation type (such as using a deep foundation at a location where a shallow foundation would be adequate). To determine the optimum solution for deformation criteria, collaboration between the geotechnical engineer and the structural engineer is needed.

Within the context of foundation deformation, the geotechnical limit states can be broadly categorized into vertical and horizontal deformations for any foundation type (for example, spread footings, driven piles, drilled shafts, and micropiles). Agencies often limit the deformation to values of 1 in. or less without any rational basis. The literature survey performed as part of the TRB's SHRP2 Project R19B (Kulicki, et al., 2015) revealed that the only definitive rational guidance related to the effect of foundation deformations on bridge structures is based on a report by Moulton, et al. (1985) (Moulton). From an evaluation of 314 bridges nationwide, the report offered the following conclusions:

"The results of this study have shown that, depending on type of spans, length and stiffness of spans, and the type of construction material, many highway bridges can tolerate significant magnitudes of total and differential vertical settlement without becoming seriously overstressed, sustaining serious structural damage, or suffering impaired riding quality. In particular, it was found that a longitudinal angular distortion (differential settlement/span length) of 0.004 would most likely be tolerable for continuous bridges of both steel and concrete, while a value of angular distortion of 0.005 would be a more suitable limit for simply supported bridges."

Another study (Wahls, 1983), states the following:

"In summary, it is very clear that the tolerable settlement criteria currently used by most transportation agencies are extremely conservative and are needlessly restricting the use of spread footings for bridge foundations on many soils. Angular distortions of $1/250$ of the span length and differential vertical movements of 2 to 4 in. (50 to 100 millimeters [mm]), depending on span length, appear to be acceptable, assuming that approach slabs or other provisions are made to minimize the effects of any differential movements

between abutments and approach embankments. Finally, horizontal movements in excess of 2 in. (50 mm) appear likely to cause structural distress. The potential for horizontal movements of abutments and piers should be considered more carefully than is done in current practice."

Based on the data from these two studies, Article 10.5.2.2 of *AASHTO LRFD* included the guidance summarized in Table 5-1 for the evaluation of tolerable vertical movements in terms of angular distortions. AASHTO (2002) includes the same criteria, which means these criteria are not new in LRFD specifications but can be traced back to the AASHTO (2002), based on ASD and LFD platform and to the work by Moulton.

Table 5-1: Tolerable Movement Criteria for Highway Bridges (AASHTO LRFD)

Limiting Angular Distortion, Δ_d/L_s (radians)	Type of Bridge
0.004	Multiple-span (continuous span) bridges
0.008	Simple-span bridges

The criteria in Table 5-1 suggest that for a 100-foot span, a differential settlement of 4.8 in. is acceptable for a continuous span and 9.6 in. is acceptable for a simple span. These relatively large values of differential settlement concerns structural designers, who often arbitrarily limit tolerable movements to one-half to one-quarter or one less order of magnitude (for example, 0.0004 instead of 0.004) of the values listed in Table 5-1 or develop guidance as shown in Table 5-2.

Table 5-2: Tolerable Movement Criteria for Highway Bridges (WSDOT, 2012)

Total Settlement at Pier or Abutment	Differential Settlement over 100 ft within Pier or Abutments and Differential Settlement Between Piers [Implied Limiting Angular Distortion, radians]	Action
$\delta \leq 1"$	$\Delta_{d100'} \leq 0.75"$ [0.000625]	Design and Construct
$1" < \delta \leq 4"$	$0.75" < \Delta_{d100'} \leq 3"$ [0.000625-0.0025]	Ensure structure can tolerate settlement
$\delta > 4"$	$\Delta_{d100'} > 3"$ [> 0.0025]	Need Department approval

Notes:

- δ = deformation
- < = less than
- > = greater than
- \leq = less than or equal to
- ' = feet (ft)
- " = inches

Another example of the use of more stringent criteria is from Chapter 10 of Bridge Design Guidelines of the Arizona Department of Transportation (ADOT, 2015), which states the following:

“The bridge designer should limit the settlement of a foundation per 100 ft span to 0.75 in. Linear interpolation should be used for other span lengths. Higher settlements may be used when the superstructure is adequately designed for such settlements. Any settlement that is in excess of 4.0 in, including stage construction settlements if applicable, must be approved by the ADOT Bridge Group. The designer shall also check other factors, which may be adversely affected by foundation settlements, such as rideability, vertical clearance, and aesthetics.”

The ADOT guidelines provide additional guidance in terms of the S-0 and construction-point concepts that are discussed later in this report. ADOT also provides guidance on consideration of creep as part of the evaluation of the effect of foundation deformations on bridge structures.

While from the structural integrity viewpoint, there are no technical reasons for structural designers to set arbitrary additional limits to the criteria listed in Table 5-1, there are often practical reasons based on the tolerable limits of deformation of other structures associated with a bridge (for example, approach slabs, wingwalls, pavement structures, drainage grades, utilities on the bridge, and deformations that adversely affect quality of ride). The relatively large differential settlements based on Table 5-1, should be considered in conjunction with functional or performance criteria not only for the bridge structure itself but for all associated facilities. Samtani and Nowatzki (2006) suggest the following steps:

- Step 1:** Identify all possible facilities associated with the bridge structure and the movement tolerance of those facilities. An example of a facility on a bridge is a utility (such as gas, power, and water). The owners of the facility can identify the movement tolerance of their facility. Alternatively, the facility owners should design their facilities for the movement anticipated for the bridge structure.
- Step 2:** Because of the inherent uncertainty associated with estimated values of settlement, determine the differential settlement by using conservative assumptions for geomaterial properties and prediction methods. It is important that the estimation of angular distortion be based on a realistic evaluation of the construction sequence and the magnitude of loads at each stage of the construction sequence.
- Step 3:** Compare the angular distortion from Step 2 with the various tolerances identified in Step 1 and in Table 5-1. Based on this comparison, identify the critical component of the facility. Review this critical component to check if it can be relocated or if it can be redesigned to more relaxed tolerances. Repeat this process as necessary for other

facilities. In some cases, a simple re-sequencing of the construction of the facility based on the construction sequence of the bridge structure may help mitigate the issues associated with intolerable movements.

This three-step approach can be used to develop project-specific limiting angular distortion criteria that may differ from the general guidelines listed in Table 5-1. For example, if a compressed gas line is fixed to a simple-span bridge deck and the gas line can tolerate an angular distortion of only 0.002, then the utility will limit the angular distortion value for the bridge structure, not the criterion listed in Table 5-1. However, this problem is typically avoided by providing flexible joints along the utility such that it does not control the bridge design.

5.2 Tolerable Horizontal Deformation Criteria

Horizontal deformations cause more severe and widespread problems for highway bridge structures than equal magnitudes of vertical movement. Tolerance of the superstructure to horizontal (lateral) movement will depend on bridge seat or joint widths, bearing type(s), structure type, and load distribution effects. Moulton found that horizontal movements less than 1 in. were almost always reported as being tolerable, while horizontal movements greater than 2 in. were typically considered to be intolerable. Based on this observation, Moulton recommended that horizontal movements be limited to 1.5 in. The data presented by Moulton shows that horizontal movements resulted in more damage when accompanied by settlement than when occurring alone.

5.3 Perspective on Tolerable Deformations

The AASHTO criteria are based on work done by Moulton that was based on the following:

1. 12th Edition (1977) of AASHTO *Standard Specifications for Highway Bridges*. This version of AASHTO specifications used the ASD platform and HS20-44 wheel loading or its equivalent lane loading for live loads.
2. The use of the following tolerable movements definition that is in accordance with TRB Committee A2K03 in mid 1970s:

“Movement is not tolerable if damage requires costly maintenance and/or repairs and a more expensive construction to avoid this would have been preferable.”

The base definition of tolerable movements that was used is subjective and the work is dated based on an old edition of AASHTO *Standard Specifications for Highway Bridges*, which was not calibrated based on reliability concepts like the current LRFD specifications. Additionally, Moulton indicates that attempts to establish tolerable movements from the effects of differential settlement analyses on the stresses in bridges significantly underestimated the

criteria established from field observations. One reason Moulton attributed the discrepancy between analytical studies and field observations is that the analytical studies often do not account for the construction time of a structure and that components of the foundation movement estimated based on analytical studies have already occurred before the completion of the structure. Portions of structure (for example, the bridge superstructure) that are constructed last do not have damage consistent with the level that is predicted by analytical studies which assume that all loads are applied instantaneously. Another reason supporting Moulton's observations is that building materials like concrete (especially concrete while it is curing) are able to undergo a considerable amount of stress relaxation when subjected to deformations. Under conditions of very slowly imposed deformations, the effective value of the Young's modulus of concrete is considerably lower than the value for rapid loading (Barker et al., 1991).

All of the previously described considerations were recognized by Moulton. Since the 1990s, valuable data have been collected that help quantify the amount of deformations that occurs as bridge structures are constructed. These data have led to the formulation of the construction-point concept in FHWA documents (for example, Samtani and Nowatzki, 2006) and is also discussed in chapter 6. At a minimum, adoption of the construction-point concept in the bridge design process will be a significant step in the right direction towards comparing estimated foundation movements with AASHTO criteria for tolerable deformations.

Chapter 6. Construction-Point Concept

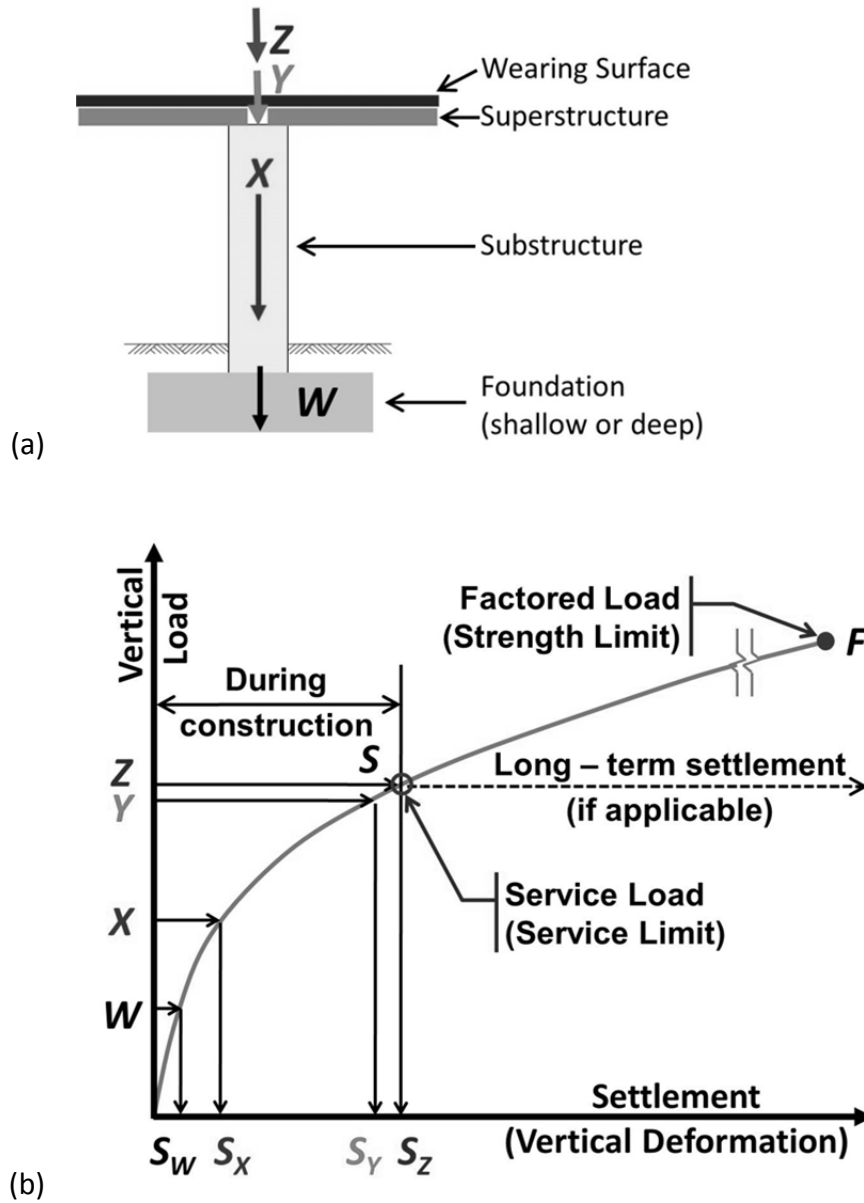
6.1 Vertical Deformation (Settlement)

Most designers analyze foundation deformations as if a weightless bridge structure is instantaneously set into place and all the loads are applied at the same time. In reality, loads are applied gradually as construction proceeds and settlements also occur gradually as construction proceeds. There are several critical construction points or stages during construction that should be evaluated separately by the designer. Figure 6-1 shows the critical construction stages and their associated load-displacement behavior. Formulation of settlements as shown in Figure 6-1 would permit an assessment of settlements up to that point that can affect the bridge superstructure. For example, the settlements that occur before placement of the superstructure may not be relevant to the design of the superstructure. Thus, the settlements between application of loads X and Z are the most relevant.

Studies, like Sargand et al. (1999) and Sargand and Masada (2006), have documented data which indicate that the percentage of settlement between placement of beams and end-of-construction is generally between 25 to 75 percent of the total settlement, depending on the type of the superstructure and the construction sequence. This is a significant observation and therefore, it is recommended that the limit state of vertical deformations, that is, settlements, and its implications should be evaluated using the construction-point concept. This observation applies to all other deformations, for example, lateral and rotation.

While using the construction-point concept, it is important that various quantities are being measured at discrete construction stages and that the associated settlements are considered to be immediate. However, the evaluation of total settlement and the maximum (design) angular distortion, as discussed previously, must also account for long-term settlements. For example, significant long-term settlements may occur if foundations are founded on saturated clay deposits or if a layer of saturated clay falls within the zone of stress influence below the foundation, even though the foundation itself is founded on competent soil. In such cases, long-term settlements will continue under the total construction load (Z) as shown by the dashed line in Figure 6-1. Continued settlements during the service life of the structure will tend to reduce the vertical clearance under the bridge with associated problems of large vehicles impacting the bridge superstructure. The geotechnical specialist must estimate and report to the structural specialist, the magnitude of the long-term settlement that will occur during the design life of the bridge. A key point in evaluating settlements at critical construction points is that the approach requires close coordination between the structural and geotechnical specialists.

Figure 6-1: Construction-point concept for a bridge pier.



Legend

W	Load after foundation construction
X	Load after pier column/wall construction
Y	Load after superstructure construction
Z	Load after wearing surface construction
S	Service Load (SLS)
F	Factored Load (Strength Limit State)

S_W	Settlement under load W
S_X	Settlement under load X
S_Y	Settlement under load Y
S_Z	Settlement under load Z


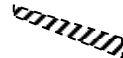
(a) Identification of critical construction points

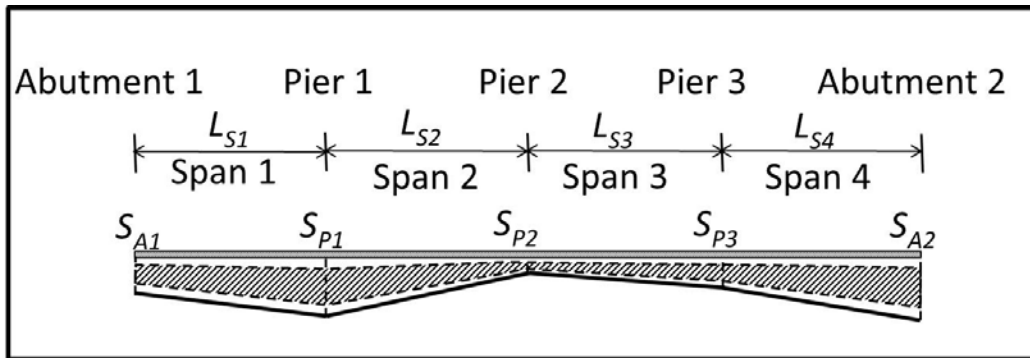
(b) conceptual load-displacement pattern for a given foundation

With respect to the example of the four-span bridge shown in Figure 4-2, the use of the construction-point concept would result in smaller settlement to be considered in the structural design. Figure 6-2 shows a comparison of the profiles of the calculated settlements (solid lines) and the actual relevant settlements (hatched pattern zones) based on the construction-point concept. The range of the hatched pattern zone can be 25 to 75 percent of the total settlement values (solid line), as previously discussed. For a given project and site-specific conditions, the actual relevant settlement profile will be within the hatched pattern zone.

Figure 6-2: Factored Angular distortion in bridges based on construction-point concept

Legend:

-  Calculated total settlement profile (refer to Figure 4.2)
-  Range of relevant settlement profile using construction-point concept



6.2 Horizontal Deformations

Horizontal deformations generally occur because of sliding and/or rotation of the foundation. Moulton indicates that horizontal deformations cause more severe and widespread problems than do equal magnitudes of vertical movement. The most common location of horizontal deformations is at the abutments, which are subject to lateral earth pressure. Horizontal movements can also occur at the piers because of lateral loads and moments at the top of the substructure unit. The estimation of the magnitudes of horizontal movements should take into account the movements associated with lateral squeeze as discussed in Samtani and Nowatzki (2006) and Samtani, et al. (2010). Lateral movements from lateral squeeze can be estimated by geotechnical specialists while lateral movements from sliding or lateral deformations of deep foundations can be estimated by structural specialists based on input from geotechnical specialists. The limiting horizontal movements are strongly dependent on the type of superstructure and the connection with that substructure; therefore, horizontal deformations are project specific.

Chapter 7. Reliability of Predicted Foundation Deformations

All analytical methods (models) for predicting foundation deformations have some degree of uncertainty. The reliability of predicted foundation deformations varies as a function of the chosen analytical method. Since the induced force effects (for example, moments) are a direct function of foundation deformations, the values of the induced force effects are only as reliable as the estimates of the foundation deformations. It is important to quantify the uncertainty in foundation deformations by calibrating the analytical method used to predict the foundation deformations using stochastic procedures. In the LRFD framework, the uncertainty is calibrated through use of load and/or resistance factors. As discussed in chapter 2, *AASHTO LRFD* considers uncertainty of foundation deformations in terms of the induced effects through the use of γ_{SE} load factor. The calibration procedure of γ_{SE} load factor is discussed chapter 8.

Chapter 8. Calibration Procedures

8.1 Relevant AASHTO LRFD Articles for Foundation Deformations

Within the context of foundation deformation, the geotechnical limit states can be broadly categorized into vertical and horizontal deformations for any foundation type (for example, spread footings, driven piles, drilled shafts, and micropiles). Table 8-1 summarizes the various relevant articles in *AASHTO LRFD* that address vertical (settlement) and horizontal deformations for various types of structural foundations.

Table 8-1: Summary of AASHTO LRFD Articles for Estimation of Vertical and Horizontal Deformation of Structural Foundations

AASHTO LRFD Article	Comment
10.6.2.4: Settlement Analyses for Spread Footings	Article 10.6.2.4 presents methods to estimate the settlement of spread footings. Settlement analysis is based on the elastic and semi-empirical Hough (1959) (Hough) method for immediate settlement and the 1-D consolidation method for long-term settlement.
10.7.2.3: Settlement (related to driven pile groups) 10.8.2.2: Settlement (related to drilled shaft groups) 10.9.2.3: Settlement (related to micropile groups)	The procedures in these Articles (10.7.2.3, 10.8.2.2 and 10.9.2.3) refer to the settlement analysis for an equivalent spread footing (see <i>AASHTO LRFD</i> , Figure 10.7.2.3.1-1).
10.7.2.4: Horizontal Pile Foundation Movement 10.8.2.4: Horizontal Movement of Shaft and Shaft Groups 10.9.2.4: Horizontal Micropile Foundation Movement	Lateral analysis based on the <i>P-y</i> method and Strain Wedge Method (SWM) is included in <i>AASHTO LRFD</i> for estimating horizontal (lateral) deformations of deep foundations.

Note:

Section 11 (Abutments, Piers and Walls), Article 11.6.2 of *AASHTO LRFD* refers back to the various Articles noted in the left column of this table. Therefore, the Articles noted in this table also apply to fill retaining walls and their foundations.

This chapter describes procedures that can be used for calibration of limit states to evaluate the effect of vertical or horizontal deformations of all structural foundation types such as footings, drilled shafts, and driven piles. The effect of foundation deformations on the bridge superstructures is discussed in the context of construction-point concept. The implementation of the calibration procedure is demonstrated in chapter 9, by using the case of immediate settlements of spread footings.

8.2 Overarching Characteristics to Be Considered

For limit states that deal with deformations, there are some overarching characteristics in terms of cause (load) and consequences to the bridge structure from limit states that are exceeded because of foundation deformations. In this context, foundation deformation may invoke several structural limit states, such as cracking of reinforced concrete structures. A key overarching characteristic to consider is that the calibration of foundation deformations must be consistent with the level of reliability that is considered in the structural service limit states.

8.2.1 Load-Driven versus Non-Load-Driven Limit States

The difference between load-driven and non-load-driven limit states is in the degree of involvement of externally-applied load components in the formulation of the limit state function. In the load-driven limit states, the damage occurs because of accumulated applications of external loads, usually live load (trucks). Examples of load-driven limit states include decompression and cracking of prestressed concrete and vibrations or deflection. The damage caused by exceeding limit states may be reversible or irreversible; therefore, the cost of repair may vary significantly. However, in non-load-driven limit states, the damage occurs because of deterioration or degradation over time and aggressive environment or as inherent behavior from certain material properties. Examples of non-load-driven limit states include penetration of chlorides leading to corrosion of reinforcement, leaking joints leading to corrosion under the joints, shrinkage cracking of concrete components, and corrosion and degradation of reinforcements in reinforced soil structures (such as, mechanically stabilized earth [MSE] walls). In these examples, the external load occurrence plays a secondary role. In case of foundation deformations, the computations are usually performed with consideration of live load (load-driven) for short-term deformations but without consideration of live load for long-term or time-dependent deformations.

8.2.2 Reversible versus Irreversible Limit States

Limit states may be categorized as reversible and irreversible. Reversible limit states are those for which no consequences remain once a load is removed from a structure. Irreversible limit states are those for which consequences remain.

Another extended concept is that of reversible-irreversible limit state, where the effect of an irreversible limit state may be reversed by intervention. An example of this concept is foundation settlement, which is an irreversible limit state with respect to the foundation elements, but may be reversible in terms of its effect on the bridge superstructure through intervention (for example, through the use of shims or jacking).

Because of their reduced service implications, irreversible limit states, which do not concern the safety of the traveling public, are calibrated to a higher probability of failure and a corresponding lower reliability index than the strength limit states. Reversible limit states are calibrated to an even lower reliability index.

8.2.3 Consequences of Exceeding Deformation-Related Limit States and Target Reliability Indices

To differentiate between different limit states according to the consequences of exceeding a limit state, the following factors should be considered:

- Whether the limit state is reversible or irreversible: Irreversible limit states may have higher target reliability than reversible limit states. Reversible-irreversible limit states may have target reliability similar to reversible limit states.
- Relative cost of repairs: Limit states that have the potential to cause damage that is costly to repair may have higher target reliability than limit states that have the potential of causing only minor damage.

For strength limit states, reliability index values in the range of 3.0 to 3.5 are used. Strength (or ultimate) limit states pertain to structural safety and the loss of load-carrying capacity. In contrast, service limit states are user-defined limiting conditions that affect the function of the structure under expected service conditions. Violation of service limit states occurs at loads much smaller than those for strength limit states. Since there is no danger of collapse if a service limit state is violated, a smaller value of target reliability index may be used for service limit states. In the case of foundation deformation such as settlement, the structural force effect is manifested in increased moments and potential cracking. The force effect due to the settlement, relative to the force effect due to dead and live loads, would generally be small because in the load factor γ_{SE} , which represents the uncertainty in estimated settlement, is only one of many load factors in all the Service and Strength limit state load combinations. The primary moments due to the sum of dead and live loads are much larger than the additional (secondary) moments because of settlement. Based on these considerations and consideration of reversible and irreversible service limit states for bridge superstructures, a target reliability index, β_T , in the range of 0.50 to 1.00 for calibration of load factor γ_{SE} for foundation deformation in the Service I limit state was used in SHRP2's *Service Limit State Design for Bridges*.

8.3 Calculation Models

While considering limit states from deformations, the load-deformation characteristics of the structure or its member are important to understand. This is because the resistance must now

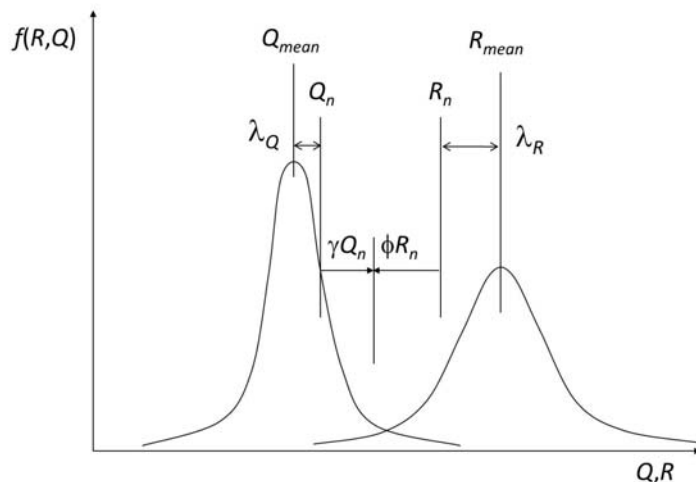
be quantified as a function of the deformation. This section discusses the extension of the *AASHTO LRFD* framework to incorporate the load-deformation behavior. This section also presents a calibration framework for foundation deformations. The proposed step-by-step procedure for calibration is described in chapter 8.3.5, which leads to a load factor for deformations based on the target reliability index that was discussed in chapter 8.2.3. This procedure is demonstrated by an example for immediate settlements of spread footings using various analytical methods in chapter 9.

8.3.1 Incorporation of Load-deformation (Q - δ) Characteristics in *AASHTO LRFD* Framework

The basic *AASHTO LRFD* framework in terms of distributions of loads and resistances is shown in Figure 8-1, where

- Q = load
- Q_{mean} = mean load
- Q_n = nominal load
- λ_Q = bias factor for load
- γ = load factor
- R = resistance
- R_{mean} = mean resistance
- R_n = nominal resistance
- λ_R = bias factor for resistance
- ϕ = resistance factor
- f = frequency

Figure 8-1: Basic *AASHTO LRFD* framework for loads and resistances



Details of the *AASHTO LRFD* framework can be found in Nowak and Collins (2013). Strength limit states were evaluated by using this framework. Determination of deformation is a necessary part of the evaluation of serviceability. Therefore, for the evaluation of deformations, the basic *AASHTO LRFD* framework shown in Figure 8-1 needs to be modified to include load-deformation or $Q-\delta$ behavior. The $Q-\delta$ behavior can be considered to be another dimension of the basic *AASHTO LRFD* framework as shown in Figure 8-2, where:

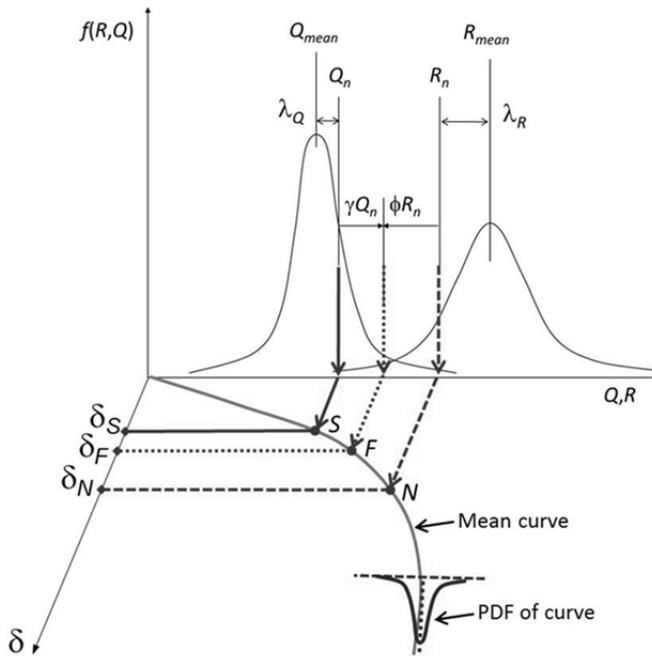
δ = deformation

δ_S = deformation at nominal load, Q_n

δ_F = deformation at factored load, $Q_F = \gamma(Q_n)$

δ_N = deformation at load corresponding to nominal resistance, R_n

Figure 8-2: Incorporation of $Q-\delta$ mechanism into the basic *AASHTO LRFD* framework



Although $Q-\delta$ curves can have many different shapes, for illustration purposes, a strain hardening curve is shown in Figure 8-2. For discussion purposes, the mean $Q-\delta$ curve is shown and the spread of the $Q-\delta$ data about the mean curve is represented schematically by a probability distribution function (PDF) that will be discussed later in this report. The various relevant load and deformation quantities shown in the $Q-\delta$ space in Figure 8-2 are shown in the regular first quadrant of the 2-D plot in Figure 8-3. Note that the nominal resistance is equated to a load that would correspond to this resistance.

Figure 8-3: Significant points of interest on the mean Q - δ curve

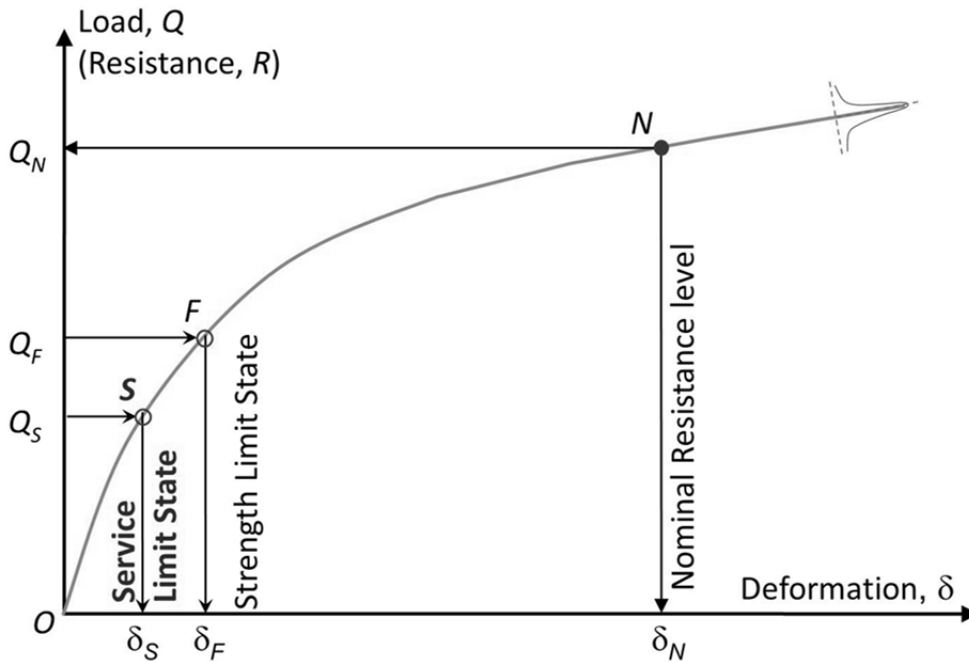


Figure 8-2 combines a number of different aspects of material behavior that covers both loads and resistances. It is important to understand the inter-relationships among the various parameters displayed on the curves. The following points are made:

- The load-deformation (Q - δ) curves shown in Figure 8-2 and Figure 8-3 represent the measured mean curves based on field measurements.
- Field measurements have upper and lower bounds with respect to the mean of the measured data. These bounds are shown schematically in Figure 8-4 and also in Figure 8-2 and Figure 8-3 through a PDF. Although PDFs for normal distributions are shown, the spread of the data along the mean may be represented by normal or nonnormal distributions, as appropriate. In general, the spread of the data around the mean curve increases with increasing deformations.
- Many theoretical methods are used to predict the load-deformation behavior. The theoretical models may predict a stiffer or softer material response compared to the actual response. A “softer” material behavior is shown in Figure 8-5. Since the bias factor is defined as the ratio of measured mean to predicted values, the bias factor for deformations, λ_δ , will vary over the full range of the Q - δ curve.

Figure 8-4: Range and distribution along a $Q-\delta$ curve

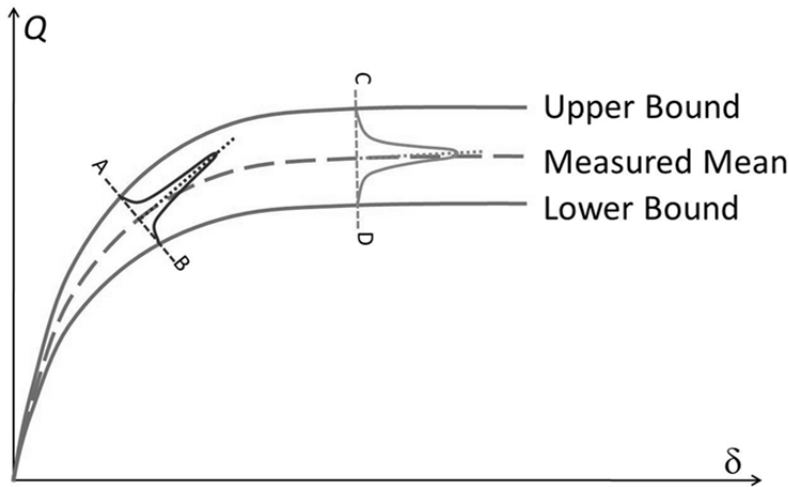
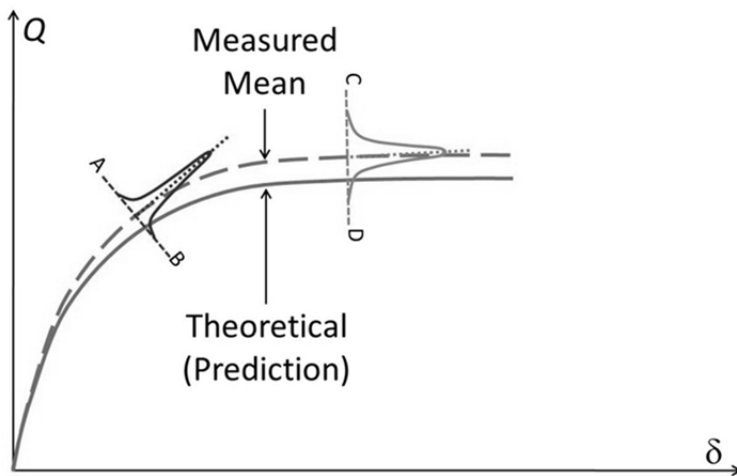


Figure 8-5: Relationship of measured mean with theoretical prediction



8.3.2 Consideration of Bias Factor in Calibration of Deformations

A varying bias factor along the $Q-\delta$ curve, although a reality, can be difficult to handle in the calibration process. However, the problem is made easier by realizing that for calibration of deformation the force effects between Points O and S as shown in Figure 8-3 are of primary interest. Point S represents the service force effects and the deformations corresponding to this point are of primary interest. Since the bias factor will generally increase with increasing deformations, the value of the bias factor at Point S will be the maximum between Point O and S and the use of the bias factor at Point S will be conservative. In this context, the bias factor at Point S is most relevant and, at a minimum, field data under full service loads are of importance in deformation calibrations. The data needed for deformation evaluations are the full range of incremental loads and deformations measured on in-service structures from the beginning of

construction of the first element (for example, the foundation) to the completion of the roadway and beyond. These data will help in evaluating the variability in predicted deformations for structural, as well as geotechnical, features. At the present time, these types of data are not routinely available; however, programs such as FHWA's Long Term Bridge Performance Program may offer a good avenue to collect such data.

8.3.3 Application of Q - δ Curves in the AASHTO LRFD Framework

The calibration of the strength limit state in AASHTO LRFD was performed by using the general concepts in Figure 8-1. This approach presumes that statistical data are available to quantify the spread of the force effects and resistances. In the context of deformations, tolerable deformations (δ_T) can be considered as resistances while the predicted deformations (δ_P) can be considered as loads. Thus, a limit state function (g) can be written as follows:

$$g = \delta_T - \delta_P \quad (8-1)$$

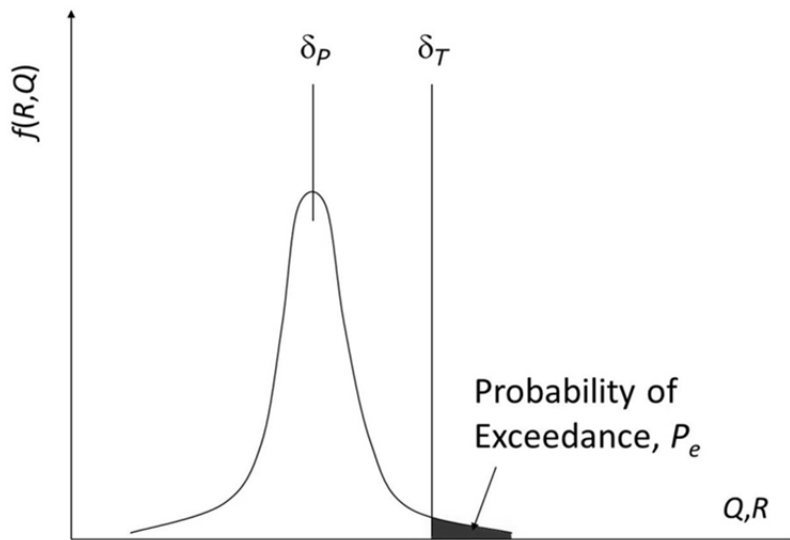
Once the deformations are expressed in the form of a limit state, probabilistic calibration processes similar to those used for the strength limit state can be used. For strength limit states, the Monte Carlo (MC) analysis is often used for calibrations. One of the assumptions of the MC procedure is that PDFs for both the load (Q) and resistance (R) are available. However, for deformation calibration, there are practical limitations to this approach. Although the statistical data for modeling the uncertainty in predicted deformations, δ_P , are available, the same is not true for tolerable deformations, δ_T . Some attempts have been made (Zhang and Ng, 2005) to evaluate the distribution of tolerable deformations, but from a geotechnical viewpoint, it may not be possible to obtain a PDF for tolerable deformation that is applicable to the various structural SLSs mentioned in chapter 1 of this report. This is largely because it is virtually impossible to identify a consistent tolerable deformation across all elements of a structure. Many variables can affect the value of tolerable deformation for a given element. To bypass these difficulties, a single deterministic value of tolerable deformation, δ_T , is often used for comparison against the potential spread of data for predicted deformations, δ_P . In practical terms, a bridge engineer often assumes a deterministic tolerable deformation that would limit deformations based on the type of the bridge structure being designed. In this case, the conventional calibration processes such as the MC procedure would not be necessary since we would have a PDF for load (Q) but a deterministic value for resistance (R). To use MC in this situation, an arbitrarily small value of standard deviation, or coefficient of variation (CV), would have to be used. Although theoretically possible, this process could lead to spurious results. An alternative approach to calibration of deformations is necessary.

When a deterministic value for δ_T is used, then using Figure 8-1 as the basis, the resistance PDF is reduced to a single value while the load PDF can be used to represent the predicted deformations. This modified treatment for deformations is shown in Figure 8-6. In this

approach, the probability of exceedance (P_e) for the predicted deformations to exceed the tolerable deformation is given by the area of the overlap of the two curves (the shaded zone shown in Figure 8-6). As the goal is to prevent deformation-related problems, P_e can be selected based on the acceptable value of target reliability index (β_T). The ratio δ_T/δ_p can be thought of as a load factor for deformations for a given probability of exceedance, P_e , corresponding to a target reliability index, β_T .

The PDF for the predicted deformations shown in Figure 8-6 is obtained from the data at Point S shown in Figure 8-2 and Figure 8-3. This is where the concept of Q - δ curve fits into the framework for calibrate based on deformations. Thus, any model that can predict a Q - δ curve can be used in the conventional *AASHTO LRFD* framework as long as the data at Point S corresponding to SLS force effects are available through field measurements. The effect of material brittleness (or ductility) can now be introduced in the *AASHTO LRFD* framework through use of an appropriate Q - δ model. Examples of Q - δ models are stress-strain curves, vertical load-settlement curves for foundations, P - y (lateral load-lateral displacement) curves for laterally loaded piles, shear force-shear strain curves, and moment-curvature curves. The proposed framework can incorporate any Q - δ model and is therefore a general framework that is applicable to structural or geotechnical aspects.

Figure 8-6: Relationship of deterministic value of tolerable deformation, δ_T , and a probability distribution function for predicted deformation, δ_p



- Q = Force effect
- R = Resistance
- δ_p = Predicted deformations (force effect)
- δ_T = Deterministic value of tolerable deformation (resistance)

8.3.4 Deterioration of Foundations and Wall Elements

Most, if not all, foundation elements are buried in geomaterials. This is also true for most earth-retaining structures. Therefore, the long-term performance of the foundation and wall elements can be affected by the corrosion and degradation potential of the geomaterials. The term “corrosion” applies to metal components while “degradation” applies to non-metal components such as polymeric soil reinforcements in MSE walls.

If the geomaterials have significant corrosion or degradation potential, then the sectional properties of the foundation and wall elements will deteriorate by reduction in the section or loss of strength, or both. The *AASHTO LRFD* specifications recognize this mode of deterioration and provide definitive guidelines. For example, *AASHTO LRFD*, Articles 10.7.5 and 10.9.5 of Section 10 (Foundations) provide guidelines for evaluation of corrosion and deterioration of driven piles and micropiles, respectively. Similarly, *AASHTO LRFD* Section 11 (Abutments, Piers and Walls) provides guidance in Article 11.8.7 for non-gravity cantilevered walls, Article 11.9.7 for anchored walls, and Articles 11.10.2.3.3 and 11.10.6.4 for MSE walls. Supplementary guidance can be found in Elias, et al. (2009) and Fishman and Withiam (2011). The *AASHTO LRFD*, Elias, et al., and Fishman and Withiam documents cross-reference a number of different publications that discuss the corrosion or degradation potential of geomaterials.

In general, the various AASHTO articles and other documents cited provide guidance for testing frequencies and protocols to evaluate the corrosion or degradation potential of various geomaterials. It is assumed that the foundation and wall designer will perform the necessary tests and, as appropriate, implement the necessary mitigation measures to minimize the inevitable effects of corrosion or degradation on the foundation, wall elements, and structures these elements support. The most common approach is to estimate the rate of corrosion or degradation over the design life of the structure and provide additional sectional or strength properties (or both) that will permit the structure to perform within its strength and serviceability requirements. For example, metal elements are often provided additional section based on the anticipated loss of metal over the design life of the structure. Concrete deterioration from sulfate attack is often mitigated by use of an appropriate type of cement.

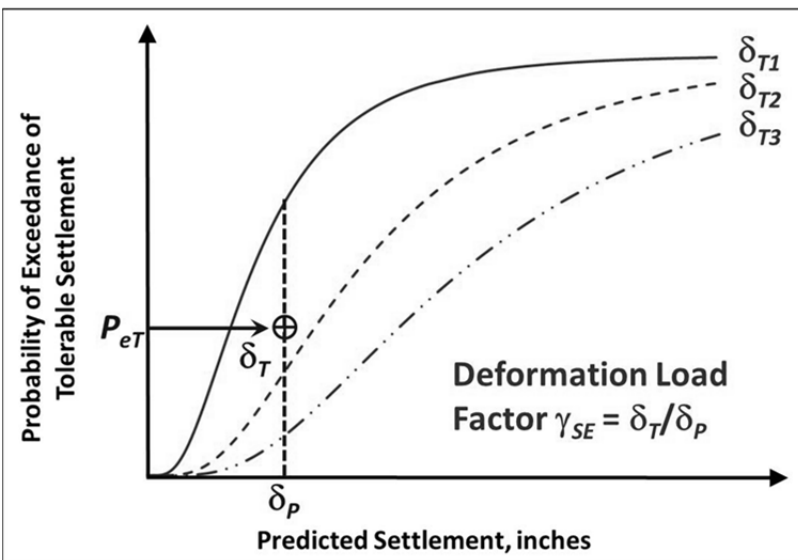
8.3.5 Determination of Load Factor for Deformations

The concept presented in Figure 8-6 assumes that the designer has unique (fixed) values of tolerable deformation (δ_T) and predicted deformation (δ_P). However, these values are functions of many parameters for a given element and the mode of deformation being evaluated. It is more practical to express the load factor for deformation as a function of the value of δ_P . The load factor is more conveniently determined by using an alternative form of the concept as shown in Figure 8-7, in which the cumulative distribution function (CDF) is used instead of the PDF. In this concept it is more convenient to use the data based on the inverse

of the bias factor since the predicted (calculated) deformation is plotted on the x-axis. The format shown in Figure 8-7 is used as follows:

1. Obtain data for predicted (δ_p) and measured (δ_M) deformations for the deformation mode of interest (for example, immediate settlement of spread footings, lateral deformation of a deep foundation, or lateral deflection at top of MSE wall). Recognize that the value of δ_M can be considered as resistance and equivalent to the tolerable settlement (δ_T).
2. Modify the data to be expressed in terms of ratio δ_p/δ_T . In geotechnical literature (Tan and Duncan, 1991) this ratio is often referred to as “accuracy.” Label this ratio as X . X is a random variable that can now be modeled by an appropriate PDF. Develop the appropriate statistics, and select a suitable distribution function. Express the data in terms of a CDF.
3. As shown in Figure 8-7, plot a family of CDF curves for a range of values of tolerable deformation (for example, $\delta_{T1} < \delta_{T2} < \delta_{T3}$) that permits the determination of values of the probability of exceedance (P_e) for a range of δ_p . The CDFs are generated by multiplying the CDF for accuracy ($X = \delta_p/\delta_T$) by selected values of tolerable deformations ($\delta_{T1}, \delta_{T2}, \delta_{T3}$). The plot shown in Figure 8-7 is referred to as a Probability Exceedance Chart (PEC).
4. Select the design value of probability of exceedance (P_{eT}) corresponding to the target reliability index (β_T), and determine the value of δ_T for a given value of δ_p , as shown in Figure 8-7.
5. Compute the value of the deformation load factor ($\gamma_{SE} = \delta_T/\delta_p$) as shown in Figure 8-7.

Figure 8-7: PEC for evaluation of load factor for a target probability of exceedance (P_{eT}) at the applicable SLS combination



The benefit of this approach is that once the designer computes (predicts) a deformation for any given deformation mechanism, then the designer simply multiplies the computed value by the deformation load factor corresponding to that value of deformation and uses the factored value for evaluation at the applicable service and strength load combinations. This concept is valid whether structural or geotechnical deformation mechanisms are evaluated. This concept is demonstrated in chapter 9.

A PEC chart is essentially a representation of CDF of accuracy, or X . Similar charts are referred to as probabilistic design charts by Das and Sivakugan (2007) and Sivakugan and Johnson (2002, 2004) and artificial neural network charts by Shahin, et al. (2002) and Musso and Provenzano (2003). Although not specifically in chart format, similar concepts are also presented in Tan and Duncan (1991) and Duncan (2000). The specific format of PEC that is developed and used here is amenable to correlation to the *AASHTO LRFD*-based concept of target reliability index.

Chapter 9. Calibration Implementation

9.1 General

AASHTO LRFD explicitly includes specific analytical methods for various features. For example, for immediate settlement of spread footings it includes a method by Hough. However, some other methods, such as Schmertmann et al. (1978) (Schmertmann), that is recommended by FHWA or another local method may be preferred by an owner based on local regional geologic conditions. Based on the calibration approach included in chapter 8, this section illustrates the calibration implementation to serve as an aid for an owner to perform a calibration of the γ_{SE} load factor for geotechnical features by using an analytical method to predict (estimate) deformation based on local geologic conditions. A step-by-step format is provided with the intention that end-users can simply substitute the appropriate data for the method and the mode of foundation deformation that they are trying to calibrate. In general, the vertical and lateral deformations for all structural-foundation types, such as footings, drilled shafts and driven piles can be calibrated by using the process described herein. The concept can also be applied to other geotechnical features such as retaining walls (for example, calibration of face deformations of MSE walls with inextensible or extensible reinforcements). To demonstrate the calibration process, the immediate vertical settlement of spread footings is used herein.

For convenience, reference is made to the widely used commercial software Microsoft Excel (References to Microsoft Excel herein are applicable to its 2007 and 2010 versions). This has been done to help simplify the calibration process without complicating the process with esoteric probabilistic principles, which in the end lead to the same result. All figures in this section have been generated using Microsoft Excel.

Table 9-1 summarizes the framework for calibration. Subsections 9.2.1 to 9.2.6 demonstrate the application of each step in Table 9-1.

Table 9-1: Basic Framework for Calibration of Deformations

Step	Comment
1. Formulate the limit state function and identify basic variables.	Identify the load and resistance parameters and formulate the limit state function. For each considered limit state, establish the acceptability criteria.
2. Identify and select representative structural types and design cases.	Select the representative components and structures to be considered, e.g., structural type could be spread footing and the design case may be immediate settlement.
3. Determine load and resistance parameters for the selected design cases.	Identify the design parameters on the basis of typical foundation types and deformations. For each considered foundation type and deformation, the parameters to be calibrated must be determined, e.g., immediate settlement of a spread footing based on Hough method, lateral deflection of driven pile group at groundline based on <i>P-y</i> method.
4. Develop statistical models for load and resistance.	Gather statistical information about the performance of the considered deformation types and prediction models. Determine the accuracy (λ) factor and statistics for loads based on prediction models. Resistance is often based on deterministic approach and its value will vary as a function of the considered structural limit state.
5. Apply the reliability analysis procedure.	Reliability can be calculated using the PEC method. In some cases, depending on the type of probability distribution function a closed form solution may be possible.
6. Review the results and develop the γ_{SE} load factors for target reliability indices.	Develop the γ_{SE} load factor for all applicable structural limits states and their corresponding target reliability indices and consideration of reversible and irreversible limit states
7. Select the γ_{SE} load factor.	Select an appropriate the γ_{SE} load factor based on owner criteria, e.g., reversible-irreversible condition.

9.2 Steps for Calibration

9.2.1 Step 1: Formulate the Limit State Functions and Identify Basic Variables

In the context of deformations, tolerable deformations (δ_T) can be considered as resistances while the predicted deformations (δ_P) can be considered as loads. Thus, a limit state function (g) can be given by Equation 9-1 (first introduced as Equation 8-1):

$$g = \delta_T - \delta_P \quad (9-1)$$

For calibration of deformations, the limit state g expressed as a ratio is more appropriate, as given by Equation 9-2:

$$g = \delta_P / \delta_T \quad (9-2)$$

9.2.2 Step 2: Identify and Select Representative Structural Types and Design Cases

To demonstrate the calibration process, immediate vertical settlement of spread footings is used as a design case. As noted earlier, in general the vertical and lateral deformations for all structural foundation types (for example, footings, drilled shafts, and driven piles) and retaining walls can be calibrated using the process described in this example.

9.2.3 Step 3: Determine Load and Resistance Parameters for the Selected Design Cases

The load and the resistance parameters for the selected design case of immediate vertical settlement of spread footings are as follows: Load is predicted (or calculated) immediate vertical settlement (δ_P) and resistance is tolerable (or limiting or measured) immediate vertical settlement (δ_T).

AASHTO LRFD uses the symbol “ S ” for foundation settlement (vertical deformation). Therefore, for further discussions, the symbol S will be used instead of δ . Similarly, while calibrating other deformation modes, an appropriate symbol may be used that defines that particular deformation mode, for example, the symbol “ y ” is used for lateral deflection of piles using the P - y method of analysis. For this example problem, load is predicted (or calculated) immediate vertical settlement (S_P) and resistance is tolerable (or limiting or measured) immediate vertical settlement (S_T).

9.2.4 Step 4: Develop Statistical Models for Load and Resistance

Table 9-2 shows a data set for spread footings based on vertical settlements of footings measured at 20 footings for 10 instrumented bridges in the northeastern United States (Gifford, et al., 1987). The bridges included five simple-span and five continuous-beam structures. Each

of the site designations in Table 9-2 represents a footing supporting a single substructure unit (abutment or pier). Four of the instrumented bridges were single-span structures. Two two-span and three four-span bridges were also monitored in addition to a single five-span structure. Nine of the structures were designed to carry highway traffic while one four-span bridge carried railroad traffic across an Interstate highway. Additional information on the instrumentation and data collection at the 10 bridges can be found in Gifford, et al. (1987). There are similar and more extensive databases for spread footings (for example, Sargand et al., 1999; Sargand and Masada, 2006; Akbas and Kulhawy, 2009; Samtani, et al., 2010) and other foundation types such as driven piles and drilled shafts. Similar databases are also available for lateral load behavior of deep foundations as well as deformations of MSE walls. However, for the purpose of this report, the calibration concepts for foundation deformations will be demonstrated by use of the limited data set for spread footings shown in Table 9-2. All concepts discussed here are applicable to other foundation or wall types and deformation patterns.

Figure 9-1 shows a plot of the data in Table 9-2 and the spread of the data about the 1:1 diagonal line, which defines the case for which the predicted and measured values are equal. Such a plot provides a visual frame of reference to judge the accuracy of the prediction method. If the data points align closely with the 1:1 diagonal line, then the predictions based on the analytical method being evaluated are close to the measured values and are more accurate than the case where the data points do not align closely with the 1:1 diagonal line. In the geotechnical literature (Tan and Duncan, 1991), “accuracy,” is defined as the mean value of the ratio of the predicted (calculated) to the measured settlements. Table 9-3 shows the values of accuracy (denoted by X , where $X = S_P/S_M$) for each footing based on the data in Table 9-2 for the following five methods:

1. Schmertmann: Method by Schmertmann et al. (1978)
2. Hough: Method by Hough (1959)
3. D’Appolonia: Method by D’Appolonia et al. (1968)
4. Peck and Bazarra: Method by Peck and Bazarra (1969)
5. Burland and Burbridge: Method by Burland and Burbridge (1984)

As noted in Step 3 of the calibration process, the value of S_M can be considered as the resistance and equivalent to the tolerable settlement (S_T). The accuracy (i.e., $X = S_P/S_M$ [or S_P/S_T]), is a random variable that can now be modeled by an appropriate PDF. To develop an appropriate PDF, an evaluation of the data spread around the mean value is needed. This evaluation involves statistical analysis and development of histograms.

Table 9-2: Data for Measured and Predicted (Calculated) Settlements Shown in Figure 9-1 Based on Gifford, et al. (1987)

Site	Settlement (in.)					
	Measured (S_M)	Predicted (Calculated) (S_P)				
		Schmertmann	Hough	D'Appolonia	Peck and Bazzara	Burland and Burbridge
#1	0.35	0.79	0.75	0.65	0.29	0.30
#2	0.67	1.85	0.94	0.39	0.16	0.12
#3	0.94	0.86	1.21	0.30	0.19	0.13
#4	0.76	0.46	1.46	0.58	0.36	0.39
#5	0.61	0.30	0.98	0.38	0.42	0.57
#6	0.42	0.52	0.61	0.50	0.17	0.34
#7	0.61	0.18	0.40	0.19	0.30	0.19
#8	0.28	0.30	0.60	0.26	0.16	0.14
#9	0.26	0.18	0.53	0.20	0.16	0.11
#10	0.29	0.29	0.40	0.23	0.16	0.09
#11	0.25	0.36	0.47	0.29	0.16	0.06
#14	0.46	0.41	1.27	0.57	0.50	0.40
#15	0.34	1.57	1.46	0.74	1.36	1.61
#16	0.23	0.26	0.74	0.39	0.17	0.17
#17	0.44	0.40	0.82	0.46	0.28	0.23
#20	0.64	1.21	0.33	0.10	0.07	0.65
#21	0.46	0.29	1.05	0.49	0.21	0.54
#22	0.66	0.54	0.84	0.56	0.52	0.31
#23	0.61	1.02	1.39	0.61	0.34	0.64
#24	0.28	0.64	0.99	0.59	0.33	0.44

Note 1: Gifford, et al. (1987) notes that data for footings at Site #12, #13, and #18 were not included because construction problems at these sites resulted in disturbance of the subgrade soils and short term settlement was increased. Data for footing at Site #19 appears to be anomalous and have been excluded in this table and Figure 9-1.

Figure 9-1: Comparison of measured and calculated (predicted) settlements based on service load data in Table 9-2

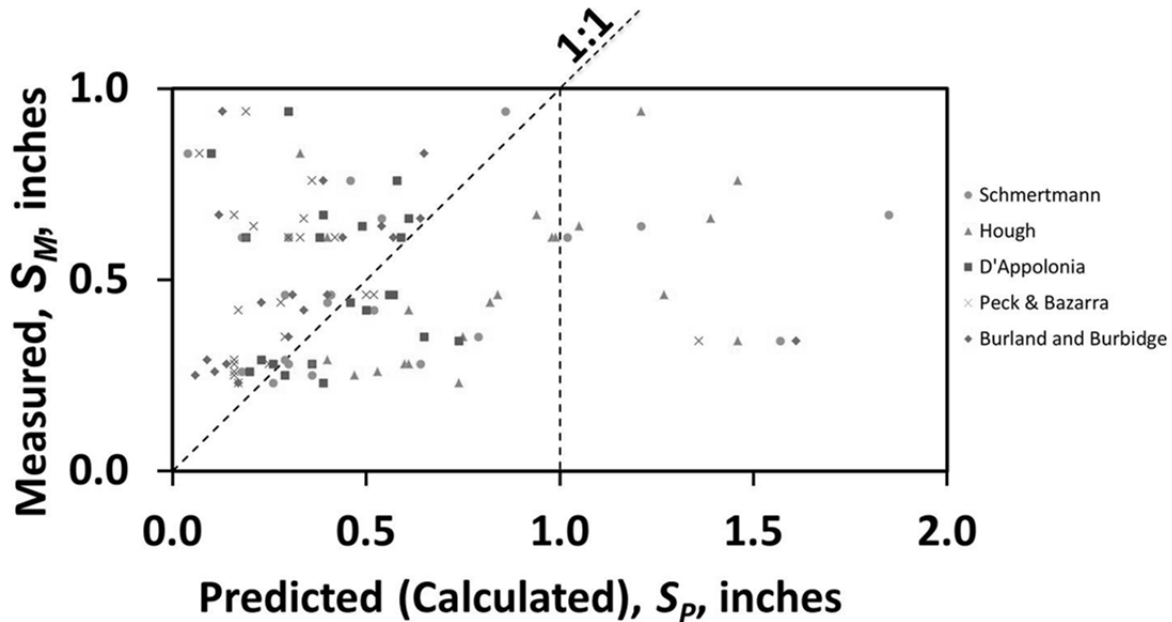


Table 9-4 presents the arithmetic mean (μ) and standard deviation (σ) values for various methods. *AASHTO LRFD* recommends the use of Hough's method, which has the smallest CV for the calculating immediate settlement. However, the Hough method is conservative by a factor of approximately 2 (see mean value in Table 9-4), which leads to unnecessary use of deep foundations instead of spread footings. FHWA (Samtani and Nowatzki, 2006; Samtani, et al. 2010) recommends the Schmertmann method because it considers not only the applied stress and its associated strain influence distribution with depth for various footing shapes, but also the elastic properties of the foundation soils, even if they are layered.

Even though FHWA and *AASHTO LRFD* recommends the Schmertmann and Hough methods, respectively, all the methods noted in Table 9-2 to Table 9-4 were evaluated as part of the calibration process because some agencies may use one of the remaining three methods as a result of past successful local practice.

Table 9-3: Accuracy ($X=S_P/S_M$) Values Based on Data Shown in Table 9-2

Site	Schmertmann	Hough	D'Appolonia	Peck and Bazzara	Burland and Burbridge
#1	2.257	2.143	1.857	0.829	0.857
#2	2.761	1.403	0.582	0.239	0.179
#3	0.915	1.287	0.319	0.202	0.138
#4	0.605	1.921	0.763	0.474	0.513
#5	0.492	1.607	0.623	0.689	0.934
#6	1.238	1.452	1.190	0.405	0.810
#7	0.295	0.656	0.311	0.492	0.311
#8	1.071	2.143	0.929	0.571	0.500
#9	0.692	2.038	0.769	0.615	0.423
#10	1.000	1.379	0.793	0.552	0.310
#11	1.440	1.880	1.160	0.640	0.240
#14	0.891	2.761	1.239	1.087	0.870
#15	4.618	4.294	2.176	4.000	4.735
#16	1.130	3.217	1.696	0.739	0.739
#17	0.909	1.864	1.045	0.636	0.523
#20	1.891	1.641	0.766	0.328	0.844
#21	0.630	1.826	1.217	1.130	0.674
#22	0.818	2.106	0.924	0.515	0.970
#23	1.672	1.623	0.967	0.541	0.721
#24	2.286	2.179	1.286	0.893	1.286

Table 9-4: Statistics of Accuracy, X , Values Based on Data Shown in Table 9-3

Statistic	Schmertmann	Hough	D'Appolonia	Peck and Bazzara	Burland and Burbridge
Count	20	20	20	20	20
Minimum	0.295	0.656	0.311	0.202	0.138
Maximum	4.618	4.294	2.176	4.000	4.735
μ	1.381	1.971	1.031	0.779	0.829
σ	1.006	0.769	0.476	0.796	0.968
CV	0.729	0.390	0.462	1.022	1.168

Note: μ = Mean; σ = Standard Deviation; CV = Coefficient of Variation ($=\sigma/\mu$)

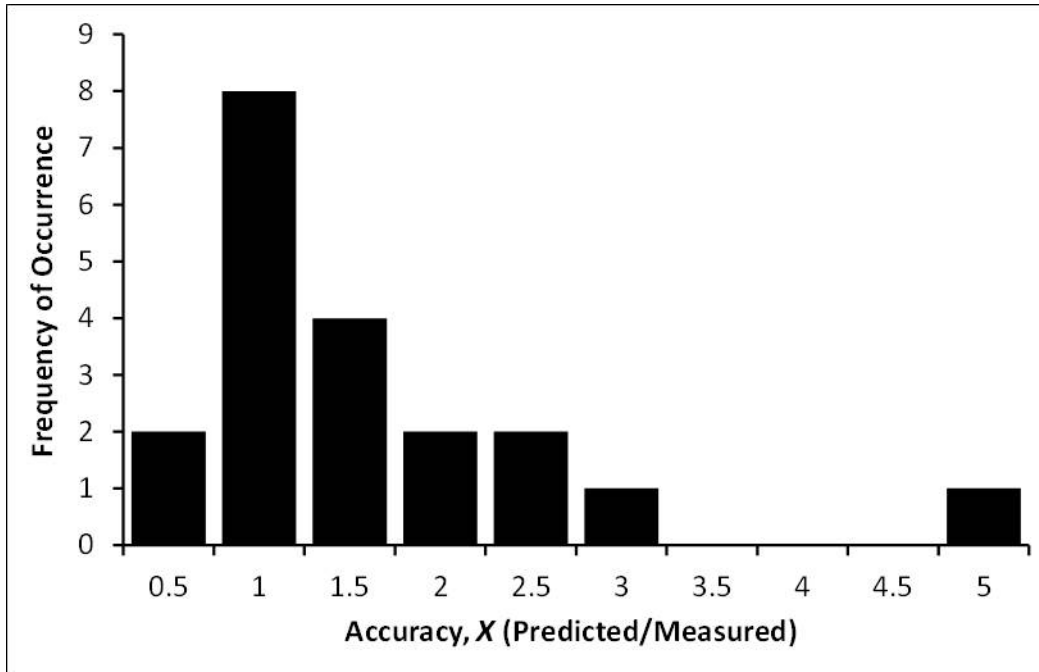
As noted earlier, accuracy ($X = S_P/S_M$) is a random variable that can be modeled by an appropriate PDF. The data for X in Table 9-3 were used to develop histograms.

The histograms of the data for X taken from Columns 2 to 6 of Table 9-3 are shown in Figures 9-2a to 9-6a, respectively. None of the histograms resemble a classical bell shape characteristic of normally distributed data. Nonnormal distributions would be more appropriate in these cases. To evaluate the deviation of the data from a classical normal PDF, the data for the value of accuracy (X) in Table 9-3 were plotted against the standard normal variable (z) to generate CDFs, as shown in Figures 9-2b to 9-6b. See Allen, et al. (2005, Chapter 5) for definition of z and procedures to develop lower graphs (b) in Figures 9-2 to 9-6. The beneficial attributes of this probability plot are discussed in Allen et al. (2005). As Figures 9-2b to 9-6b show, the data points based on Table 9-3 do not plot on the straight line, which confirms the observation of nonnormal distributions made based on the histograms in Figures 9-2a to 9-6a.

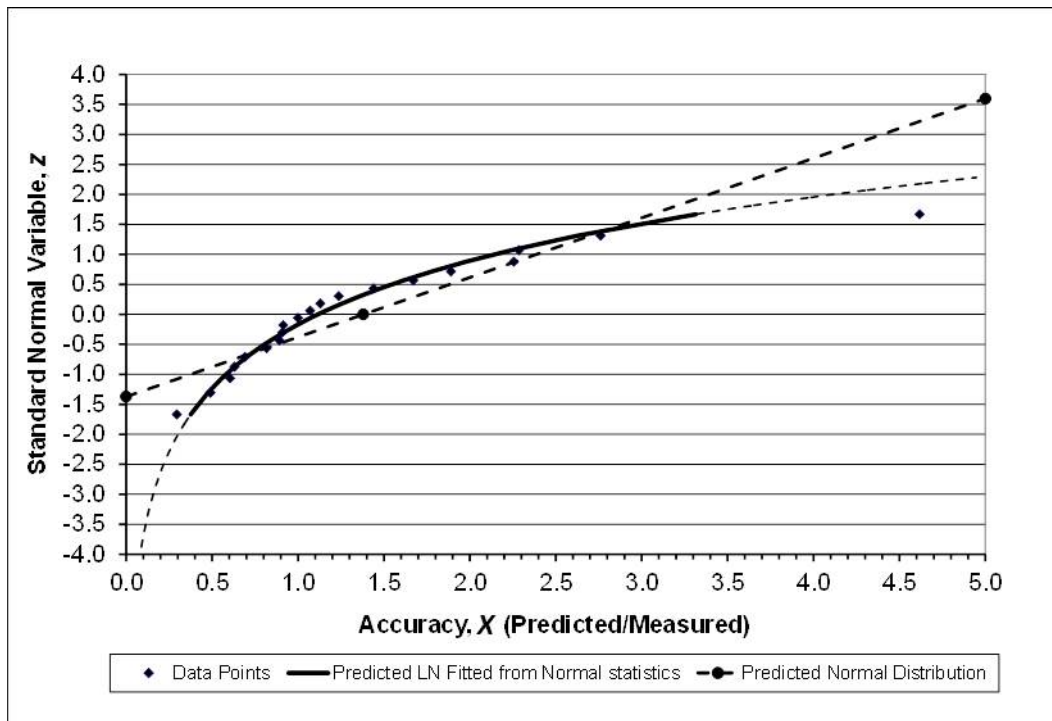
By using procedures described in Allen, et al. (2005), a lognormal distribution is used to evaluate the nonnormal data. As seen in Figures 9-2b to 9-6b, the lognormal distribution fits the data better than the normal distribution. The lognormal distribution, which is valid between values of 0 and $+\infty$, is used in these figures because (a) immediate settlement cannot have negative values, and (b) lognormal PDFs have been used in the past for nonnormal distributions during calibration of the strength limit state for geotechnical, as well as structural, features in the *AASHTO LRFD* framework. For foundation deformations, a PDF with an upper bound and lower bound (beta distribution) instead of open tail(s) (normal or lognormal distribution) may be more appropriate because the conditions represented by an open-tail PDF are not physically possible when one considers foundation deformations. As noted, the lognormal PDF is used here to be consistent with the PDFs that have been used in the LRFD calibration processes to-date. Guidance for the selection of an appropriate PDF and development of the distribution parameters shown in Table 9-5 is provided in Nowak and Collins (2013) or other similar books that deal with probabilistic methods.

Values of the lognormal mean and lognormal standard deviation are needed to use the lognormal PDF. These values can be obtained by using correlations with the mean and standard deviation values for normal distribution or calculated directly from the natural logarithm (\ln) of the values of the data points. Table 9-5 presents the values for correlated mean (μ_{LNC}) and correlated standard deviation (σ_{LNC}). Table 9-6 shows the lognormal of accuracy values of data in Table 9-3, and Table 9-7 presents the values for arithmetic mean (μ_{LNA}) and arithmetic standard deviation (σ_{LNA}) based on the $\ln(X)$ values in Table 9-6.

Figure 9-2: Schmertmann method: (a) histograms for accuracy (X), and (b) plot of standard normal variable (z) as a function of the X

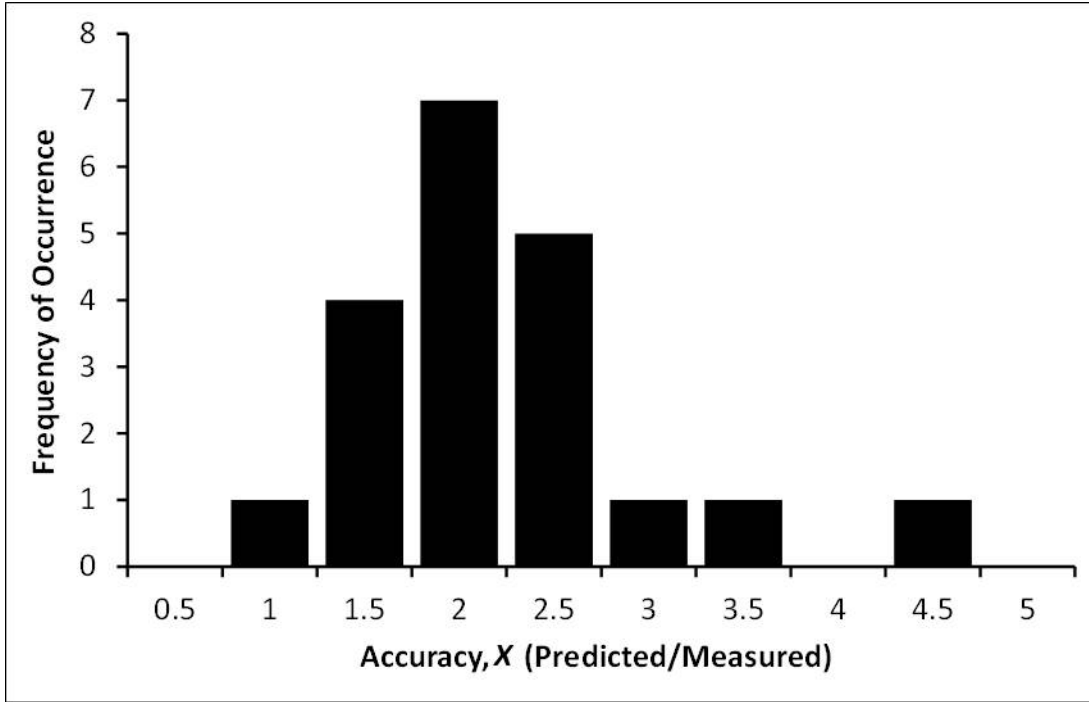


(a)

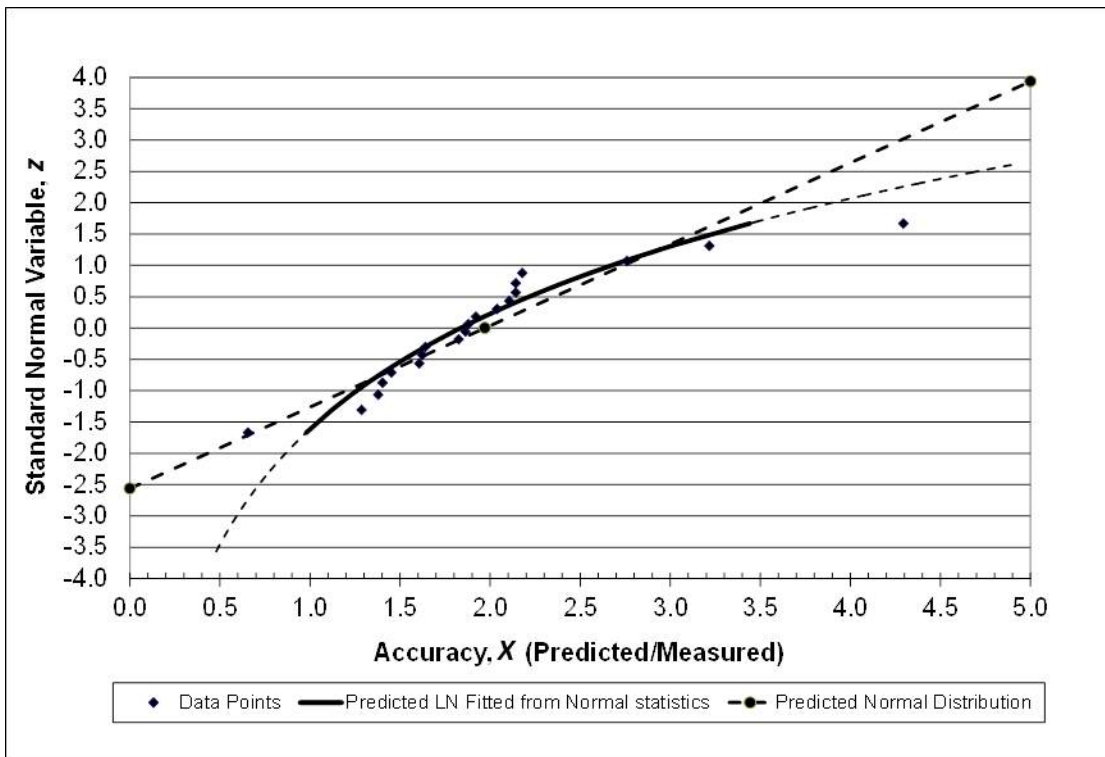


(b)

Figure 9-3: Hough method: (a) histograms for accuracy (X), and (b) plot of standard normal variable (z) as a function of the X

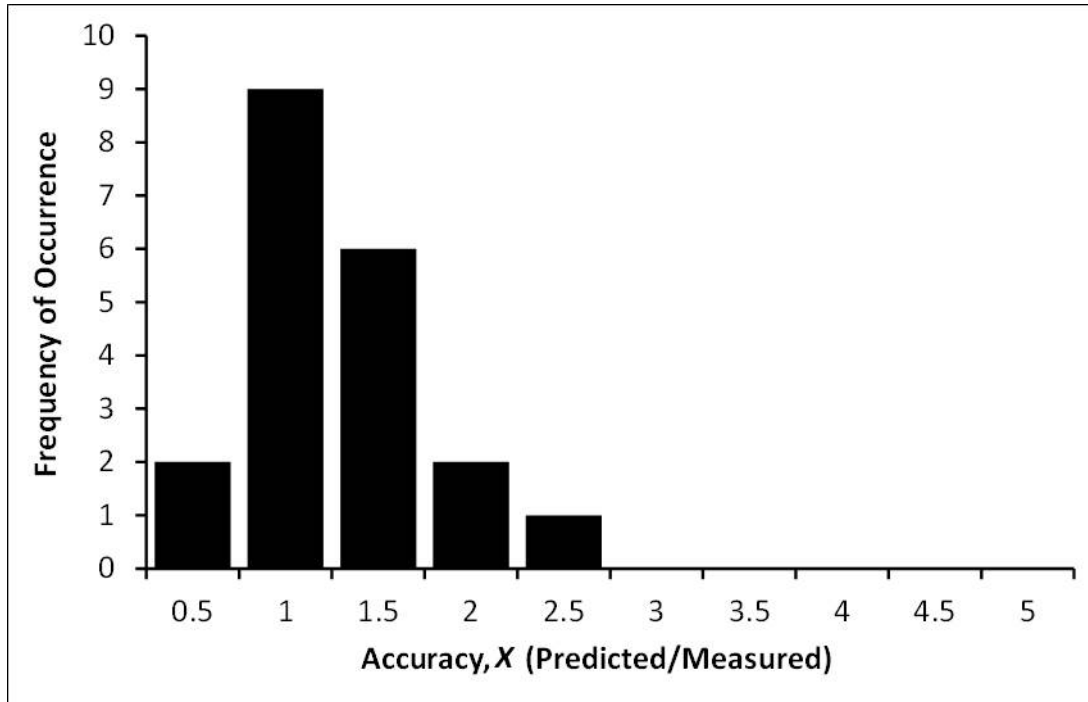


(a)

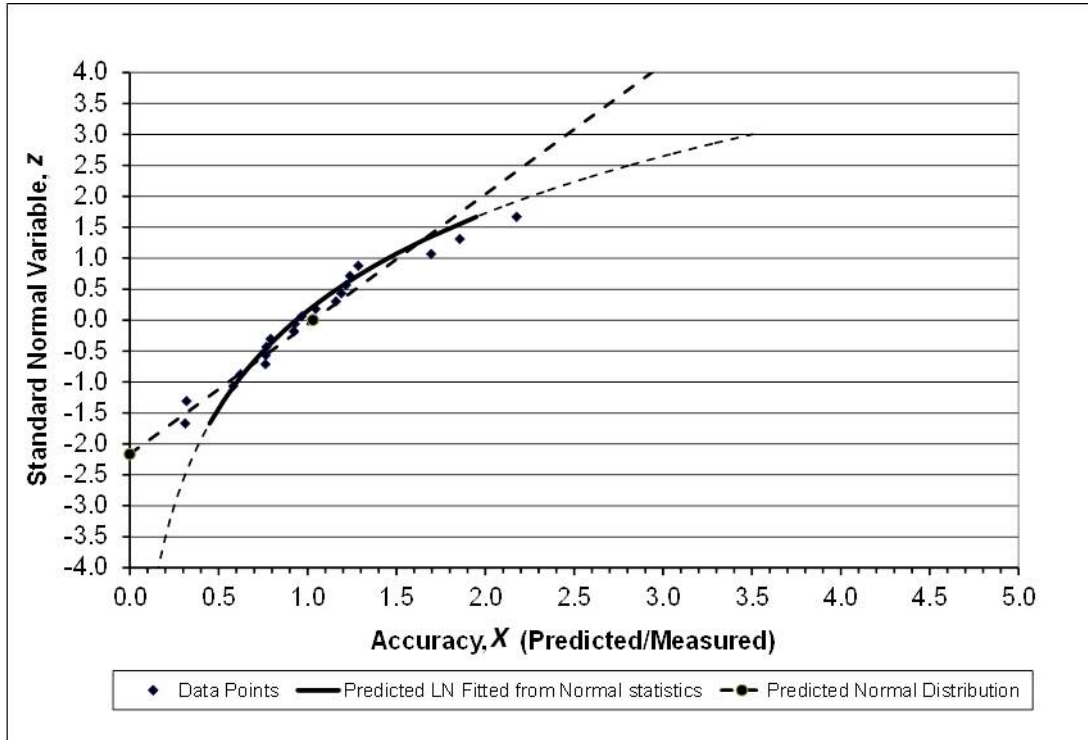


(b)

Figure 9-4: D'Appolonia method: (a) histograms for accuracy (X), and (b) plot of standard normal variable (z) as a function of the X

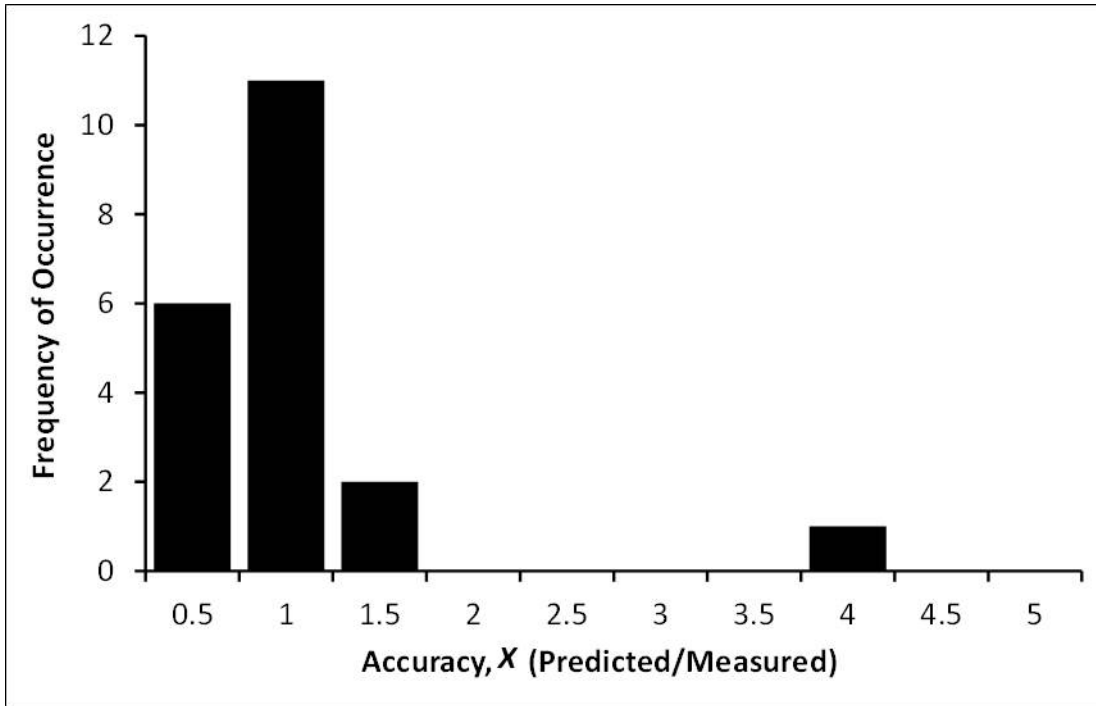


(a)

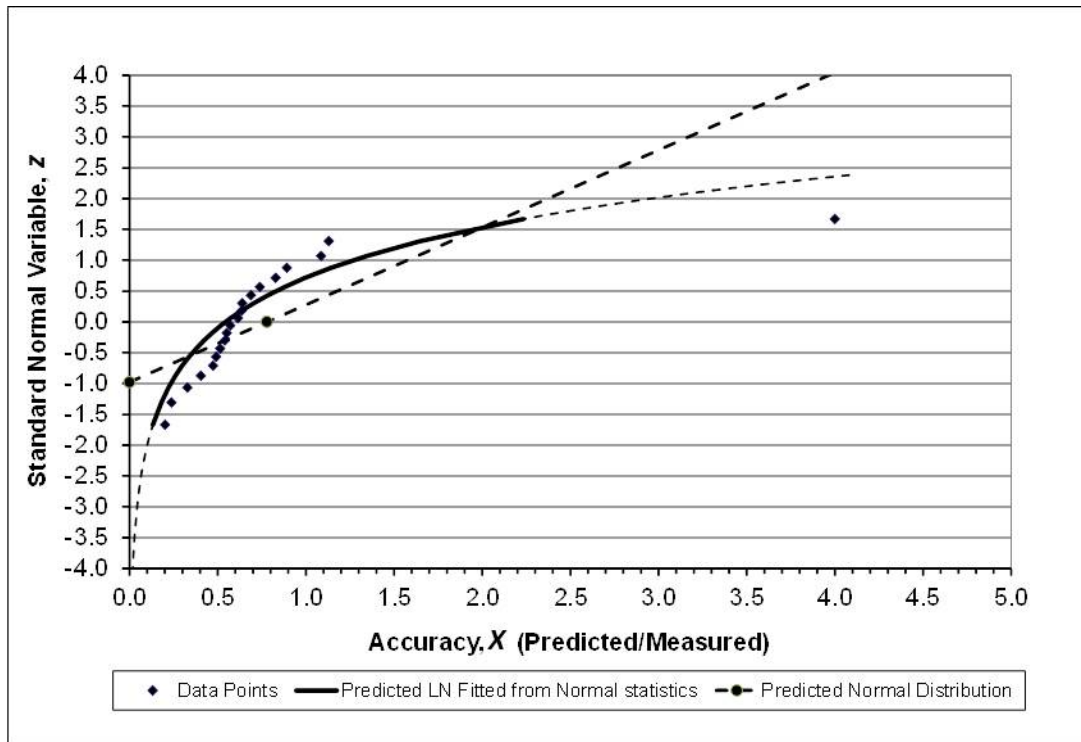


(b)

Figure 9-5: Peck and Bazarra method: (a) histograms for accuracy (X), and (b) plot of standard normal variable (z) as a function of the X

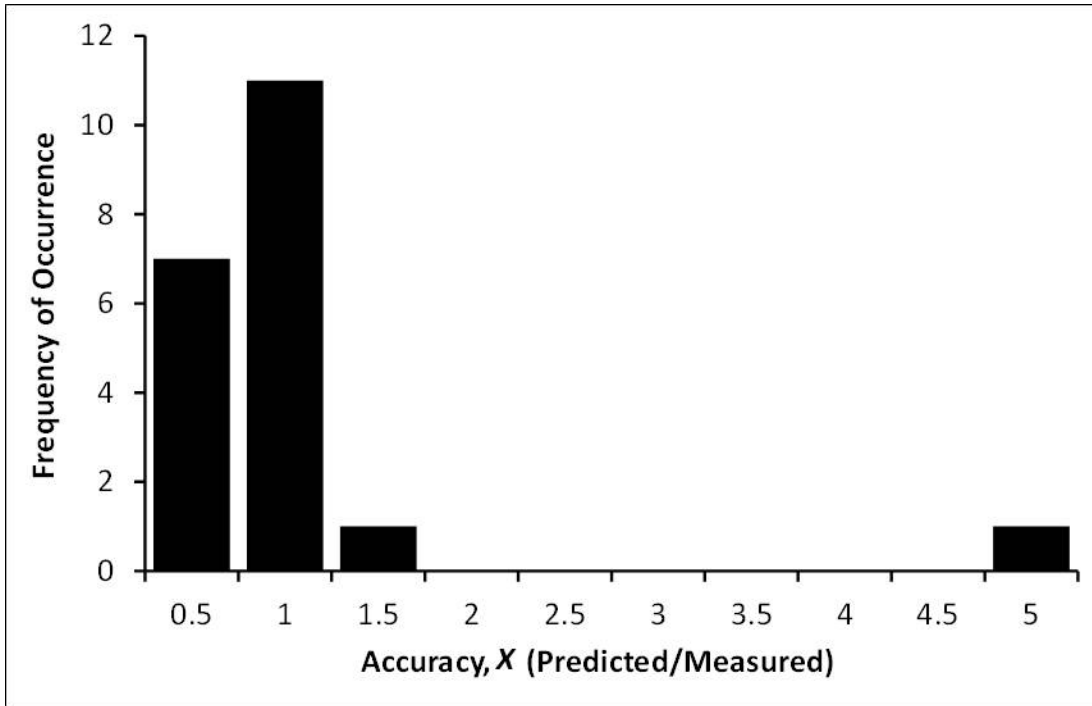


(a)

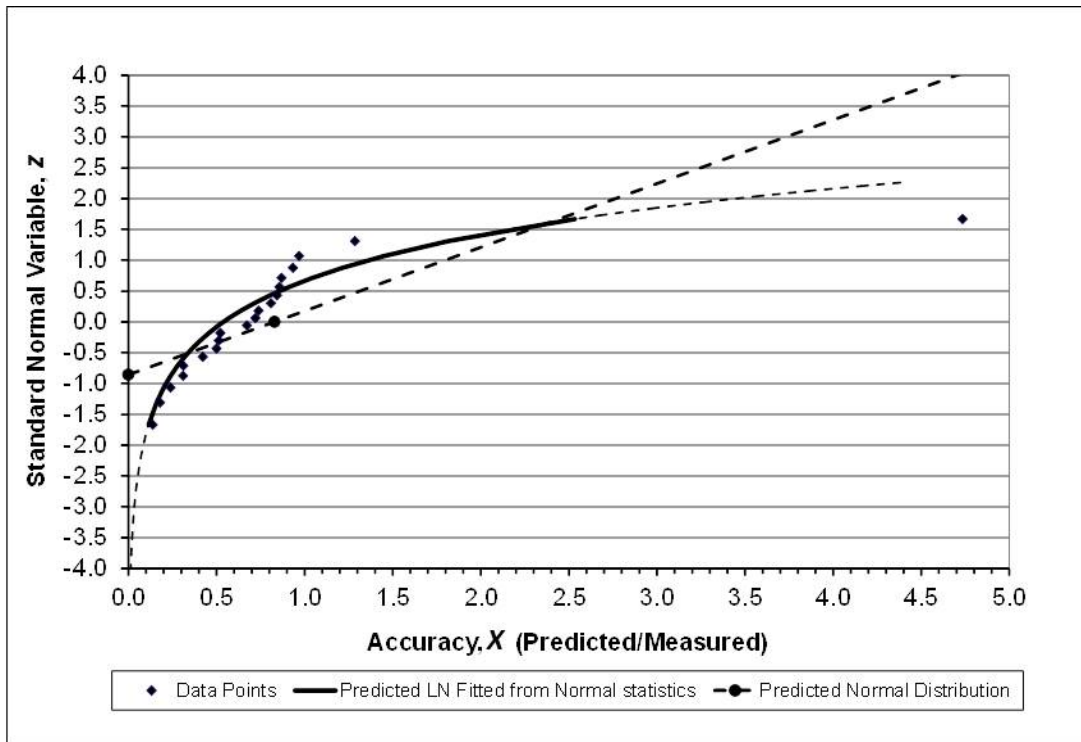


(b)

Figure 9-6: Burland and Burbridge method: (a) histograms for accuracy (X), and (b) plot of standard normal variable (z) as a function of the X



(a)



(b)

Table 9-5: Correlated Statistics of Accuracy (X) for Lognormal PDFs

Statistic	Schmertmann	Hough	D'Appolonia	Peck and Bazzara	Burland and Burbridge
μ_{LNC}	0.1095	0.6076	-0.0665	-0.6078	-0.6177
σ_{LNC}	0.6528	0.3766	0.4398	0.8459	0.9274

Note: The correlated mean (μ_{LNC}) and standard deviation (σ_{LNC}) values for lognormal distribution were calculated from the normal (arithmetic) mean (μ) and standard deviation (σ) values in Table 9-4, respectively, by using the following equations based on idealized normal and lognormal PDFs:

$$\mu_{LNC} = \ln(\mu) - 0.50(\sigma_{LNC})^2; \sigma_{LNC} = [\ln\{(\sigma/\mu)^2 + 1\}]^{0.5}$$

Table 9-6: Lognormal of Accuracy Values [ln(X)] Based on Data Shown in Table 9-3

Site	Schmertmann	Hough	D'Appolonia	Peck and Bazzara	Burland and Burbridge
#1	0.8141	0.7621	0.6190	-0.1881	-0.1542
#2	1.0157	0.3386	-0.5411	-1.4321	-1.7198
#3	-0.0889	0.2525	-1.1421	-1.5989	-1.9783
#4	-0.5021	0.6529	-0.2703	-0.7472	-0.6672
#5	-0.7097	0.4741	-0.4733	-0.3732	-0.0678
#6	0.2136	0.3732	0.1744	-0.9045	-0.2113
#7	-1.2205	-0.4220	-1.1664	-0.7097	-1.1664
#8	0.0690	0.7621	-0.0741	-0.5596	-0.6931
#9	-0.3677	0.7122	-0.2624	-0.4855	-0.8602
#10	0.0000	0.3216	-0.2318	-0.5947	-1.1701
#11	0.3646	0.6313	0.1484	-0.4463	-1.4271
#14	-0.1151	1.0155	0.2144	0.0834	-0.1398
#15	1.5299	1.4572	0.7777	1.3863	1.5550
#16	0.1226	1.1686	0.5281	-0.3023	-0.3023
#17	-0.0953	0.6225	0.0445	-0.4520	-0.6487
#20	0.6369	0.4951	-0.2671	-1.1144	-0.1699
#21	-0.4613	0.6022	0.1967	0.1226	-0.3947
#22	-0.2007	0.7448	-0.0788	-0.6633	-0.0308
#23	0.5141	0.4842	-0.0333	-0.6144	-0.3267
#24	0.8267	0.7787	0.2513	-0.1133	0.2513

Table 9-7: Statistics of $\ln(X)$ Values Based on Data Shown in Table 9-6

Statistic	Schmertmann	Hough	D'Appolonia	Peck and Bazzara	Burland and Burbridge
Count	20	20	20	20	20
Minimum	-1.2205	-0.4220	-1.1664	-1.5989	-1.9783
Maximum	1.5299	1.4572	0.7777	1.3863	1.5550
μ_{LNA}	0.1173	0.6114	-0.0793	-0.4854	-0.5161
σ_{LNA}	0.6479	0.3807	0.5029	0.6226	0.7731

Note: μ_{LNA} = arithmetic mean of $\ln(X)$ values;
 σ_{LNA} = arithmetic standard deviation of $\ln(X)$ values

The correlated and the arithmetic values of the mean (μ_{LNC} and μ_{LNA} , respectively) and standard deviation (σ_{LNC} and σ_{LNA} , respectively) for lognormal distributions are not equal. This is because the correlated values were based on derivations for an idealized lognormal distribution and not a sample distribution from actual data, which may not necessarily fit an idealized lognormal distribution. In contrast, the arithmetic values are obtained by taking the arithmetic mean and standard deviation directly from the $\ln(X)$ value of each data point noted in Column 2 to 6 of Table 9-3.

It is important to use the appropriate values of mean and standard deviation based on the syntax for a lognormal distribution function used by a particular computational program. For example, if one is using the @RISK program by Palisade Corporation, then the RISKLOGNORM function in that program is based on arithmetic values (μ and σ) of the normal distribution. In contrast, the Microsoft Excel LOGNORMDIST (or LOGNORM.DIST) function uses the arithmetic mean (μ_{LNA}) and standard deviation (σ_{LNA}) values of $\ln(X)$. Use of improper values of mean and standard deviation can lead to drastically different results. This issue is of critical importance because calibration in this report, as mentioned earlier, is based on Microsoft Excel.

Figure 9-7 shows the CDFs for Accuracy, X , for various analytical methods based on use of the LOGNORM.DIST function in 2010 version of Microsoft Excel using the μ_{LNA} and σ_{LNA} values noted in Table 9-7. These CDFs can now be used to develop the PEC discussed in chapter 8.3.5 for various analytical methods.

Figure 9-7: Cumulative Distribution Functions (CDFs) for various analytical methods for estimation of immediate settlement of spread footings.

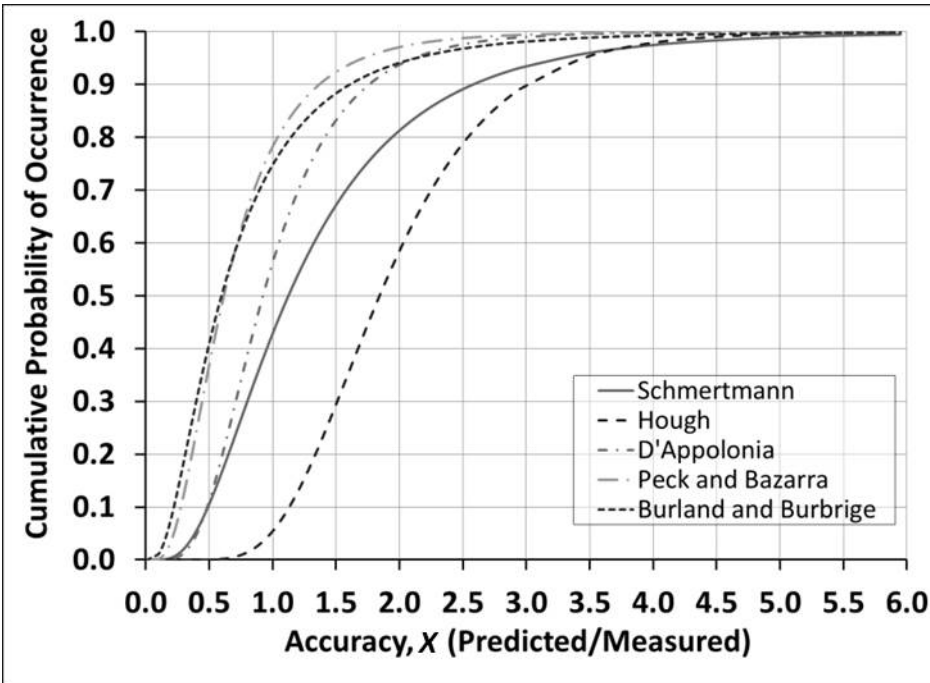
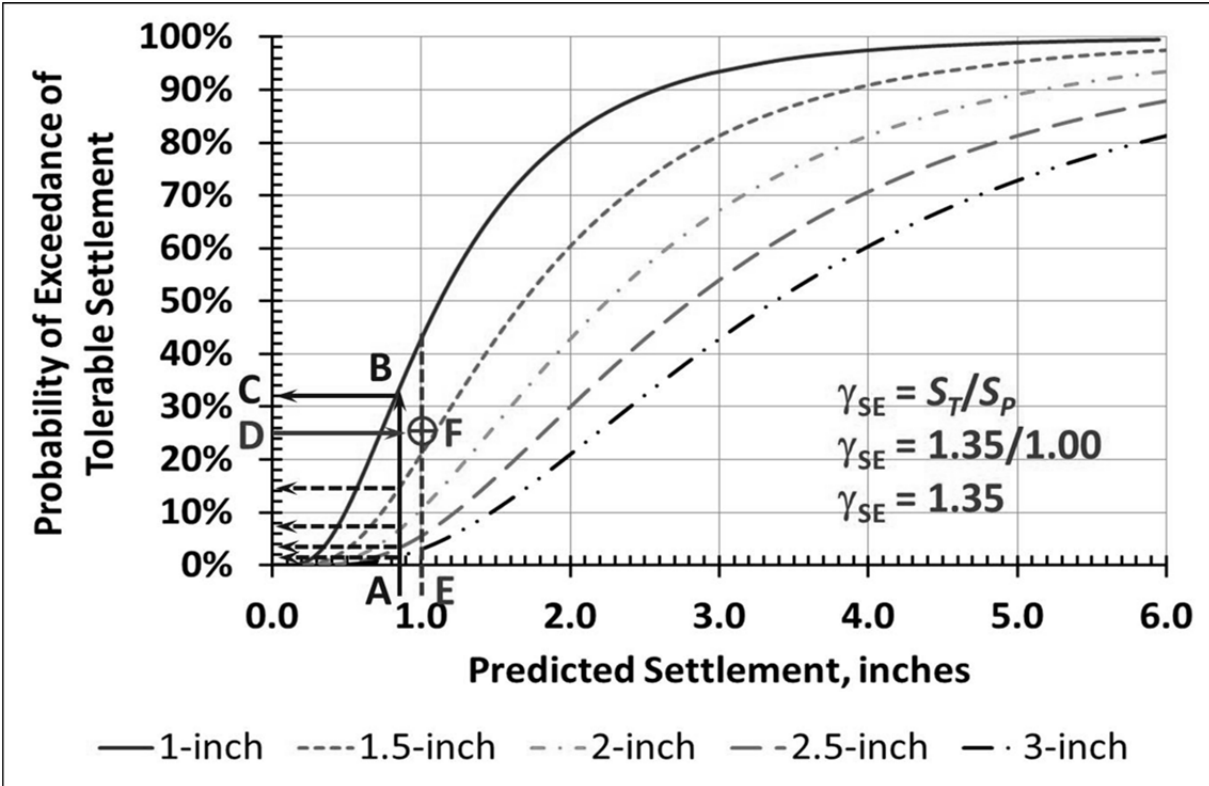


Figure 9-8 shows the PEC for method by Schmertmann, et al. (1978). This figure was developed by scaling (multiplying) the accuracy values for Schmertmann in Figure 9-7, by dimensional values of S_T , i.e., $S_T = 1$ in., 2 in., and so on. For example, Figure 9-7 indicates a cumulative probability of about 0.8 for an accuracy of 2.0. In Figure 9-8 if the values of S_p/S_T is multiplied by $S_T = 2.0$, the result is a value of $S_p = 4.0$ at a cumulative probability of 0.8 which is now shown as a percentage called probability of exceedance of about 80%. Using this procedure, the probability of exceedance corresponding to a given predicted settlement can now be readily determined. For example, assume that the geotechnical engineer has predicted a settlement of 0.85 in. The probability of exceedance of 1 in. in this case is approximately 32 percent. This can be found by drawing line AB, finding the intersection of the line with the curve for 1 in., drawing line BC, and reading the value from the ordinate of the PEC in Figure 9-8. Four additional curves for settlements of 1.5, 2, 2.5, and 3 in. are shown in Figure 9-8. Using the procedure demonstrated for the example above (see dashed arrows in Figure 9-8), if the predicted (calculated) value is 0.85 in., then the probability of the measured value being greater than 1.5, 2, 2.5, and 3 in. is approximately 14 percent, 6 percent, 3 percent, and 2 percent, respectively.

Figure 9-8: PEC for Schmertmann method



A load factor for settlement, γ_{SE} , can be determined using the procedure in chapter 8.3.5. For example, assume the predicted settlement is 1 in. To determine the value of γ_{SE} for a 25 percent target probability of exceedance (P_{eT}) draw a horizontal line from Point D on the ordinate corresponding to a value of 25 percent. Next, draw a vertical line from Point E on the abscissa corresponding to a value of 1 in. Locate the point of intersection, F, which lies between the curves for 1 in. and 1.5 in. Interpolating between the two curves leads to a value of approximately 1.35 in. Based on the definition of γ_{SE} noted above, the value of γ_{SE} is equal to 1.35 in./1.0 in., or 1.35.

PECs for other analytical methods noted in Figure 9-7 are given in Figures 9-9 to 9-12. Those PECs can be used in a similar manner as demonstrated for the PEC for the Schmertmann method.

Figure 9-9: PEC for Hough method

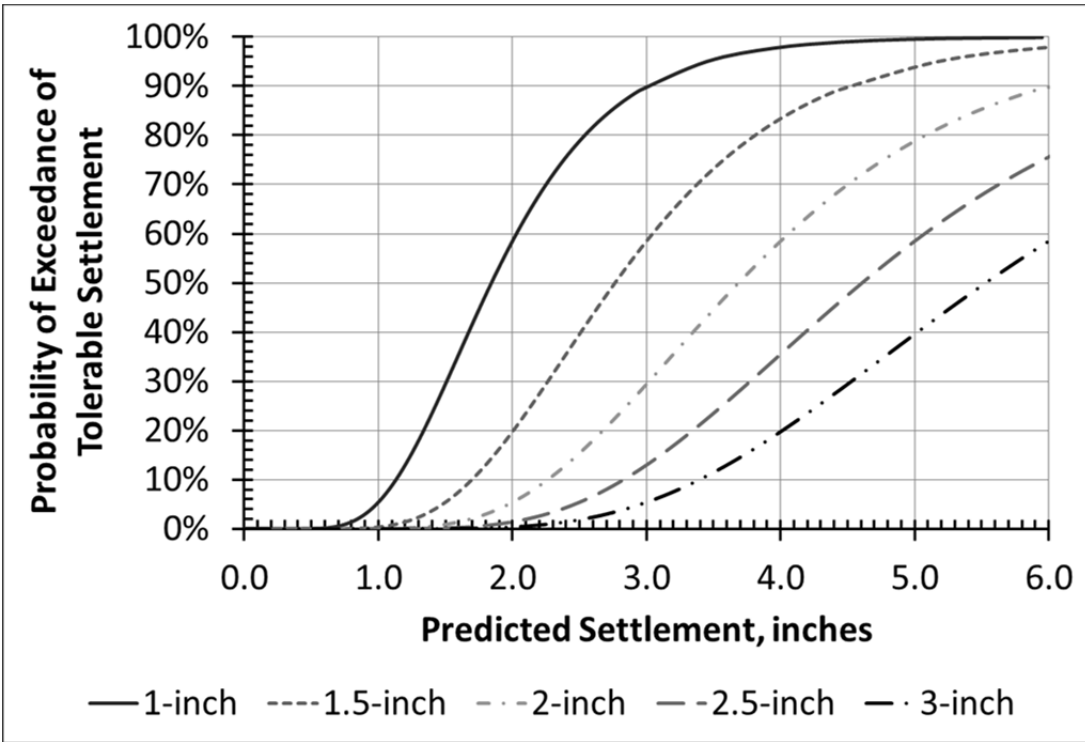


Figure 9-10: PEC for D'Appolonia method

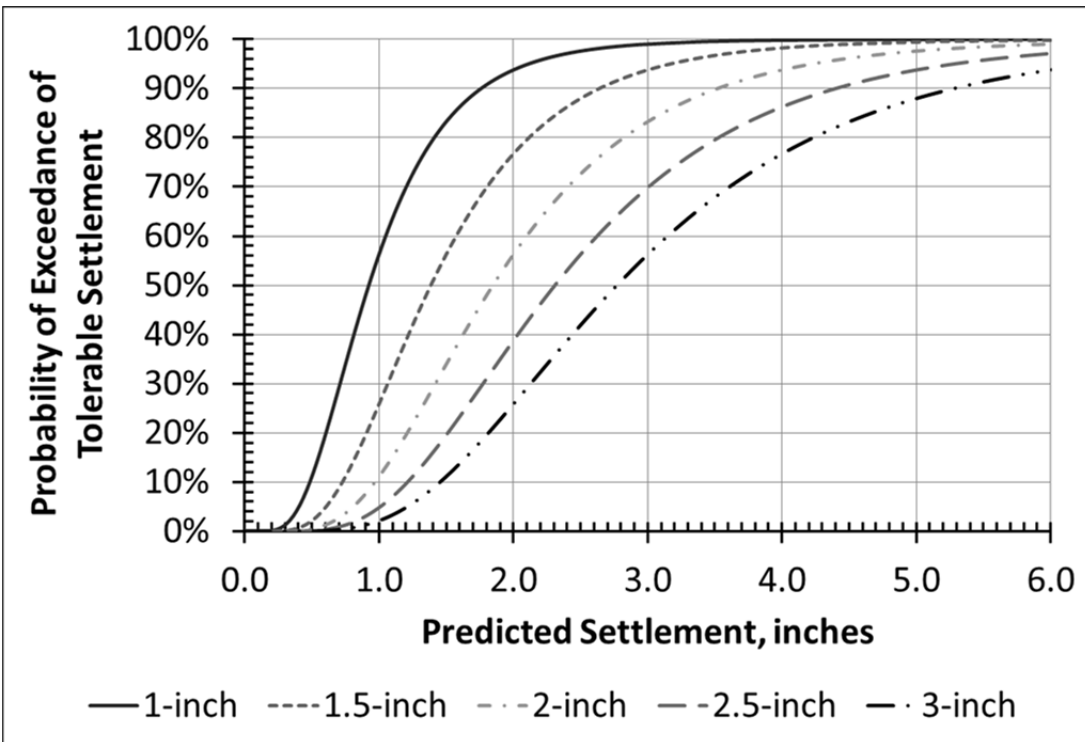


Figure 9-11: PEC for Peck and Bazarra method

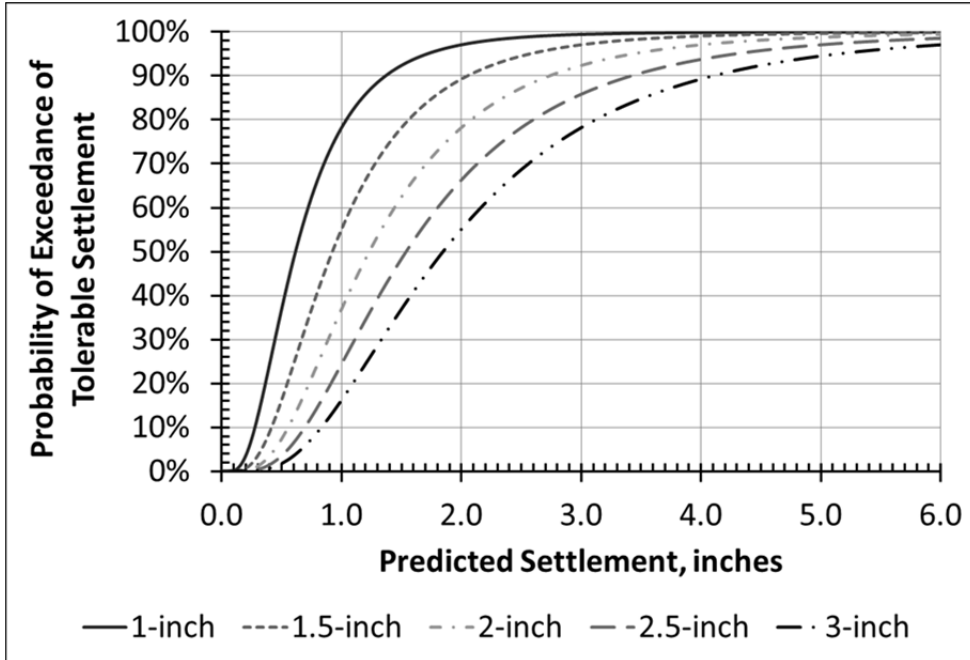
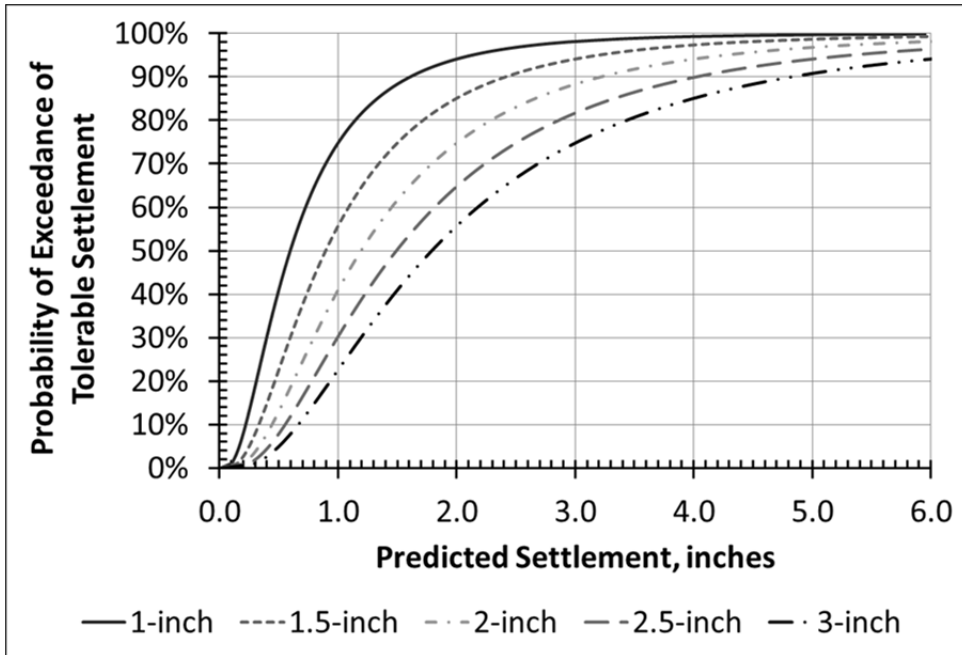


Figure 9-12: PEC for Burland and Burbridge method



9.2.5 Step 5: Apply the Reliability Analysis Procedure

The estimation of load factor for settlement, γ_{SE} , in terms of probability of exceedance was demonstrated in the previous step. In *AASHTO LRFD* framework, calibrations are expressed in terms of reliability index (β). β can be expressed in terms of P_e of a predicted value by using Equation 9-3, which applies to normally distributed data. As observed from Step 4, lognormal distributions have been used. Furthermore, the CV values noted in Table 9-4 are large. For a normal random variable, the relationship between β and P_e depends only on the CV (one parameter) but for a lognormal distribution, it depends on the mean and standard deviation, or the mean and CV (two parameters). Therefore, the reliability index should be based on lognormal function. However, for $\beta < 2.0$ there is not a significant practical difference in the P_e values for data that are normally or lognormally distributed for a wide range of CVs noted in Table 9-4. An assumption of a normal distribution is generally conservative in the sense that for a given β it gives a larger P_e compared to a lognormal distribution. Furthermore, the normal distribution has been conventionally been assumed for strength limit states in *AASHTO LRFD* (as well as other international codes), which have reliability index values larger than 2.0. The key consideration is that the type of distribution is not as important as being consistent and not mixing different distributions while comparing β values. Based on these considerations, use of the Microsoft Excel formula in Equation 9-3 that assumes normally distributed data is considered to be acceptable for service limit state calibrations.

Table 9-8 and Figure 9-13 were generated by using Equation 9-3:

$$\beta = \text{NORMSINV}(1-P_e) \quad (9-3)$$

The correlation between β and P_e , can now be used to rephrase the discussion earlier with respect to Figure 9-8. In that discussion, as an example, it was assumed that the geotechnical engineer has predicted a settlement of 0.85 in. From Figure 9-8, it was determined that the probability of exceedance of 1, 1.5, 2, 2.5, and 3 in was approximately 32 percent, 14 percent, 6 percent, 3 percent, and 2 percent, respectively. Using Table 9-8 (or Figure 9-13 or Equation 9-3), the results can now be expressed in terms of reliability index values. If the predicted settlement is 0.85 in. then the assumption of tolerable settlement values of 1, 1.5, 2, 2.5, and 3 in. means a reliability index of approximately 0.45, 1.10, 1.55, 1.90, and > 2.00 in., respectively.

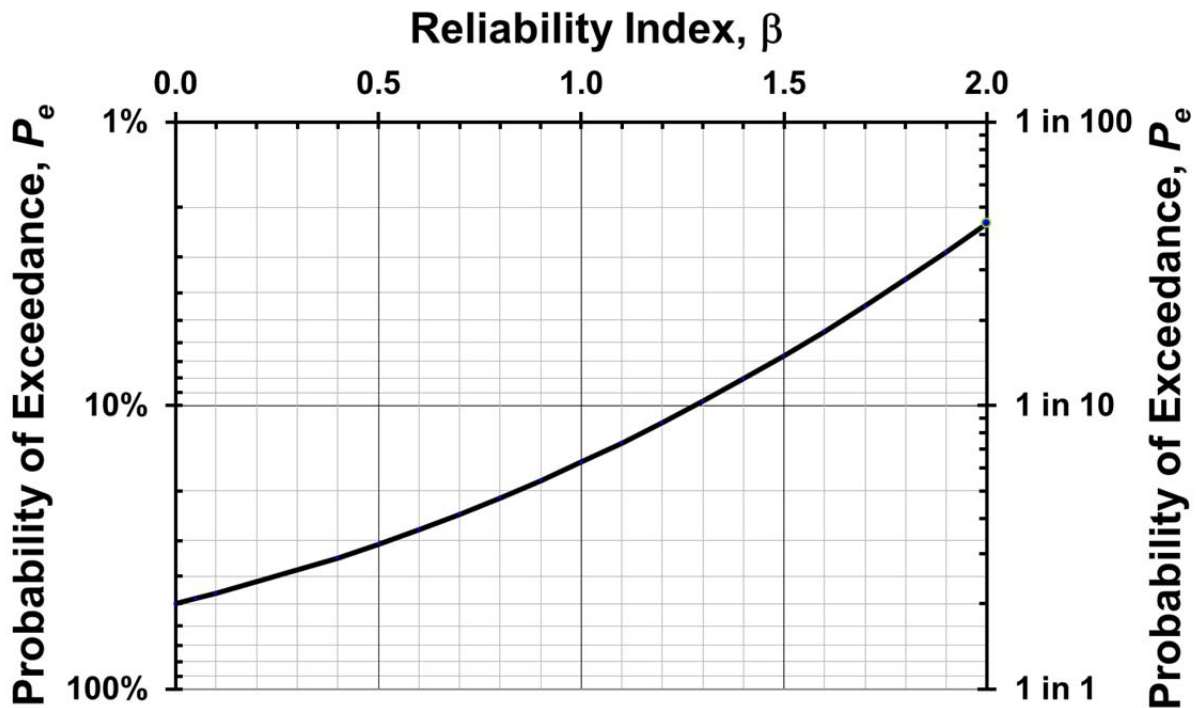
The following example demonstrates the determination of γ_{SE} in terms of β by using Microsoft Excel.

Table 9-8: Values of β and Corresponding P_e Based on Normally Distributed Data

β	P_e , %	β	P_e , %	β	P_e , %	β	P_e , %	
2.00	2.28	1.50	6.68	1.00	15.87	0.50	30.85	
1.95	2.56	1.45	7.35	0.95	17.11	0.45	32.64	
1.90	2.87	1.40	8.08	0.90	18.41	0.40	34.46	
1.85	3.22	1.35	8.85	0.85	19.77	0.35	36.32	
1.80	3.59	1.30	9.68	0.80	21.19	0.30	38.21	
1.75	4.01	1.25	10.56	0.75	22.66	0.25	40.13	
1.70	4.46	1.20	11.51	0.70	24.20	0.20	42.07	
1.65	4.95	1.15	12.51	0.65	25.78	0.15	44.04	
1.60	5.48	1.10	13.57	0.60	27.43	0.10	46.02	
1.55	6.06	1.05	14.69	0.55	29.12	0.05	48.01	
							0.00	50.00

Note: Linear interpolation may be used as an approximation for intermediate values

Figure 9-13: Relationship between β and P_e for the case of a single load and single resistance



Example: The geotechnical engineer has predicted settlement $S_p = 0.85$ in. using the Schmertmann method. The owner has specified that the SLS design for the bridge shall be performed using a reliability index (β) of 0.50. What is the value of γ_{SE} and the tolerable settlement that the bridge designer should use?

Solution: The load factor, γ_{SE} , is a function of the probability of exceedance, P_e , of the foundation deformation under consideration, which in this example is the immediate settlement of spread footings calculated by using the analytical method of Schmertmann. Based on either Equation 9-3 or Table 9-8, a value of $P_e \approx 0.3085$ (or 30.85%) is obtained for $\beta = 0.50$.

Equation 9-4 is the formula used in Microsoft Excel to determine a value of accuracy (X) in terms of P_e , the mean value (μ_{LNA}), and the standard deviation (σ_{LNA}) of the lognormal distribution function as computed in Step 4. The value of X represents the probability of the accuracy value (S_p/S_T) being less than a specified value.

$$P_e = \text{LOGNORMDIST}(X, \mu_{LNA}, \sigma_{LNA}) \quad (9-4)$$

From Table 9-7, for the Schmertmann method, $\mu_{LNA} = 0.1173$, $\sigma_{LNA} = 0.6479$. The goal is to determine the value of X that gives $P_e = 0.3085$. For this example, the expression for P_e can be written as follows:

$$P_e = \text{LOGNORMDIST}(X, 0.1173, 0.6479) = 0.3085 \text{ or } 30.85\% \quad (9.5)$$

Using Goal Seek in Microsoft Excel, X (i.e., S_p/S_T) ≈ 0.813 . Note that in the 2010 version of Microsoft Excel, another function LOGNORM.DIST is also available that can be used. In this case, the same result ($X \approx 0.813$) is obtained by using the following syntax and using the Goal Seek function to determine X ("TRUE" indicates the use of a CDF):

$$P_e = \text{LOGNORM.DIST}(X, 0.1173, 0.6479, \text{TRUE}) = 0.3085$$

In the context of the AASHTO LRFD framework, the load factor, γ_{SE} , is the reciprocal of X . For immediate settlement of spread footings based on the method of Schmertmann, $\gamma_{SE} = 1/0.813 \approx 1.23$.

As per the AASHTO LRFD framework, the load factor is rounded-up to the nearest 0.05; therefore, $\gamma_{SE} = 1.25$ should be used.

In the bridge design example, the bridge designer should use a settlement value of $(\gamma_{SE})(S_p) = (1.25)(0.85 \text{ in.}) = 1.06$ in. to assess the effect of settlement on the bridge structure. This value can also be obtained using the graphic technique explained earlier with respect to Figure 9-8. The example that was demonstrated with respect to Figure 9-8, also assumed a tolerable settlement of 0.85 in., where it was found that a settlement of 1 in. would imply a 32 percent

probability of exceedance. These values are close to the value of 1.06 in. for a 30.85 percent probability of exceedance obtained here. Given that the load factor is rounded to the nearest 0.05, the result from the graphic technique is sufficiently accurate.

The procedure demonstrated in the above example can be used to develop the values of γ_{SE} for any desired β using the lognormal distribution of X for method of Schmertmann. A similar approach can be used for other analytical methods and distributions.

Table 9-9 presents the values of γ_{SE} results for various analytical methods shown in Figure 9-1 and Table 9-2. Note γ_{SE} values less than 1.0 should not be allowed to prevent the risk of bridges being underdesigned. Furthermore, the values of γ_{SE} should be rounded to the nearest 0.05 because not doing so implies a level of confidence that is not justified by the available data. Table 9-10 presents values of γ_{SE} that are bounded by 1.0 and rounded to the nearest 0.05.

Table 9-9: Computed Values of γ_{SE} for Various Methods to Estimate Immediate Settlement of Spread Footings on Cohesionless Soils

Reliability Index, β	Values of γ_{SE}				
	Schmertmann	Hough	D'Appolonia	Peck and Bazzara	Burland and Burbridge
0.00	0.89	0.54	1.08	1.62	1.68
0.50	1.23	0.66	1.39	2.22	2.47
1.00	1.70	0.79	1.79	3.03	3.63
1.50	2.35	0.96	2.30	4.13	5.34
2.00	3.25	1.16	2.96	5.64	7.86
2.50	4.49	1.41	3.81	7.71	11.58
3.00	6.21	1.70	4.89	10.52	17.04
3.50	8.59	2.06	6.29	14.36	25.08

Table 9-10: Proposed Values of γ_{SE} for Various Methods to Estimate Immediate Settlement of Spread Footings on Cohesionless Soils

Reliability Index, β	Values of γ_{SE}				
	Schmertmann	Hough	D'Appolonia	Peck and Bazzara	Burland and Burbridge
0.00	1.00	1.00	1.10	1.60	1.70
0.50	1.25	1.00	1.40	2.20	2.45
1.00	1.70	1.00	1.80	3.05	3.65
1.50	2.35	1.00	2.30	4.15	5.35
2.00	3.25	1.15	2.95	5.65	7.85
2.50	4.50	1.40	3.80	7.70	11.60
3.00	6.20	1.70	4.90	10.50	17.05
3.50	8.60	2.05	6.30	14.35	25.10

Notes: The values of γ_{SE} have been rounded to the nearest 0.05. The values of γ_{SE} have been limited to 1.00 or larger.

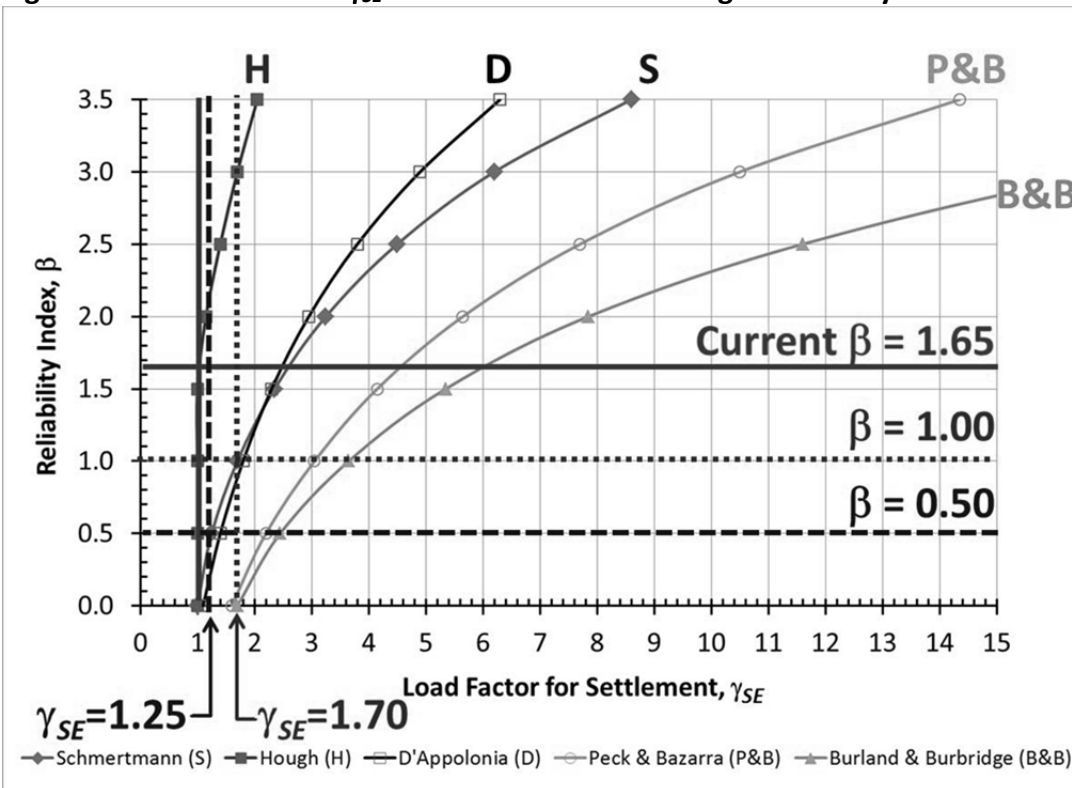
9.2.6 Step 6: Review the Results and Selection of Load Factor for Settlement, γ_{SE}

Figure 9-14 shows a plot of γ_{SE} versus β based on the data shown in Table 9-10. The current practice based on *AASHTO LRFD* is as follows:

1. Use the Hough method to estimate immediate settlements
2. Use $\gamma_{SE} = 1.0$.

The data in Table 9-10 and the graph in Figure 9-14 imply that $\beta \approx 1.65$ corresponds to current practice noted above. $\beta \approx 1.65$ is based on the data set in Table 9-2. If additional data were included, or if a different regional data set was to be used then the value of β may be different. However, based on a review of state practices performed as part of Samtani and Nowatzki (2006) and Samtani, et al. (2010), it is anticipated that, based on its inherent conservatism, the value of β is anticipated to be large and greater than 1.0 for Hough method and $\gamma_{SE} = 1.0$. The majority of the data points for Hough method plot below $\gamma_{SE} = 1.0$ which suggests a significant conservatism in the Hough method. This is consistent with the earlier observation that the Hough method is conservative (overpredicts) by a factor of approximately two (see Table 9-4), which leads to unnecessary use of deep foundations instead of spread footings.

Figure 9-14: Evaluation of γ_{SE} based on current and target reliability indices



Based on a consideration of reversible and irreversible limit states for bridge superstructures, as shown earlier, a target reliability index (β_T) in the range of 0.50 to 1.00 for calibration of load factor γ_{SE} for foundation deformation limit state is acceptable. Settlement is clearly an irreversible limit state with respect to the foundation elements but may be reversible through intervention with respect to the superstructure. This type of logic would lead to consideration of 0.50 as the target reliability index for calibration of immediate settlements under spread footings on cohesionless soils.

In Figure 9-14, the horizontal bold dashed line corresponds to $\beta = 0.50$ for SLS evaluation. For $\beta = 0.50$, if a $\gamma_{SE} = 1.25$ is adopted, then it would encompass 3 of the 5 methods. The value of $\gamma_{SE} = 1.25$ includes the Schmertmann method, which is currently recommended by Samtani and Nowatzki (2006) and Samtani, et al. (2010) and is commonly used in US practice. Based on these observations, a $\gamma_{SE} = 1.25$ is recommended. Using similar approach, for $\beta = 1.00$, a $\gamma_{SE} = 1.70$ can be adopted.

9.2.7 Step 7: Select Value of γ_{SE}

Table 9-11 shows the target reliability index, β_T , values for various structural limit states based on the work done as part of SHRP2's *Service Limit State Design for Bridges* and the discussions as part of proposed ballot items by AASHTO SCOBS meetings. Table 9-11 shows reliability index values much smaller than the typical reliability index values of 3.0 to 3.5 for strength limit state which is consistent with earlier discussions in chapter 8.1.1.

As demonstrated in Steps 5 and 6, the γ_{SE} value can be determined for any reliability index (β) for various analytical methods. Use of the format shown in Figure 9-14 will lead to better regional practices in the sense that owners desiring to calibrate their local practices can readily see the implication of a certain method on the selection and cost of a foundation system. This is because the Figure 9-14 chart shows the reliability of various methods and permits selection of an appropriate method that would lead to selection of a proper foundation system for a given set of β and γ_{SE} , that is, not use a deep foundation system when a spread foundation would be feasible. The agency that is calibrating a value of γ_{SE} based on a locally-accepted analytical method must ensure that the chosen value of γ_{SE} is consistent with the serviceability of the substructure and superstructure design, as discussed in Step 6.

Table 9-11: Target Reliability Index, γ_{SE} for Various Structural Limit States (Kulicki, et al., 2015)

Limit State	Target Reliability Index, β_T	Approx P_e (Note 1)
Fatigue I and Fatigue II limit states for steel components	1.0	16%
Fatigue I for compression in concrete and tension in reinforcement	0.9 (Compression) 1.1 (Tension)	18% 14%
Tension in prestressed concrete components	1.0 (Normal environment) 1.2 (Severe environment)	16% 11%
Crack control in decks (Note 2)	1.6 (Class 1) 1.0 (Class 2)	5% 16%
Service II limit state for yielding of steel and for bolt slip (Note 2)	1.8	4%

Note 1: P_e is based on "Normal" Distribution

Note 2: Although smaller values of reliability index can be used as per R19B, the subcommittees have expressed a desire not to change the values implied by the current standard.

Chapter 10. Meaning and Effect of γ_{SE} in Bridge Design Process

The meaning and use of γ_{SE} must be understood in the specific context of structural implications within the *AASHTO LRFD* framework. The main point is that the value of γ_{SE} is used to assess the structural implications such as generation of additional (secondary) moments within a given span because of settlement of one of the support elements and effect on the riding surface, and conceivably even appearance and roadway damage issues. If taken literally, the value of $\gamma_{SE} = 1.25$ in the example could be interpreted to mean that the settlement, δ_p , predicted by the Schmertmann method, which needs to be increased by 25 percent, will lead to 25 percent more total force effects (for example, moments). However, this literal interpretation is not entirely correct because the value of γ_{SE} (1.25 in this case) is just one of the many load factors in the Service and Strength limit state load combinations within the overall *AASHTO LRFD* framework.

The additional moments because of the effect of settlement are dependent on the stiffness of the bridge and the angular distortion. A limited study (Schopen, 2010) of several two- and three-span steel and prestressed concrete continuous bridges selected from the National Cooperative Highway Research Program (NCHRP) Project 12-78 (Mlynarski et al., 2011) database, showed that allowing the full angular distortion suggested in Table 5-1 could result in an increase in the factored Strength I moments, as little as 10 percent for the more flexible units considered to more than double the moment from only the factored dead and live load moments for the stiffer units. These order of magnitude estimates are based on elastic analysis without consideration of creep which could significantly reduce the moments, especially for relatively stiff concrete bridges. For example, a W 36 x 194 rolled beam with a 10 in. x 1-7/8 in. bottom cover plate composite with a 96 in. x 7-3/4 in. deck is presented in Sen et al. (2011). The computed moments of inertia for the basic beam, short-term composite and long-term composite sections were in the approximate ratio 1:2:3. This indicates consideration of construction sequence, an appropriate choice of section properties, and possibly a time-dependent calculation of creep effects could be beneficial. Use of the construction-point concept would also mitigate the settlement moments. Schopen's results suggest that the use of permissible angular distortions approaching those currently allowed by *AASHTO LRFD* requires careful consideration of the particular bridge and its design objectives. This suggests that if the computed angular distortions are between the current practice of various agencies (as discussed in chapter 5) and the *AASHTO LRFD* limiting angular distortion criteria shown in Table 5-1, the resulting angular distortions may be tolerable and yet economy may be realized.

Appendix C presents example problems that explore the effect of including γ_{SE} in the bridge design process.

Chapter 11. Incorporating Values of γ_{SE} in AASHTO LRFD

The calibration of *SE* load factor leads to load factors equal to or greater than 1.0 based on the chosen target reliability index. Either Table 3.4.1-3 of *AASHTO LRFD* (see Figure 3-3) can be expanded to include values of *SE* load factor since this table include load factors for superimposed deformations, or a similar additional table can be developed. The latter approach is proposed since it is anticipated that further research will lead to additional values of *SE* load factors related to various foundation types and deformations. Table 11-1 presents proposed *SE* load factors, γ_{SE} .

Table 11-1: Load Factors for *SE* Loads

Deformation	<i>SE</i>
Immediate Settlement <ul style="list-style-type: none"> • Hough method • Schmertmann method • Local method 	1.00 1.25 *
Consolidation settlement	1.00
Lateral deformation <ul style="list-style-type: none"> • <i>P-y</i> or SWM soil-structure interaction method • Local method 	1.00 *

*To be determined by the Owner based on local geologic conditions.

The values of γ_{SE} in Table 11-1 are based on a target reliability index of 0.50, which assume that the effect of irreversible foundation deformations on the bridge superstructure will be reversed by intervention (for example, shimming and jacking). If intervention to relieve the superstructure is not practical or desirable for a given bridge type, then larger values of γ_{SE} consistent with target reliability index of 1.00 or larger should be considered based on procedures described in this report.

An owner may choose to use a local method that provides better estimation of foundation movement for local geologic conditions compared to methods noted in Section 10 (Foundations) of *AASHTO LRFD*. In such cases, the owner will have to calibrate the γ_{SE} value for the local method using the procedures described in chapters 8 and 9.

The value of $\gamma_{SE}=1.00$ for consolidation (long-term settlement time-dependent) settlement assumes that the estimation of consolidation settlement is based on appropriate laboratory and field tests to determine parameters (rather than correlations with index properties of soils) in the consolidation settlement equations in Article 10.6.2.4.3 of *AASHTO LRFD*.

The value of γ_{SE} for soil-structure interaction methods in Table 11-1 for estimation of lateral deformations may be increased to larger than 1.0 based on local experience and calibration using procedures described in chapter 9 in this report.

Chapter 12. The “S_f0” Concept

Chapters 8 and 9 have demonstrated a method to quantify uncertainty of predicted deformations for analytical models. The model uncertainty was calibrated and expressed through the load factor γ_{SE} . While all analytical models for estimating settlements have some degree of uncertainty, the uncertainty of the calculated differential settlement is larger than the uncertainty of the calculated total settlement at each of the two support elements used to calculate the differential settlement (for example, between an abutment and a pier, or between two adjacent piers). If one support element actually settles less than the amount calculated while the other support element actually settles the amount calculated, the actual differential settlement will be larger than the difference between the two values of calculated settlement at the support elements.

The larger uncertainty of calculated differential settlement could be because of a number of factors. One such factor is the temporal and spatial uncertainties that are associated with inherent randomness of natural processes. The temporal uncertainties are from a time-related variability that may occur at a given support location and the possibility that this variability is not the same at all support locations. In contrast, variability that can occur over different support locations at a given time is referenced as spatial variability. Mathematical models, such as those discussed in chapter 9, use simplified assumptions to account for these variabilities but their success in doing so is a function of the level of subsurface investigations (field and laboratory) and interpretations of the subsurface data. These uncertainties can be reduced by increased and better subsurface investigations using appropriate investigative and interpretive techniques, but can never be completely addressed. This is further complicated by factors such as uncertainties due to variabilities in regional design and construction practices, maintenance protocols, and local environment leading to deterioration. Such uncertainties cannot be accounted for in a national code, which includes specific methods that were developed in a certain geographical region based on geologic formations specific to that region. For example, use of a prediction model that was developed based on data in the northeast U.S. for glacial till may not produce reliable results when applied to other regional geologic conditions such as cemented soil in the desert southwest U.S. Although some uncertainties can be addressed by a load factor, such as γ_{SE} for a certain model, there are additional uncertainties that must be accounted for particularly when differential settlements are considered. Quantification of such additional uncertainties (sometimes categorized as epistemic uncertainties) may not be possible and therefore practical limit state criteria need to be established to incorporate deformation into the bridge design process.

As was noted earlier in the report, *AASHTO LRFD* states, “Force effects due to extreme values of differential settlement among substructures and within individual substructure units shall be considered.” This requirement is consistent with the knowledge that not all uncertainties associated with foundation deformations can be accounted for by a single load factor γ_{SE} for a certain model for prediction of deformation. Based on these considerations and guidance in Barker, et al. (1991) and Samtani and Nowatzki (2006), the following limit state criteria are suggested to estimate a realistic value of differential settlement and angular distortion:

- The actual factored settlement of any support element could be as large as the factored settlement value calculated by using a given method.
- The actual factored settlement of the adjacent support element could be less, taken as zero in the limit, instead of the value calculated by using the same given method.

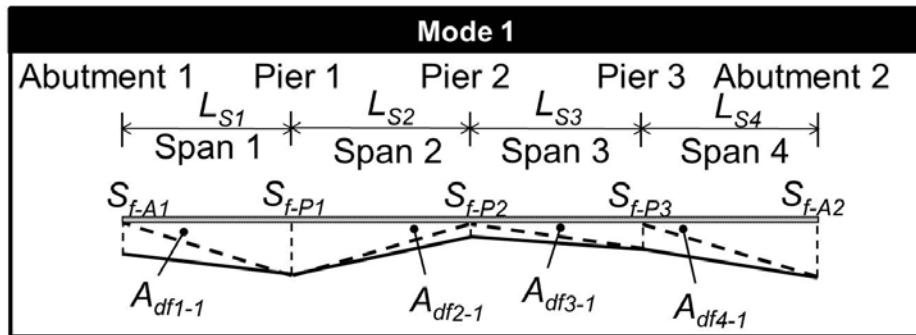
This concept is referred herein as the “ S_f -0” concept², with a value of S_f representing full factored settlement at one support of a span and a value of “0” representing zero settlement at an adjacent support. Use of the S_f -0 approach would result in an estimated maximum possible differential settlement between two adjacent supports equal to the larger of the two factored total settlements calculated at either end of any span. This approach also helps create the extreme values of differential settlement as required by Article 3.12.6 of *AASHTO LRFD*.

The application of the S_f -0 concept can be illustrated by considering the example of the four-span bridge in Figure 3-2. Before the application of the S_f -0 concept, the computed settlements S_{A1} , S_{P1} , S_{P2} , S_{P3} and S_{A2} are factored by multiplying each settlement by the γ_{SE} factor applicable to the method that was used to compute that particular settlement. The factored settlement values are labeled as S_{f-A1} , S_{f-P1} , S_{f-P2} , S_{f-P3} and S_{f-A2} . The factored differential settlement and the corresponding factored angular distortion values computed using the S_f -0 approach are shown in Figure 12-1. There are two possible modes, Mode 1 and Mode 2 depending on which support settlement is assumed to be zero. The values of factored differential settlement and corresponding factored angular distortions in the inset tables in Figure 12-1 represent the maximum values for each span according to the criteria above and should be used for design. The symbols are in accordance with Δ_{i-j} and A_{di-j} where i represents the span number (1 to 4) and j represents the mode (1 and 2). The hypothetical settlement profile assumed for computation of the factored angular distortion for each span is represented by the dashed lines in Figure 12-1. It should not be confused with the calculated factored total settlement profile that is represented by the solid lines. From the viewpoint of the damage to the bridge

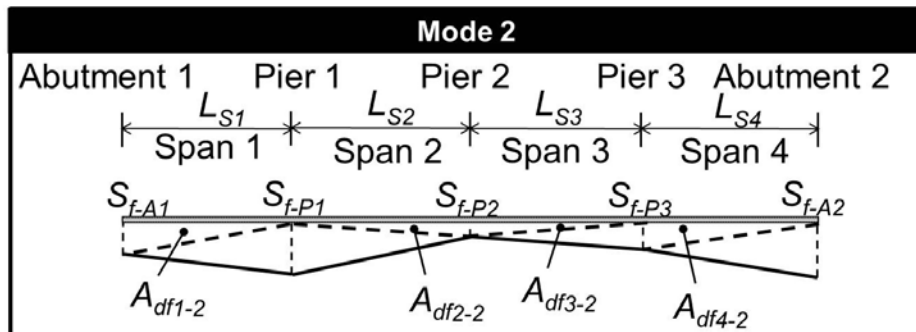
² This discussion is based on the consideration of settlement (vertical deformation). The S_f -0 concept can be considered in general terms as δ -0 concept where δ is a general symbol to designate any deformation (vertical, lateral or rotational).

superstructure, the concept shown in Figure 12-1 is more important for continuous span structures than single span structures because of the ability of the latter to permit larger movements at support elements.

Figure 12-1: Estimation of maximum factored angular distortion in bridges – Mode 1 and Mode 2



Span	Factored Differential Settlement	Factored Angular Distortion
1	$\Delta_{f1-1} = S_{f-P1}$ (assume $S_{f-A1} = 0$)	$A_{df1-1} = \Delta_{f1-1}/L_{S1}$
2	$\Delta_{f2-1} = S_{f-P1}$ (assume $S_{f-P2} = 0$)	$A_{df2-1} = \Delta_{f2-1}/L_{S2}$
3	$\Delta_{f3-1} = S_{f-P3}$ (assume $S_{f-P2} = 0$)	$A_{df3-1} = \Delta_{f3-1}/L_{S3}$
4	$\Delta_{f4-1} = S_{f-A2}$ (assume $S_{f-P3} = 0$)	$A_{df4-1} = \Delta_{f4-1}/L_{S4}$



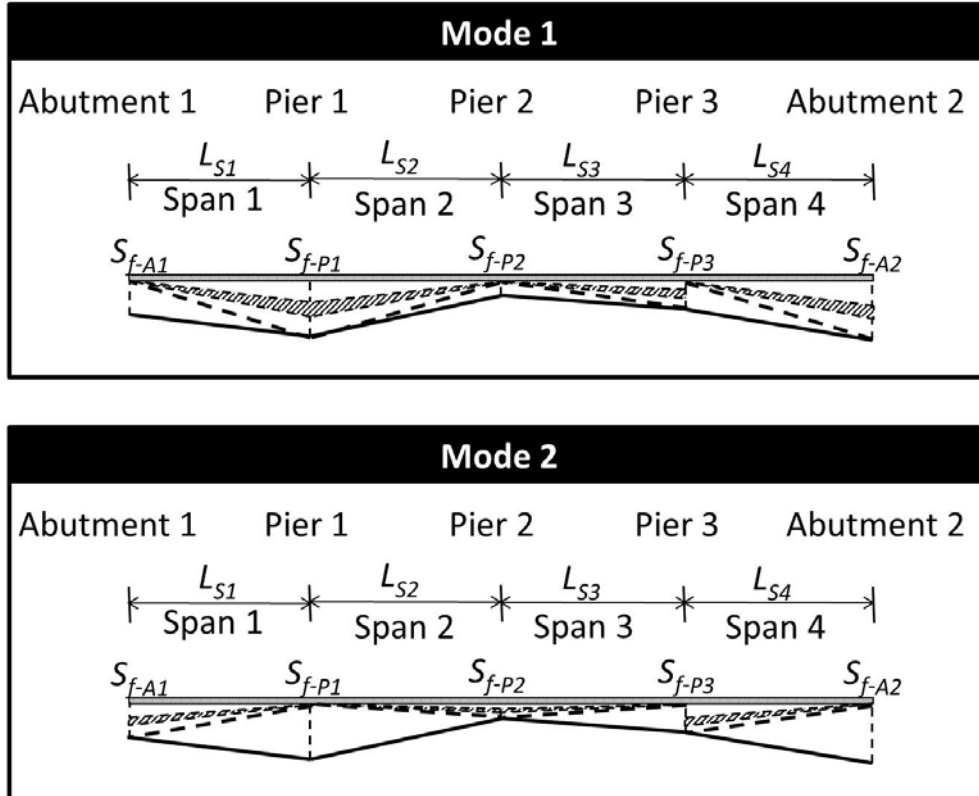
Span	Factored Differential Settlement	Factored Angular Distortion
1	$\Delta_{f1-2} = S_{f-A1}$ (assume $S_{f-P1} = 0$)	$A_{df1-2} = \Delta_{f1-2}/L_{S1}$
2	$\Delta_{f2-2} = S_{f-P2}$ (assume $S_{f-P1} = 0$)	$A_{df2-2} = \Delta_{f2-2}/L_{S2}$
3	$\Delta_{f3-2} = S_{f-P2}$ (assume $S_{f-P3} = 0$)	$A_{df3-2} = \Delta_{f3-2}/L_{S3}$
4	$\Delta_{f4-2} = S_{f-P3}$ (assume $S_{f-A2} = 0$)	$A_{df4-2} = \Delta_{f4-2}/L_{S4}$

With respect to the example of the four-span bridge and the angular distortions as shown in the inset table in Figure 12-1, the use of the construction-point concept (Figure 6-2) would result in smaller angular distortions to be considered in the structural design. This will be true of any bridge evaluation. Using Figure 12-1 as a reference, Figure 12-2 shows a comparison of the profiles of the factored total settlements (solid lines), hypothetical maximum angular distortions (dashed lines) and the actual relevant angular distortions (hatched pattern zones) based on the construction-point concept. The range of the hatched pattern zone can be 25 to 75 percent of the factored total settlement value at the location where full settlement is assumed. For a given project and site-specific conditions, the actual relevant angular distortion profile will be represented by a dashed line within the hatched pattern zone. The relevant angular distortion would then be compared with the limit state criteria for angular distortions provided in *AASHTO LRFD* Article 10.5.2.2 and Table 5-1 herein.

Figure 12-2: Factored angular distortion in bridges based on construction-point concept

Legend:

- Calculated factored total settlement profile (refer to Figure 4-2)
- Hypothetical factored settlement profile assumed for computation of maximum angular distortion
- Range of factored relevant angular distortions using construction-point concept



12.1 Foundations Proportioned for Equal Settlement

Occasionally geotechnical and structural specialists will try to proportion foundations for equal settlement. In this case, the argument is made that there will be no differential settlement. While this concept may work for a building structure because the footprint is localized, it is incorrect to assume a zero differential settlement for a long linear highway structure, such as a bridge or a wall because of the inevitable variation of the geomaterial properties along the length of the structure. Furthermore, as noted earlier, the prediction of settlements from any given method is uncertain in itself.

For highway structures, even where the foundations are proportioned for equal settlement, evaluation of differential settlement is recommended, assuming that the actual settlement of any support element could be as large as the value calculated by using a given method while at the same time, the actual settlement of the adjacent support element would be zero.

Chapter 13. Flow Chart to Consider Foundation Deformations in Bridge Design Process

Figure 13-1 shows a flow chart to consider foundation deformation in the bridge design process. The flow chart has two distinct parts, left and right. The left part outlines the process that a bridge designer may use without explicit consideration of foundation deformations other than what is required in the 7th Edition of *AASHTO LRFD*, i.e. without considering the method-specific load factor, γ_{SE} , the construction-point concept or the δ -0 concept. For convenience this will be called the “legacy loop”. The right part provides the recommended procedure to factor the deformations and evaluate the effect on the structure using the factored deformations. The sequence of activities in the deformation loop is based on the discussions in this report, which includes the method-specific load factor, γ_{SE} , the construction-point concept, or the δ -0 concept. For convenience, this will be called the “refined (deformation) loop”. The flow chart applies to any type of foundation deformation and hence the symbol δ is used for deformations. If the flow chart is used for settlement, then symbol “*S*” may be substituted for δ .

It is not the intention of the illustrated design process to universally require additional design effort beyond what is required by the 7th edition of *AASHTO LRFD*, or approved owner policies that take advantage of well-documented past geotechnical practice. For example, if the geomaterials at a site are well understood and past experience shows that a deep foundation is the best option, or that a given service-bearing pressure results in acceptable foundation deformations with minimal structural or geometric consequences, then the decision to base a new design on legacy practices is a viable option. If, on the other hand, site conditions are not within past successful practice, there is a desire to consider possible economies of design that alter the experience base, or the structure requires more careful consideration of possible foundation deformations, then the additional provisions embodied in the refined (deformation) loop will result in a more thorough assessment of the implications of foundation deformations and the associated impact on the design and economy of the bridge.

Three notes are provided in the flow chart to include additional guidance for the designer.

Some of the key points associated with the flow chart are as follows:

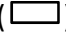
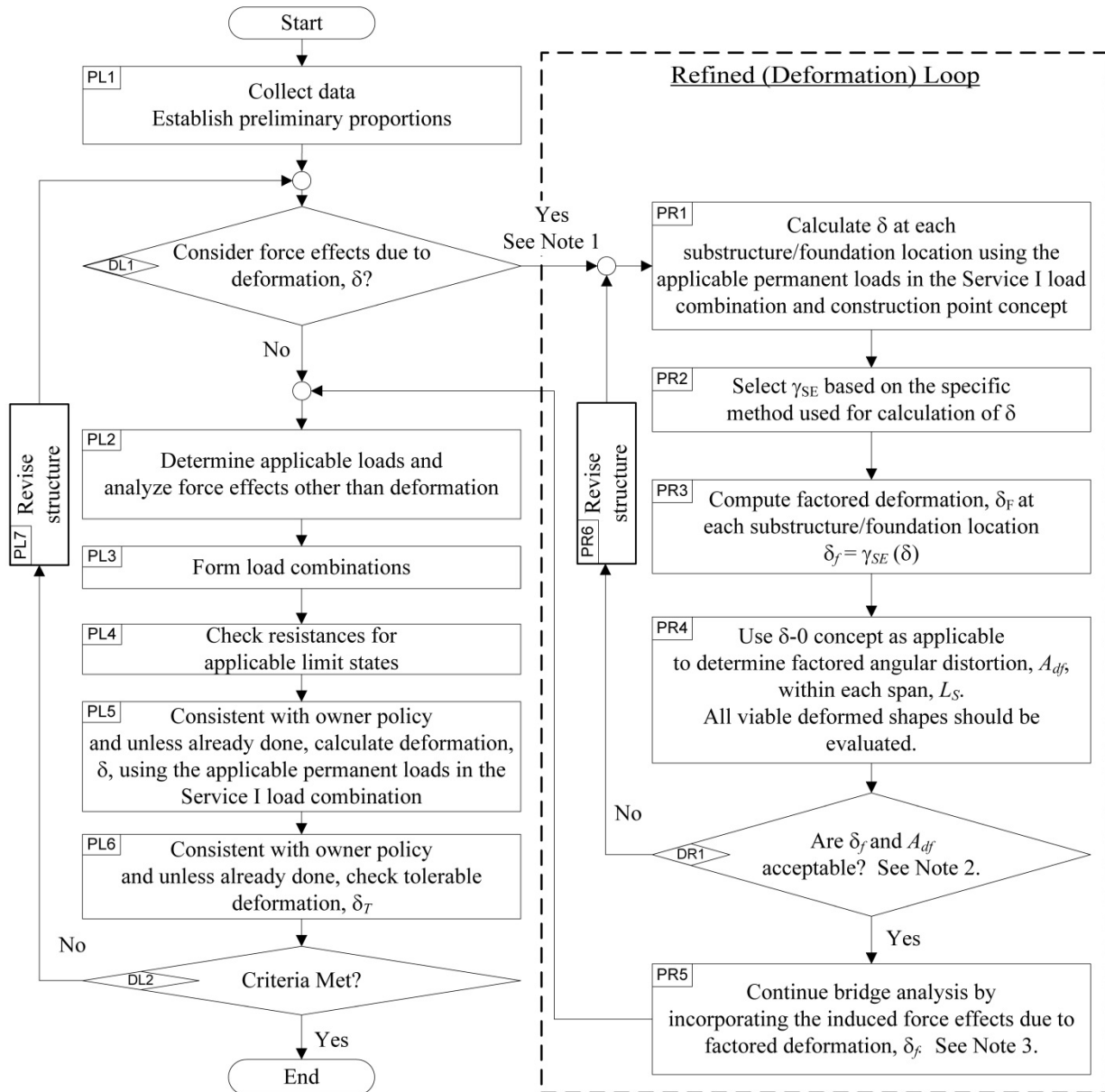
1. The process (“P”) related steps are indicated in rectangular boxes (). In the left (“L”) part, there are six process boxes labeled PL1 to PL6. In the right (“R”) part, there are five process boxes labeled PR1 to PR5.

Figure 13-1: Consideration of foundation deformation in bridge design process



Note 1: It may be efficient to run some early design iterations without including this loop until the proportions of the bridge are well developed, and then include this loop to consider the force effects from differential deformations.

Note 2: Compare A_{df} to permissible angular distortion criteria and δ_f to permissible values at abutment interfaces and within spans in terms of vertical clearance under bridge. Guidance in Article 10.5.2 may be used to establish permissible values. Owner may establish other permissible values.

Note 3: Note that the γ_{SE} is used to factor the deformations as shown in this flow chart. γ_{SE} also appears in Table 3.4.1-1 (Load Combinations and Load Factors). This does not imply a second application of γ_{SE} in the load combinations but rather it is an acknowledgement that the deformations have already been factored. Use of the factored deformations in a structural analysis program ensures that the output is factored value.

2. The decision (“D”) related steps are indicated by diamond boxes (\diamond). In the left part, there are two decision boxes labeled DL1 and DL2. The right part contains one decision box labeled DR1.
3. The left and right parts are connected at two levels. The first connection is established when a bridge designer decides to proceed with either the legacy or refined (deformation) loop in box DL1. The second connection is established after box PR5, once the designer has determined a favorable resolution of “Yes” to the decision in box DR1.
4. If the resolution to either box DL2 is “No,” then the structure is revised and the flow chart is re-entered at box DL1. Likewise, if the resolution at DR1 is “No” the structure is revised and the flowchart is re-entered at box PR1
5. If the answer is “No” at box DL1, then the designer goes through the process provided in boxes PL2 to PL6 using the legacy approach as follows:
 - In box PL2, structural analysis proceeds without use of the construction-point or δ -0 concepts as they are not incorporated into the legacy approach. Consideration of foundation deformations is consistent with the owner’s implementation of the 7th edition of *AASHTO LRFD*.
 - Box PL3 indicates use of Table 3.4.1-1 of *AASHTO LRFD*, as applicable to the situation at hand. Depending on the owner’s policies, the values of γ_{SE} will effectively be zero or unity. In this case, the deformation may be evaluated based on past local experience with similar structures.
6. If the answer is “Yes” at box DL1, then the designer goes through the process provided in boxes PR1 to PR5, using the refined (deformation) approach. Note 1 is provided as guidance about entering the right side. The design proceeds as follows:
 - After the calculation of δ for the indicated loads in box PR1 and adjusting them for the construction-point concept, they are scaled (factored) as indicated in box PR3 using the method-specific values of γ_{SE} determined in box PR2.
 - These factored deformations, δ_f , are used along with the δ -0 concept to calculate the factored angular distortions, A_{df} in box PR4.
 - In box DR1, the values of δ_f and A_{df} are compared to the applicable criteria. These criteria are geometric, not structural. Note 2 provides additional guidance.
 - If the results are not acceptable the structure is revised and the design process returns to box PR1 to evaluate the modified structure.
 - If the results at box DR1 are acceptable, the structural force effects from the factored deformations, δ_f , are calculated and are carried into the remaining steps of the legacy

loop. Note 3 is vital to the correct formulation of load combinations using Table 3.4.1-1 in box PL5.

7. The “Criteria” in box DL2 can include any criteria related to bridge design, such as deck grades, joint distress, crack control, and moment and shear resistance.
8. In boxes PL5 and PL6, the phrase “unless already done” acknowledges the possibility that the actions in these boxes may already have been performed by a designer who is entering these boxes after completing the right part of the flow chart.
9. If all structural and geometric criteria are satisfied in box DL2, the design is satisfactory; if not, the structure is modified and the design process returns to box DL1.

Chapter 14. Proposed Modifications to *AASHTO LRFD* Bridge Design Specifications

The work presented in this report can be considered for modifications of Section 3 and Section 10 of *AASHTO LRFD* as follows:

1. In Article 3.4.1, include a new load factor table for SE as shown in Table 11-1, with appropriate specifications and commentary to explain the various values of the SE load factor.
2. In Article 10.5.2.2, include a step-by-step procedure and appropriate commentary for implementation of the γ_{SE} load factor in conjunction with the construction-point and $S_f=0$ concept.
3. In Section 3, as an appendix, include the flow chart for incorporation of foundation deformations in the bridge design process.
4. Include method by Schmertmann in Article 10.6.2.4.2.

These proposed draft modifications for Section 3 of *AASHTO LRFD* are included in Appendix D while those for Section 10 of *AASHTO LRFD* are included in Appendix E.

Chapter 15. Application of Calibration Procedures

Although the focus of this report is calibration of foundation deformations, the calibration procedures described are general and can be considered for calibration of any civil engineering feature. The calibration procedure developed in SHRP2's *Service Limit State Design for Bridges* and explained herein provides additional tools for continued development of reliability-based design specifications. There are two particular classes of problems that can be treated with the calibration procedure used in this report:

- Class A: This involves situations where consideration of deformations is required to inform the “two-hump” distribution of load and resistance, or their proxies, as illustrated in Figure 8-2. In the illustrated situation, the calibration has to account for load-deformation characteristics and the distribution of load and resistance.
- Class B: This involves situations where there is so little data on the distribution of either loads or resistances, or their proxies, that one of them needs to be considered as determinant, where there is no variability as shown in Figure 8-6, and Monte-Carlo simulation is unstable.

Class A problems are typical of geotechnical features where the load-deformation ($Q-\delta$) curves have a much flatter initial portion compared to the steep initial portions for structural materials, such as concrete and steel. During the calibration of service limit states in SHRP2's *Service Limit State Design for Bridges*, Class B problems arose several times, where the variability of resistance proxy could not be established and the calibration process described in this report for a geotechnical service limit state was adapted for structural service limit states. Extension to strength limit state calibration is also possible.

One use of the calibration procedure described in this report is further research and development of γ_{SE} load factors for other types of deformations, features such as retaining structures, and use of other deformation calculation methods than those documented herein. The γ_{SE} load factors that are developed in the future can be included in Table 11-1. Three examples within the geotechnical field are as follows:

1. Lateral deformation of deep foundations: In this case a figure similar to Figure 9-1 will need to be developed based on data from methods such as the $P-y$ method and SWM. The remainder of the calibration process will remain identical as shown in chapter 9.
2. Face movements of MSE walls: In this case, a figure similar to Figure 9-1 will need to be developed based on data from MSE walls with inextensible and extensible reinforcements. Within each category, different reinforcement materials types and configurations can be

included (for example, steel strips, steel grids, geogrids, and geotextiles). The remainder of the calibration process will remain identical as shown in chapter 9.

3. Pullout out resistance of soil reinforcements: In this case, a figure similar to Figure 9-1 will need to be developed based on pullout test data for soil reinforcements embedded in different soil types (such as, native, compacted, sand, and clay) and different soil reinforcements (such as, anchors and nails). The remainder of the calibration process will remain identical as shown in chapter 9.

Chapter 16. Summary

This report was developed as part of IAP and focuses on the work related to foundation deformations developed as part of SHRP2's *Service Limit State Design for Bridges*. Its purpose was to explain the implementation of calibrations for foundation deformations into the bridge design process. The scope was to bring together the relevant content of SHRP2's *Service Limit State Design for Bridges* (Kulicki, et al., 2015) and additional materials developed since the issuance of the TRB SHRP2's R19B report. Examples of these materials include flow charts and examples that provide background information as part of AASHTO's balloting process for incorporation of the γ_{SE} load factor and other associated modifications in *AASHTO LRFD Bridge Design Specifications*.

The consideration of foundation deformations in the bridge design process can lead to the use of cost-effective structures with more efficient foundation systems. The proposed approach and modifications will help avoid overly conservative criteria that can lead to (a) foundations that are larger than needed, or (b) a choice of less economical foundation type (such as, using a deep foundation at a location where a shallow foundation would be adequate).

Implementation of the proposed procedures may often allow consideration of larger foundation deformations. The associated structural and geometric impacts can be mitigated by the construction-point concept and the δ -0 concept. These are incorporated into the design process following the recommended specification revisions illustrated in the flowchart found in chapter 13. The revised design procedures and the method-specific load factor are combined to produce flexibility in comparing the alternative foundations and structures and provide more uniform serviceability and safety.

Chapter 17. References

AASHTO. 2002. *Standard Specifications for Highway Bridges*, 17th ed. American Association of State Highway and Transportation Officials, Washington, D.C.

AASHTO LRFD. 2014. *AASHTO LRFD Bridge Design Specifications*, 7th ed. American Association of State Highway and Transportation Officials, Washington, D.C.

ADOT (2015). See Section 10, Article 10.5.2.2 in Bridge Design Guidelines at <http://www.azdot.gov/business/engineering-and-construction/bridge/guidelines>

Akbas, S., and F. Kulhawy. 2009. Axial Compression of Footings in Cohesionless Soils: I—Load-Settlement Behavior. *ASCE Journal of Geotechnical and Geoenvironmental Engineering*, Vol. 135, No. 11, pp. 1562–1574.

Allen, T., A. Nowak, and R. Bathurst. 2005. *Transportation Research Circular E-C079: Calibration to Determine Load and Resistance Factors for Geotechnical and Structural Design*. Transportation Research Board of the National Academies, Washington, D.C. <http://onlinepubs.trb.org/onlinepubs/circulars/ec079.pdf>.

Barker, R., J. Duncan, K. Rojiani, P. Ooi, C. Tan, and S. Kim. 1991. *NCHRP Report 343: Manuals for the Design of Bridge Foundations: Shallow Foundations, Driven Piles, Retaining Walls and Abutments, Drilled Shafts, Estimating Tolerable Movements, Load Factor Design Specifications, and Commentary*. TRB, National Research Council, Washington, D.C.

Burland, J., and M. Burbridge. 1984. Settlement of Foundations on Sand and Gravel. *Proceedings, Part I, Institution of Civil Engineers*, Vol. 78, No. 6, pp. 1325–1381.

D’Appolonia, D., E. D’Appolonia, and R. Brissette. 1968. Settlement of Spread Footings on Sand. *ASCE Journal of Soil Mechanics and Foundations Division*, Vol. 94, No. 3, pp. 735–762.

Das, B., and B. Sivakugan. 2007. Settlements of Shallow Foundations on Granular Soil: An Overview. *International Journal of Geotechnical Engineering*, No. 1, pp. 19–29.

Duncan, J. 2000. Factors of Safety and Reliability in Geotechnical Engineering. *ASCE Journal of Geotechnical and Geoenvironmental Engineering*, Vol. 126, No. 4, pp. 307–316.

Elias, V., K. Fishman, B. Christopher, and R. Berg. 2009. *Corrosion/Degradation of Soil Reinforcements for Mechanically Stabilized Earth Walls and Reinforced Soil Slopes*. FHWA-NHI-09-087. National Highway Institute, Federal Highway Administration, Washington, D.C.

Fishman, K., and J. Withiam. 2011. *NCHRP Report 675: LRFD Metal Loss and Service-Life Strength Reduction Factors for Metal-Reinforced Systems*. TRB, National Research Council, Washington, D.C.

- Geotechnical Design Manual*. 2012. M 46-03.07. Washington State Department of Transportation, Olympia.
- Gifford, D., S. Kraemer, J. Wheeler, and A. McKown. 1987. *Spread Footings for Highway Bridges*. FHWA/RD-86-185. Haley and Aldrich, Cambridge, Mass.
- Grant, R., J. Christian, and E. Vanmarcke. 1974. Differential Settlement of Buildings. *ASCE Journal of the Geotechnical Engineering Division*, Vol. 100, No. 9, pp. 973–991.
- Hough, B. 1959. Compressibility as the Basis for Soil Bearing Value. *ASCE Journal of the Soil Mechanics and Foundations Division*, Vol. 85, No. 4, pp. 11–40.
- Kulicki, J., W. Wassef, D. Mertz, A. Nowak, N. Samtani, and H. Nassif. 2015. *Bridges for Service Life Beyond 100 Years: Service Limit State Design*. SHRP 2 Report S2-R19B-RW-1, SHRP2 Renewal Research, Transportation Research Board. National Research Council, The National Academies, Washington, D.C.
- Mlynarski, M., W. Wassef, and A. Nowak. 2011. *NCHRP Report 700: A Comparison of AASHTO Bridge Load Rating Methods*. NCHRP Project 12-78, TRB, National Research Council, Washington, D.C.
- Moulton, L., H. Ganga Rao, and G. Halvorsen. 1985. *Tolerable Movement Criteria for Highway Bridges*. FHWA/RD-85-107. West Virginia University, Morgantown.
- Musso, A., and P. Provenzano. 2003. Discussion of Predicting Settlement of Shallow Foundations Using Neural Networks. *ASCE Journal of Geotechnical and Geoenvironmental Engineering*, Vol. 129, No. 12, pp. 1172–1175.
- Nielson, B. 2005. *Analytical Fragility Curves for Highway Bridges in Moderate Seismic Zones*. A Thesis presented to The Academic Faculty in partial fulfillment of the requirements for the Degree of Doctor of Philosophy, School of Civil and Environmental Engineering, Georgia Institute of Technology.
- Nowak, A., and K. Collins. 2013. *Reliability of Structures*. McGraw-Hill, New York.
- Peck, R., and A. Bazaraa. 1969. Discussion of Settlement of Spread Footings on Sand. *ASCE Journal of the Soil Mechanics and Foundations Division*, Vol. 95, No. 3, pp. 900–916.
- Samtani, N., A. Nowatzki, and D. Mertz. 2010. *Selection of Spread Footings on Soils to Support Highway Bridge Structures*. FHWA RC/TD-10-001. Federal Highway Administration Resource Center, Matteson, Ill.
- Samtani, N., and E. Nowatzki. 2006. *Soils and Foundations: Volumes I and II*. FHWA-NHI-06-088 and FHWA-NHI-06-089. Federal Highway Administration, U.S. Department of Transportation.

- Sargand, S., and T. Masada. 2006. *Further Use of Spread Footing Foundations for Highway Bridges*. State Job No. 14747(0), FHWA-OH-2006/8. Ohio Research Institute for Transportation and the Environment, Athens; Ohio Department of Transportation, Columbus; and Office of Research and Development, Federal Highway Administration, U.S. Department of Transportation.
- Sargand, S., T. Masada, and R. Engle. 1999. Spread Footing Foundation for Highway Bridge Applications. *ASCE Journal of Geotechnical and Geoenvironmental Engineering*, Vol. 125, No. 5, pp. 373–382.
- Schmertmann, J., P. Brown, and J. Hartman. 1978. Improved Strain Influence Factor Diagrams. *ASCE Journal of the Geotechnical Engineering Division*, Vol. 104, No. 8, pp. 1131–1135.
- Schopen, D. 2010. *Analyzing and Designing for Substructure Movement in Highway Bridges: An LRFD Approach*. Master's thesis. University of Delaware, Newark.
- Sen, M., A. Hedefine, and J. Swindlehurst. 2011. "Beam and Girder Bridges," Chapter 12 in *Structural Steel Designer's Handbook*, 5th ed. Editors: Brockenbrough, R., and F. Merritt, McGraw-Hill, New York.
- Shahin, M., H. Maier, and M. Jaksa. 2002. Predicting Settlement of Shallow Foundations Using Neural Networks. *ASCE Journal of Geotechnical and Geoenvironmental Engineering*, Vol. 128, No. 9, pp. 785–793.
- Sivakugan, N., and K. Johnson. 2002. Probabilistic Design Chart for Settlements of Shallow Foundations in Granular Soils. *Australian Civil Engineering Transactions*, No. 43, pp. 19–24.
- Sivakugan, N., and K. Johnson. 2004. Settlement Predictions in Granular Soils: A Probabilistic Approach. *Geotechnique*, Vol. 54, No. 7, pp. 499–502.
- Skempton, A., and D. MacDonald. 1956. Allowable Settlement of Buildings. *Proceedings, Part III, Institution of Civil Engineers*, No. 5, pp. 727–768.
- Tan, C., and J. Duncan. 1991. Settlement of Footings on Sands: Accuracy and Reliability. *Proc., Geotechnical Engineering Congress 1991, ASCE Geotechnical Special Publication No. 27*, Vol. 1, pp. 446–455.
- WSDOT. 2012. *Geotechnical Design Manual*. M 46-03.07. Washington State Department of Transportation, Olympia.
- Wahls, H. 1983. *NCHRP Synthesis of Highway Practice 107: Shallow Foundations for Highway Structures*. TRB, National Research Council, Washington, D.C.
- Zhang, L., and A. Ng. 2005. Probabilistic Limiting Tolerable Displacements for Serviceability Limit State Design of Foundations. *Geotechnique*, Vol. 55, No. 2, pp. 151–161.

Appendix A
Conventions

Appendix A. Conventions

Documents from various sources such as AASHTO, FHWA, and SHRP2 are referenced in this paper. Each reference document has its own style and organization, which often creates confusion during cross-referencing of documents. For instance, the AASHTO bridge design specifications based on the Load and Resistance Factor Design (LRFD) platform are organized in sections and articles in a two-column format, while FHWA documents are organized in chapters and sections in single-column format. Different fonts (for example, Times New Roman, and Calibri), font styles (such as regular and *italic*), and font sizes (for example, 12 point and 10 point) are used in different documents. Finally, different styles for referencing other documents are used. The following are the important points with respect to convention used in this report:

1. AASHTO LRFD Bridge Design Specifications are referenced as *AASHTO LRFD* to fulfill AASHTO's citation requirements. Similarly, the format of AASHTO's *Standard Specifications for Highway Bridges* is used to refer to the AASHTO bridge design specifications based on the Allowable Stress Design (ASD) and Load Factor Design (LFD) platform.
2. *AASHTO LRFD* refers to the 7th edition issued in 2014 and its subsequent interims.
3. A document reference that is unique and often cited is referenced with a single word after the first usage. For example, after an initial reference as Moulton et al. (1985), it is subsequently referenced in the body of the report simply as Moulton.
4. A specific section or article within *AASHTO LRFD* is referenced "Section # of *AASHTO LRFD*". Similar convention is followed for a specific Article in *AASHTO LRFD*.
5. The approach of chapter and section in a single-column format with 12 point Calibri font is used except for Appendices D and E, which use the two-column section and article format with 10 point Times New Roman font because these appendices include proposed modifications for *AASHTO LRFD*.
6. Since this report will be used for input related to modifications in *AASHTO LRFD*, the notations are italicized to be consistent with *AASHTO LRFD*. For example, *S* and Δ_f .
7. *AASHTO LRFD* uses the word "deformation" and "movement" interchangeably when discussing foundations or bridge supports. The word "deformation" is used in this report unless a direct quote is provided from a document where the word "movement" was used.

Appendix B
Application of γ_{SE} Load Factor

Appendix B. Application of γ_{SE} Load Factor

Figure 6.1 shows the construction-point concept. The horizontal dashed line in Figure 6.1b is annotated with “Long-term settlement (if applicable)”. In the text related to Figure 6.1 in Chapter 6, it is stated that “...long-term settlements will continue under the total construction load (Z) as shown by the dashed line in Figure 6.1”. The proposed design approach incorporates the construction-point concept in conjunction with the γ_{SE} load factor. Table 11-1 provides the value of γ_{SE} load factors for the immediate and consolidation type settlements. This appendix provides a numerical example to illustrate the application of the γ_{SE} load factor for the case where a support element such as an abutment or a pier may experience long-term consolidation settlement after the short-term immediate settlement.

Example: Assume a four-span bridge similar to that shown in Figure 12-2. Table B-1 provides the predicted settlements along with the methods used for computing the predicted settlement. For the data given in Table B-1, develop the factored total relevant settlement, S_f , values that will be used for bridge structural analysis.

Table B-1: Predicted Settlements

Support Element	Unfactored Predicted Settlements				
	Immediate Settlement (Note 1)			Consolidation Settlement (in.) (Note 2)	Total Relevant Settlement, S_{tr} (in.) (Note 3)
	Total (in.)	Relevant (in.)	Prediction Method		
Abutment 1	1.90	0.80	Schmertmann	2.00	2.80
Pier 1	3.20	1.90	Hough	3.60	5.50
Pier 2	2.00	0.90	Hough	3.20	4.10
Pier 3	2.10	1.20	Schmertmann	4.00	5.20
Abutment 2	1.50	0.70	Schmertmann	1.90	2.60

Note 1: The total immediate settlement is based on the assumption of instantaneous application of all loads while the relevant settlement is based on the assumption of loads due to superstructure only. With respect to Figure 6.1, the relevant immediate settlement is based on loads after the completion of the substructure. In other words, the difference between the total and relevant values represents the magnitude of settlement that occurs prior to the construction of the superstructure.

Note 2: The consolidation settlement is based on the total load of the structure.

Note 3: The total relevant settlement is obtained by adding the relevant immediate settlement and the consolidation settlement.

The computations of the factored total relevant settlement, S_f , at each support element are as follows:

Abutment 1: From Table 11-1, $\gamma_{SE} = 1.25$ for Schmertmann method and $\gamma_{SE} = 1.00$ for consolidation settlement. Thus, $S_f = (1.25)(0.80 \text{ in.}) + (1.00)(2.00 \text{ in.}) = 3.00 \text{ in.}$

Pier 1: From Table 11-1, $\gamma_{SE} = 1.00$ for Hough method and $\gamma_{SE} = 1.00$ for consolidation settlement. Thus, $S_f = (1.00)(1.90 \text{ in.}) + (1.00)(3.60 \text{ in.}) = 5.50 \text{ in.}$

Pier 2: From Table 11-1, $\gamma_{SE} = 1.00$ for Hough method and $\gamma_{SE} = 1.00$ for consolidation settlement. Thus, $S_f = (1.00)(0.90 \text{ in.}) + (1.00)(3.20 \text{ in.}) = 4.10 \text{ in.}$

Pier 3: From Table 11-1, $\gamma_{SE} = 1.25$ for Schmertmann method and $\gamma_{SE} = 1.00$ for consolidation settlement. Thus, $S_f = (1.25)(1.20 \text{ in.}) + (1.00)(4.00 \text{ in.}) = 5.50 \text{ in.}$

Abutment 2: From Table 11-1, $\gamma_{SE} = 1.25$ for Schmertmann method and $\gamma_{SE} = 1.00$ for consolidation settlement. Thus, $S_f = (1.25)(0.70 \text{ in.}) + (1.00)(1.90 \text{ in.}) = 2.78 \text{ in.}$

Table B-2 summarizes the computed factored total relevant settlements, S_f , at each support element. These values are used for the bridge structural analysis.

Table B-2: Summary of Factored Total Relevant Settlements

Support Element	Factored Total Relevant Settlement, S_f (in.)
Abutment 1	3.00
Pier 1	5.50
Pier 2	4.10
Pier 3	5.50
Abutment 2	2.78

This example deliberately used different methods for prediction of immediate settlement at different support elements to illustrate the process of computation of factored total relevant settlement, S_f . In practice, the same method of predicting immediate settlement is often used.

Appendix C
Examples (Developed by AECOM)

Appendix C. Examples

This appendix presents examples that demonstrate application of the process to incorporate the effect of foundation deformations in the bridge design process. The right side of the flow chart in Figure 13-1 is used in the demonstration. The purpose of these example problems is to show the effect of applying the proposed specifications revisions on the controlling moments and shears in several bridges.

The examples are based on several recently constructed continuous span steel I-girder bridges by AECOM. Table C-1 shows the characteristic of the bridges.

Table C-1: Bridge Characteristics

Example	Material	Span lengths (ft)	Girder Spacing
1	Steel I-Girders	50, 50	7 ft-2 in.
2	Steel I-Girders	168, 293, 335, 165	11 ft-2 in.
3	Steel I-Girders	120, 140, 140, 140, 120	12 ft-3 in.

The examples examine the following force effects due to foundation settlement (SE):

- Maximum positive moment within each span along with the minimum (i.e. maximum negative) moment at the same location
- Maximum moment and minimum moment (i.e. maximum negative) at each intermediate support
- Maximum shear at each abutment
- Maximum and minimum shear on both sides of intermediate supports

During the design procedure, the magnitude of settlement at each support at different stages of construction will be determined by bridge designer based on input provided by the geotechnical engineer. For these examples, the following assumptions have been made³:

1. Use of Schmertmann's method to predict immediate settlement at all support locations.
2. No long-term consolidation settlements. Thus, the total settlement, S_t , in these example problems is equal to the immediate settlement.

³ Use site-specific data for actual projects. The values chosen for the examples are for illustration purpose only.

3. The values of the total settlement, S_t , chosen reflect typical settlement magnitudes expected for similar bridges.
4. The values of total relevant settlement, S_{tr} , are 50% of total settlement, S_t .

The settlement data can be organized using the format shown in Tables C-2 to C-5. Each of these tables is briefly discussed below:

- Table C-2 shows the assumed predicted total settlements, S_t . These values should be computed as per first part of box PR1 of the flowchart of Figure 13-1. These are settlements based on the assumptions of instantaneous application of all loads.

Table C-2: Predicted Total Settlements, S_t

Example	Unfactored Predicted Settlement, S_t (in.)					
	Abutment 1	Pier 1	Pier 2	Pier 3	Pier 4	Abutment 2
1	0.8	1.6	N/A	N/A	N/A	0.6
2	1.9	3.9	4.8	1.9	N/A	2.5
3	0.9	1.5	1.8	1.0	2.3	1.4

- Table C-3 shows the estimated total relevant settlements, S_{tr} . These values are as per second part of box PR1 of the flowchart of Figure 13-1. These are settlements computed after consideration of construction-point concept. For this example problem, these values are assumed to be 50% of the predicted total settlements, S_t .

Table C-3: Estimated Total Relevant Settlements, S_{tr}

Example	Unfactored Total Relevant Settlement, S_{tr} (in.)					
	Abutment 1	Pier 1	Pier 2	Pier 3	Pier 4	Abutment 2
1	0.40	0.80	N/A	N/A	N/A	0.30
2	0.95	1.95	2.40	0.95	N/A	1.25
3	0.45	0.75	0.90	0.50	1.15	0.70

- Table C-4 shows the compute factored total relevant Settlements, S_f . These values are computed by multiplying the estimated total relevant settlements, S_{tr} , from Table C-3 by the applicable load factor for the method used to estimate the settlement. This is done as per box PR3 and PR4 of the flowchart of Figure 13-1. For the purpose of the examples, assume that the owner will select a target reliability index, $\beta = 0.50$ and since the settlements were computed by Schmertmann's method, the applicable load factor, γ_{SE} is 1.25 based on Table 11-1. The values in Table C-4 are those that will be used in the structural analysis as per box PR5 in the flow chart of the flowchart of Figure 13-1.

Table C-4: Factored Total Relevant Settlements, S_f

Example	Factored Total Relevant Settlement, S_f (in.)					
	Abutment 1	Pier 1	Pier 2	Pier 3	Pier 4	Abutment 2
1	0.50	1.00	N/A	N/A	N/A	0.38
2	1.19	2.44	3.00	1.19	N/A	1.56
3	0.56	0.94	1.13	0.63	1.44	0.88

Note: $S_f = \gamma_{SE} (S_{tr})$

- Table C-5 shows the factored angular distortion, A_{df} , calculated as per box PR4 of the flowchart of Figure 13-1. The angular distortion for any span is calculated by dividing the factored total relevant settlement, S_f , at one end of the span (taken from Table C-4) by the span length then the calculation is repeated using the factored total relevant settlement at the other end of each span. By following this process, all viable modes of deformation profiles will be evaluated. (e.g., see Mode 1 and Mode 2 example in Figure 12-1).

Table C-5: Compute Factored Angular Distortions, A_{df}

Example	Factored Angular Distortion, A_{df} (rad.)				
	Mode 1: S_f at the left end of the span divided by the span length				
	Span 1	Span 2	Span 3	Span 4	Span 5
1	0.0008	0.0017	N/A	N/A	N/A
2	0.0006	0.0007	0.0007	0.0006	N/A
3	0.0004	0.0006	0.0007	0.0004	0.0010
Example	Mode 2: S_f at the right end of the span divided by the span length				
	Span 1	Span 2	Span 3	Span 4	Span 5
	1	0.0017	0.0006	N/A	N/A
2	0.0012	0.0009	0.0003	0.0008	N/A
3	0.0007	0.0007	0.0004	0.0009	0.0006

The calculated factored total relevant settlement, S_f , and the factored angular deformation, A_{df} , can then be evaluated in accordance to box DR1 of the of the flowchart of Figure 13-1. See Note 2 in flowchart for guidance on comparison of angular distortion values. The factored settlements in Table C-4 can be evaluated based on project specific criteria. If acceptability criteria are satisfied, then proceed to box PR5 of the flowchart and evaluate induced force effects due to the values in Table C-4 and incorporate these force effects into the bridge design by going to box PL2 of the flowchart.

Each of the example problems is organized in a set of 14 tables with 7 tables applicable to moment and 7 applicable to shear considerations. Each example problem has 4 pages with 2 pages applicable to moment computations and 2 pages applicable to shear computations. Page numbers for each example problem are noted in the upper right hand corner of each page.

The organization of the tables is discussed using Example 1 as an illustration. The tables in other examples are organized in a similar manner.

- Tables E1-M1 and E1-S1 provide the values of moment and shear that were computed by a bridge design program.
- Table E1-M2 provides the values of the predicted unfactored total settlement, S_t , at each support element. For convenience, the values in Table E1-S2 are repeated in Table E1-M2.
- Table E1-M3 provides the values of the estimated unfactored relevant settlement, S_{tr} , at each support element. For convenience, the values in Table E1-S3 are repeated in Table E1-M3.
- Table E1-M4 provides the values of the factored relevant settlement, S_f , at each support element. For convenience, the values in Table E1-S4 are repeated in Table E1-M4.
- The top three rows of Table E1-M5 contain the unfactored moments (copied from the corresponding top three rows of Table E1-M1). The next three rows in Table E1-M5 contain values of moments calculated by scaling the moments determined based on unit (1 in.) settlement in the last three rows of Table E1-M1. The computation of values in last nine rows of Table E1-M5 are demonstrated below for moment at Pier 1 location (similar computations apply at other support locations)⁴:
 - Effect of unfactored S_{tr} at Abutment 1: $(0.40 \text{ in.}/1.00 \text{ in.})(-277 \text{ kip-ft}) = -111 \text{ kip-ft}$
 - Effect of unfactored S_{tr} at Pier 1: $(0.80 \text{ in.}/1.00 \text{ in.})(555 \text{ kip-ft}) = 444 \text{ kip-ft}$
 - Effect of unfactored S_{tr} at Abutment 1: $(0.30 \text{ in.}/1.00 \text{ in.})(-277 \text{ kip-ft}) = -83 \text{ kip-ft}$
 - Total unfactored effect of S_{tr} at all supports:
 - +ve value: $0 \text{ kip-ft} + 444 \text{ kip-ft} = 444 \text{ kip-ft}$
 - -ve value: $-111 \text{ kip-ft} - 83 \text{ kip-ft} = -194 \text{ kip-ft}$
 - Total factored effect of settlement using $\gamma_{SE} = 1.00 S_t$:
 - +ve value: $(1.60 \text{ in.}/1.00 \text{ in.})(555 \text{ kip-ft}) (1.00) = 888 \text{ kip-ft}$
 - -ve value: $(0.80 \text{ in.}/1.00 \text{ in.})(-277 \text{ kip-ft})(1.00) + (0.60 \text{ in.}/1.00 \text{ in.})(-277 \text{ kip-ft}) (1.00) = -388 \text{ kip-ft}$
 - Total factored effect of settlement using $\gamma_{SE} = 1.25$ and S_{tr} :
 - +ve value: $(0.80 \text{ in.}/1.00 \text{ in.}) (1.25)(555 \text{ kip-ft}) = 555 \text{ kip-ft}$
 - -ve value: $(0.40 \text{ in.}/1.00 \text{ in.}) (1.25)(-277 \text{ kip-ft}) + (0.30 \text{ in.}/1.00 \text{ in.}) (1.25) (-277 \text{ kip-ft}) = 242 \text{ kip-ft}$

⁴ Values are rounded to nearest whole number.

- For comparison purposes, three cases of Service 1 and Strength 1 load combinations were developed as follows in Tables E1-M6 and E1-M7:
 - **Case 1:** DL + LL with no settlement. This case represents designs performed without consideration of settlement. In this case, dead load and live load are factored according to the load factors for Service I and Strength I load combinations.
 - **Case 2:** DL + LL with settlement using load factor $\gamma_{SE} = 1.0$. This case represents the procedure as per the current *AASHTO LRFD* provisions related to incorporation of the settlement (assuming $\gamma_{SE} = 1.0$). In this case, (a) dead load and live load are factored according to the load factors for Service I and Strength I load combinations, and (b) the total settlement, S_t , with a load factor $\gamma_{SE} = 1.0$ is used.
 - **Case 3:** DL + LL with settlement using construction-point concept and method-specific load factor γ_{SE} . This case represents the proposed design procedure that incorporates the construction-point concept along with method-specific load factor γ_{SE} . In this case, (a) dead load and live load are factored according to the load factors for Service I and Strength I load combinations, and (b) the relevant settlements, S_{tr} , is used with the load factor appropriate to the method used to estimate the settlement. In the examples, Schmertmann's method is assumed and, thus, a load factor $\gamma_{SE} = 1.25$ is assumed as noted earlier.

The numerical computations in Tables E1-M6 and E1-M7 are based on the equations in the first columns of these tables and the corresponding values from Table E1-M5. Consideration of individual settlements or groups of settlements is required by Article 3.12.6 of *AASHTO LRFD*. This is analogous to the S_f -0 concept in Chapter 12 in that the purpose of the provision is to account for the possibility that some of the foundation units may settle less than predicted, or even undergo no settlement. Use of the word "consideration" denotes that judgment may be used to reduce the number of conditions to be investigated. For demonstration purposes these examples were developed assuming that the worst possible set of settlements for each individual force effect was realized. This was done by summing all the positive and all the negative moments and shears at each point of interest in the example structure. The sum of the positive settlement contributions, factored as shown, were combined with the dead load and positive live load contributions to determine the maximum value of the force effect under consideration. The sum of the negative settlement contributions, factored as shown, was combined with the dead load and the negative live contributions to determine the minimum value of the force effect under consideration.

- The numerical computations in Tables E1-S5, E1-S6 and E1-S7 follow the approach similar to the corresponding tables E1-M5, E1-M6 and E1-M7, respectively.

C.1 Evaluation of Results

For each example, the following two comparisons are made for both of the moment and shear results:

- Case 3 is compared to Case 1 to show the difference between the results after incorporating the proposed design procedures and designs performed ignoring settlement.
- Case 3 is compared to Case 1 to show the difference between the results after incorporating the proposed design procedures and designs performed using current design procedures and taking settlement into consideration.

As all results are compared for both the maximum and minimum values of the force effects, the ratios representing the controlling force effects are shown in bold typeface. Settlement should not be used to reduce the permanent force effects. This is the purpose of the requirement that "Load combinations which include settlement shall also be applied without settlement." in Article 3.4.1 of *AASHTO LRFD*. For ease of following the calculations, this requirement was not implemented in the examples. However, the values of various ratios not affected by the provision were highlighted.

The following general observations are made:

1. Generally, the values from Case 3 may be larger or smaller than the results from Case 1 or Case 2 depending on the magnitude of the differential settlement and the direction of the angular rotation in different spans.
2. For the three steel I-girder bridges with the settlements assumed for the examples, the difference in the controlling moments and shears is not significant for Bridges 2 and 3 regardless of whether Case 3 is compared to Case 1 or Case 2. The difference is more significant for Bridge 1. This indicates that the factored design force effects for shorter spans will be affected by the proposed provisions more than longer spans.
3. In performing the design, if including the settlement decreases a certain force effect at a section, the force effect calculated ignoring the effect of the settlement should be used for the design.
4. Based on a comparison of the ratios, it is observed that the induced force effects for Case 3 ($\gamma_{SE} > 1.0$) as compared to Case 2 ($\gamma_{SE} = 1.0$) in accordance with current *AASHTO LRFD* specifications are not in direct proportion to the value of the load factor, i.e., $\gamma_{SE} = 1.25$. This was expected as the effect of the settlement is one of several components combined to determine the design load effect for a load combination. The exact value of the change in total force effects would be a function of many factors such as bridge

superstructure type and configuration, substructure type, foundation type, and use of construction-point concept. In general, the use of the construction-point concept reduces the effect of the settlement on the total force effects. In the example problems, the changes in total force effects did not significantly alter the controlling values for design. In such cases, consideration could be given to use of more efficient and cost-effective foundation types as well as other appropriate members of the bridge structure.

Example 1**Two-Span Bridge, Span Lengths 50 ft and 50 ft, Girder Spacing 7 ft-2 in.****Moment Comparison****Table E1-M1**

Moment (kip-ft)				
		Span 1 - 0.4L	Pier 1	Span 2 - 0.6L
Unfactored DL moment (No Settlement)		256	-453	256
Unfactored LL moment	+ve	486	0	486
	-ve	-116	-370	-116
Unfactored effect of 1 in. settlement at Abutment 1		-111	-277	-111
Unfactored effect of 1 in. settlement at Pier 1		222	555	222
Unfactored effect of 1 in. settlement at Abutment 2		-111	-277	-111

Predicted Unfactored Total Settlements, S_t

Use appropriate method. Schmertmann method is assumed for this example.

Estimated Unfactored Relevant Settlements, S_{tr}

Should be calculated based on the site-specific soil conditions and loads at different stages of the bridge. Assumed as 50% of S_t for this example.

Factored Relevant Settlements, S_f

For $\beta = 0.50$ and Schmertmann method, the load factor $\gamma_{SE} = 1.25$

Table E1-M2

Predicted Unfactored Total Settlements, S_t (in.)		
Abutment 1	Pier 1	Abutment 2
0.80	1.60	0.60

Table E1-M3

Estimated Unfactored Relevant Settlements, S_{tr} (in.)		
Abutment 1	Pier 1	Abutment 2
0.40	0.80	0.30

Table E1-M4

Factored Relevant Settlements, S_f (in.)		
Abutment 1	Pier 1	Abutment 2
0.50	1.00	0.38

Table E1-M5

		Moment (kip-ft)		
		Span 1 - 0.4L	Pier 1	Span 2 - 0.6L
Unfactored DL moment (No Settlement)		256	-453	256
Unfactored LL moment	+ve	486	0	486
	-ve	-116	-370	-116
Effect of unfactored S_{tr} at Abutment 1		-44	-111	-44
Effect of unfactored S_{tr} at Pier 1		178	444	178
Effect of unfactored S_{tr} at Abutment 2		-33	-83	-33
Total unfactored effect of S_{tr} at all supports	+ve	178	444	178
	-ve	-78	-194	-78
Total factored effect of settlement using $\gamma_{SE} = 1.00$ and S_t	+ve	355	888	355
	-ve	-155	-388	-155
Total factored effect of settlement using $\gamma_{SE} = 1.25$ and S_{tr}	+ve	222	555	222
	-ve	-97	-242	-97

Table E1-M6

Service I Comparison

		Moment (kip-ft)		
		Span 1 - 0.4L	Pier 1	Span 2 - 0.6L
Case 1: 1.0 DL + 1.0 LL without SE	Max	742	-453	742
	Min	140	-823	140
Case 2: 1.0 DL + 1.0 LL + γ_{SE} SE (use $\gamma_{SE} = 1.00$ and S_t)	Max	1097	435	1097
	Min	-15	-1211	-15
Case 3: 1.0 DL + 1.0 LL + γ_{SE} SE (use $\gamma_{SE} = 1.25$ and S_{tr})	Max	964	102	964
	Min	43	-1065	43
Ratio of Case 3 to Case 1	Max	1.299	-0.225	1.299
	Min	0.306	1.295	0.306
Ratio of Case 3 to Case 2	Max	0.879	0.234	0.879
	Min	-2.784	0.880	-2.784

Table E1-M7

Strength I Comparison

		Moment (kip-ft)		
		Span 1 - 0.4L	Pier 1	Span 2 - 0.6L
Case 1: 1.25 DL + 1.75 LL without SE	Max	1171	-566	1171
	Min	117	-1214	117
Case 2: 1.25 DL + 1.75 LL + γ_{SE} SE (use $\gamma_{SE} = 1.00$ and S_t)	Max	1526	322	1526
	Min	-38	-1602	-38
Case 3: 1.25 DL + 1.75 LL + γ_{SE} SE (use $\gamma_{SE} = 1.25$ and S_{tr})	Max	1393	-11	1393
	Min	20	-1456	20
Ratio of Case 3 to Case 1	Max	1.190	0.020	1.190
	Min	0.170	1.200	0.170
Ratio of Case 3 to Case 2	Max	0.913	-0.035	0.913
	Min	-0.518	0.909	-0.518

Example 1**Two-Span Bridge, Span Lengths 50 ft and 50 ft, Girder Spacing 7 ft-2 in.****Shear Comparison****Table E1-S1**

Shear (kip)					
		Right of Abutment 1	Left of Pier 1	Right of Pier 1	Left of Abutment 2
Unfactored DL shear (No settlement)		27.4	-45.5	45.5	-27.4
Unfactored LL shear	+ve	67.4	0.0	79.1	7.5
	-ve	-7.5	-79.1	0.0	-67.4
Unfactored effect of 1 in. settlement at Abutment 1		-5.5	-5.5	5.5	5.5
Unfactored effect of 1 in. settlement at Pier 1		11.1	11.1	-11.1	-11.1
Unfactored effect of 1 in. settlement at Abutment 2		-5.5	-5.5	5.5	5.5

Predicted Unfactored Total Settlements, S_t

Use appropriate method. Schmertmann method is assumed for this example.

Estimated Unfactored Relevant Settlements, S_{tr}

Should be calculated based on the site-specific soil conditions and loads at different stages of the bridge. Assumed as 50% of S_t for this example.

Factored Relevant Settlements, S_f

For $\beta = 0.50$ and Schmertmann method, the load factor $\gamma_{SE} = 1.25$

Table E1-S2

Predicted Unfactored Total Settlements, S_t (in.)		
Abutment 1	Pier 1	Abutment 2
0.80	1.60	0.60

Table E1-S3

Estimated Unfactored Relevant Settlements, S_{tr} (in.)		
Abutment 1	Pier 1	Abutment 2
0.40	0.80	0.30

Table E1-S4

Factored Relevant Settlements, S_f (in.)		
Abutment 1	Pier 1	Abutment 2
0.50	1.00	0.38

Table E1-S5

		Shear (kip)			
		Right of Abutment 1	Left of Pier 1	Right of Pier 1	Left of Abutment 2
Unfactored DL shear (No settlement)		27.4	-45.5	45.5	-27.4
Unfactored LL shear	+ve	67.4	0.0	79.1	7.5
	-ve	-7.5	-79.1	0.0	-67.4
Effect of unfactored S_{tr} at Abutment 1		-2.2	-2.2	2.2	2.2
Effect of unfactored S_{tr} at Pier 1		8.9	8.9	-8.9	-8.9
Effect of unfactored S_{tr} at Abutment 2		-1.7	-1.7	1.7	1.7
Total unfactored effect of S_{tr} at all supports	+ve	9	9	4	4
	-ve	-4	-4	-9	-9
Total factored effect of settlement using $\gamma_{SE} = 1.00$ and S_t	+ve	18	18	8	8
	-ve	-8	-8	-18	-18
Total factored effect of settlement using $\gamma_{SE} = 1.25$ and S_{tr}	+ve	11	11	5	5
	-ve	-5	-5	-11	-11

Table E1-S6

		Shear (kip)			
		Right of Abutment 1	Left of Pier 1	Right of Pier 1	Left of Abutment 2
Service I Comparison					
Case 1: 1.0 DL + 1.0 LL without SE	Max	94.8	-45.5	124.6	-19.9
	Min	19.9	-124.6	45.5	-94.8
Case 2: 1.0 DL + 1.0 LL + γ_{SE} SE (use $\gamma_{SE} = 1.00$ and S_t)	Max	112.5	-27.8	132.4	-12.2
	Min	12.2	-132.4	27.8	-112.5
Case 3: 1.0 DL + 1.0 LL + γ_{SE} SE (use $\gamma_{SE} = 1.25$ and S_{tr})	Max	105.9	-34.4	129.5	-15.1
	Min	15.1	-129.5	34.4	-105.9
Ratio of Case 3 to Case 1	Max	1.117	0.756	1.039	0.757
	Min	0.757	1.039	0.756	1.117
Ratio of Case 3 to Case 2	Max	0.941	1.240	0.978	1.239
	Min	1.239	0.978	1.240	0.941

Table E1-S7

		Shear (kip)			
		Right of Abutment 1	Left of Pier 1	Right of Pier 1	Left of Abutment 2
Strength I Comparison					
Case 1: 1.25 DL + 1.75 LL without SE	Max	152.2	-56.9	195.3	-21.2
	Min	21.2	-195.3	56.9	-152.2
Case 2: 1.25 DL + 1.75 LL + γ_{SE} SE (use $\gamma_{SE} = 1.00$ and S_t)	Max	169.9	-39.1	203.1	-13.4
	Min	13.4	-203.1	39.1	-169.9
Case 3: 1.25 DL + 1.75 LL + γ_{SE} SE (use $\gamma_{SE} = 1.25$ and S_{tr})	Max	163.3	-45.8	200.2	-16.3
	Min	16.3	-200.2	45.8	-163.3
Ratio of Case 3 to Case 1	Max	1.073	0.805	1.025	0.771
	Min	0.771	1.025	0.805	1.073
Ratio of Case 3 to Case 2	Max	0.961	1.170	0.986	1.217
	Min	1.217	0.986	1.170	0.961

Example 2**Four-Span Bridge, Span Lengths 168 FT, 293 FT, 335 FT, and 165 Ft, Girder Spacing 12 ft-3 in.****Moment Comparison****Table E2-M1**

		Moment (kip-ft)						
		Span 1 - 0.4L	Pier 1	Span 2 - 0.5L	Pier 2	Span 3 - 0.5L	Pier 3	Span 4 - 0.8L
Unfactored DL moment (No Settlement)		3884	-15561	8001	-33891	13513	-25824	1651
Unfactored LL moment	+ve	6401	2807	8639	1166	9741	2662	4379
	-ve	-3171	-10609	-3174	-13208	-2257	-14582	-2270
Unfactored effect of 1 in. settlement at Abutment 1		-329	-822	-273	278	84	-110	-22
Unfactored effect of 1 in. settlement at Pier 1		702	1753	609	-534	-161	212	43
Unfactored effect of 1 in. settlement at Pier 2		-469	-1174	-79	1016	344	-328	-65
Unfactored effect of 1 in. settlement at Pier 3		192	452	-479	-1409	321	2050	411
Unfactored effect of 1 in. settlement at Abutment 2		-82	-208	221	651	-587	-1825	-364

Predicted Unfactored Total Settlements, S_t

Use appropriate method. Schmertmann method is assumed for this example.

Table E2-M2

Predicted Unfactored Total Settlements, S_t (in.)				
Abutment 1	Pier 1	Pier 2	Pier 3	Abutment 2
1.90	3.90	4.80	1.90	2.50

Estimated Unfactored Relevant Settlements, S_{tr}

Should be calculated based on the site-specific soil conditions and loads at different stages of the bridge. Assumed as 50% of S_t for this example.

Table E2-M3

Estimated Unfactored Relevant Settlements, S_{tr} (in.)				
Abutment 1	Pier 1	Pier 2	Pier 3	Abutment 2
0.95	1.95	2.40	0.95	1.25

Factored Relevant Settlements, S_f

For $\beta = 0.50$ and Schmertmann method, the load factor $\gamma_{SE} = 1.25$

Table E2-M4

Factored Relevant Settlements, S_f (in.)				
Abutment 1	Pier 1	Pier 2	Pier 3	Abutment 2
1.19	2.44	3.00	1.19	1.56

		Moment (kip-ft)						
		Span 1 - 0.4L	Pier 1	Span 2 - 0.5L	Pier 2	Span 3 - 0.5L	Pier 3	Span 4 - 0.8L
Unfactored DL moment (No Settlement)		3884	-15561	8001	-33891	13513	-25824	1651
Unfactored LL moment	+ve	6401	2807	8639	1166	9741	2662	4379
	-ve	-3171	-10609	-3174	-13208	-2257	-14582	-2270
Effect of unfactored S_{tr} at Abutment 1		-313	-781	-259	264	80	-105	-21
Effect of unfactored S_{tr} at Pier 1		1369	3418	1188	-1041	-314	413	84
Effect of unfactored S_{tr} at Pier 2		-1126	-2818	-190	2438	826	-787	-156
Effect of unfactored S_{tr} at Pier 3		182	429	-455	-1339	305	1948	390
Effect of unfactored S_{tr} at Abutment 2		-103	-260	276	814	-734	-2281	-455
Total unfactored effect of S_{tr} at all supports	+ve	1551	3848	1464	3516	1210	2361	474
	-ve	-1541	-3859	-904	-2380	-1048	-3173	-632
Total factored effect of settlement using $\gamma_{SE} = 1.00$ and S_t	+ve	3103	7696	2928	7033	2421	4722	949
	-ve	-3081	-7717	-1808	-4760	-2095	-6346	-1264
Total factored effect of settlement using $\gamma_{SE} = 1.25$ and S_{tr}	+ve	1939	4810	1830	4395	1513	2951	593
	-ve	-1926	-4823	-1130	-2975	-1310	-3966	-790

		Moment (kip-ft)						
		Span 1 - 0.4L	Pier 1	Span 2 - 0.5L	Pier 2	Span 3 - 0.5L	Pier 3	Span 4 - 0.8L
Service I Comparison								
Case 1: 1.0 DL + 1.0 LL without SE	Max	10285	-12754	16640	-32725	23254	-23162	6030
	Min	713	-26170	4827	-47099	11256	-40406	-619
Case 2: 1.0 DL + 1.0 LL + γ_{SE} SE (use $\gamma_{SE} = 1.00$ and S_t)	Max	13388	-5059	19568	-25693	25675	-18440	6979
	Min	-2368	-33887	3019	-51859	9161	-46752	-1883
Case 3: 1.0 DL + 1.0 LL + γ_{SE} SE (use $\gamma_{SE} = 1.25$ and S_{tr})	Max	12224	-7944	18470	-28330	24767	-20211	6623
	Min	-1213	-30993	3697	-50074	9946	-44372	-1409
Ratio of Case 3 to Case 1	Max	1.189	0.623	1.110	0.866	1.065	0.873	1.098
	Min	-1.701	1.184	0.766	1.063	0.884	1.098	2.276
Ratio of Case 3 to Case 2	Max	0.913	1.570	0.944	1.103	0.965	1.096	0.949
	Min	0.512	0.915	1.225	0.966	1.086	0.949	0.748

		Moment (kip-ft)						
		Span 1 - 0.4L	Pier 1	Span 2 - 0.5L	Pier 2	Span 3 - 0.5L	Pier 3	Span 4 - 0.8L
Strength I Comparison								
Case 1: 1.25 DL + 1.75 LL without SE	Max	16057	-14539	25120	-40323	33938	-27622	9727
	Min	-694	-38017	4447	-65478	12942	-57799	-1909
Case 2: 1.25 DL + 1.75 LL + γ_{SE} SE (use $\gamma_{SE} = 1.00$ and S_t)	Max	19159	-6844	28047	-33291	36359	-22900	10676
	Min	-3776	-45734	2639	-70237	10846	-64144	-3173
Case 3: 1.25 DL + 1.75 LL + γ_{SE} SE (use $\gamma_{SE} = 1.25$ and S_{tr})	Max	17996	-9729	26949	-35928	35451	-24670	10320
	Min	-2620	-42840	3317	-68453	11632	-61765	-2699
Ratio of Case 3 to Case 1	Max	1.121	0.669	1.073	0.891	1.045	0.893	1.061
	Min	3.774	1.127	0.746	1.045	0.899	1.069	1.414
Ratio of Case 3 to Case 2	Max	0.939	1.422	0.961	1.079	0.975	1.077	0.967
	Min	0.694	0.937	1.257	0.975	1.072	0.963	0.851

Example 2**Four-Span Bridge, Span Lengths 168 FT, 293 FT, 335 FT, and 165 Ft, Girder Spacing 12 ft-3 in.****Shear Comparison****Table E2-S1**

		Shear (kip)							
		Right of Abutment 1	Left of Pier 1	Right of Pier 1	Left of Pier 2	Right of Pier 2	Left of Pier 3	Right of Pier 3	Left of Abutment 2
Unfactored DL shear (No settlement)		157.1	-345.5	384.0	-526.5	564.0	-502.5	428.5	-100.7
Unfactored LL shear	+ve	159.5	15.4	213.9	12.9	232.3	26.0	203.7	63.1
	-ve	-43.4	-191.7	-36.3	-224.4	-9.9	-229.9	-14.8	-158.7
Unfactored effect of 1 in. settlement at Abutment 1		-4.9	-4.9	3.8	3.8	-1.2	-1.2	0.7	0.7
Unfactored effect of 1 in. settlement at Pier 1		10.4	10.4	-7.8	-7.8	2.2	2.2	-1.3	-1.3
Unfactored effect of 1 in. settlement at Pier 2		-7.0	-7.0	7.5	7.5	-4.0	-4.0	2.0	2.0
Unfactored effect of 1 in. settlement at Pier 3		2.7	2.7	-6.4	-6.4	10.3	10.3	-12.4	-12.4
Unfactored effect of 1 in. settlement at Abutment 2		-1.2	-1.2	2.9	2.9	-7.4	-7.4	11.1	11.1

Predicted Unfactored Total Settlements, S_t

Use appropriate method. Schmertmann method is assumed for this example.

Table E2-S2

Predicted Unfactored Total Settlements, S_t (in.)				
Abutment 1	Pier 1	Pier 2	Pier 3	Abutment 2
1.90	3.90	4.80	1.90	2.50

Estimated Unfactored Relevant Settlements, S_{tr} Should be calculated based on the site-specific soil conditions and loads at different stages of the bridge. Assumed as 50% of S_t for this example.**Table E2-S3**

Estimated Unfactored Relevant Settlements, S_{tr} (in.)				
Abutment 1	Pier 1	Pier 2	Pier 3	Abutment 2
0.95	1.95	2.40	0.95	1.25

Factored Relevant Settlements, S_f For $\beta = 0.50$ and Schmertmann method, the load factor $\gamma_{SE} = 1.25$ **Table E2-S4**

Factored Relevant Settlements, S_f (in.)				
Abutment 1	Pier 1	Pier 2	Pier 3	Abutment 2
1.19	2.44	3.00	1.19	1.56

		Shear (kip)							
		Right of Abutment 1	Left of Pier 1	Right of Pier 1	Left of Pier 2	Right of Pier 2	Left of Pier 3	Right of Pier 3	Left of Abutment 2
Unfactored DL shear (No settlement)		157.1	-345.5	384.0	-526.5	564.0	-502.5	428.5	-100.7
Unfactored LL shear	+ve	159.5	15.4	213.9	12.9	232.3	26.0	203.7	63.1
	-ve	-43.4	-191.7	-36.3	-224.4	-9.9	-229.9	-14.8	-158.7
Effect of unfactored S_{tr} at Abutment 1		-4.7	-4.7	3.6	3.6	-1.1	-1.1	0.6	0.6
Effect of unfactored S_{tr} at Pier 1		20.4	20.4	-15.2	-15.2	4.3	4.3	-2.5	-2.5
Effect of unfactored S_{tr} at Pier 2		-16.8	-16.8	17.9	17.9	-9.6	-9.6	4.8	4.8
Effect of unfactored S_{tr} at Pier 3		2.5	2.5	-6.0	-6.0	9.8	9.8	-11.8	-11.8
Effect of unfactored S_{tr} at Abutment 2		-1.6	-1.6	3.7	3.7	-9.2	-9.2	13.8	13.8
Total unfactored effect of S_{tr} at all supports	+ve	23	23	25	25	14	14	19	19
	-ve	-23	-23	-21	-21	-20	-20	-14	-14
Total factored effect of settlement using $\gamma_{SE} = 1.00$ and S_t	+ve	46	46	50	50	28	28	38	38
	-ve	-46	-46	-43	-43	-40	-40	-29	-29
Total factored effect of settlement using $\gamma_{SE} = 1.25$ and S_{tr}	+ve	29	29	31	31	18	18	24	24
	-ve	-29	-29	-27	-27	-25	-25	-18	-18

		Shear (kip)							
		Right of Abutment 1	Left of Pier 1	Right of Pier 1	Left of Pier 2	Right of Pier 2	Left of Pier 3	Right of Pier 3	Left of Abutment 2
Service I Comparison									
Case 1: 1.0 DL + 1.0 LL without SE	Max	317	-330	598	-514	796	-476	632	-38
	Min	114	-537	348	-751	554	-732	414	-259
Case 2: 1.0 DL + 1.0 LL + γ_{SE} SE (use $\gamma_{SE} = 1.00$ and S_t)	Max	362	-284	648	-463	825	-448	671	1
	Min	68	-583	305	-794	514	-772	385	-288
Case 3: 1.0 DL + 1.0 LL + γ_{SE} SE (use $\gamma_{SE} = 1.25$ and S_{tr})	Max	345	-302	629	-482	814	-459	656	-14
	Min	85	-566	321	-778	529	-757	396	-277
Ratio of Case 3 to Case 1	Max	1.090	0.913	1.053	0.939	1.022	0.963	1.038	0.362
	Min	0.747	1.053	0.924	1.035	0.955	1.034	0.957	1.069
Ratio of Case 3 to Case 2	Max	0.953	1.060	0.971	1.041	0.987	1.024	0.979	-17.149
	Min	1.254	0.970	1.052	0.980	1.029	0.981	1.028	0.963

		Shear (kip)							
		Right of Abutment 1	Left of Pier 1	Right of Pier 1	Left of Pier 2	Right of Pier 2	Left of Pier 3	Right of Pier 3	Left of Abutment 2
Strength I Comparison									
Case 1: 1.25 DL + 1.75 LL without SE	Max	475	-405	854	-636	1112	-583	892	-16
	Min	120	-767	416	-1051	688	-1030	510	-404
Case 2: 1.25 DL + 1.75 LL + γ_{SE} SE (use $\gamma_{SE} = 1.00$ and S_t)	Max	521	-359	905	-585	1140	-554	931	23
	Min	74	-813	374	-1093	648	-1070	481	-432
Case 3: 1.25 DL + 1.75 LL + γ_{SE} SE (use $\gamma_{SE} = 1.25$ and S_{tr})	Max	504	-376	886	-604	1129	-565	916	8
	Min	92	-796	390	-1078	663	-1055	492	-422
Ratio of Case 3 to Case 1	Max	1.060	0.929	1.037	0.951	1.016	0.970	1.027	-0.544
	Min	0.761	1.037	0.936	1.025	0.964	1.024	0.965	1.044
Ratio of Case 3 to Case 2	Max	0.967	1.048	0.979	1.032	0.991	1.019	0.985	0.370
	Min	1.231	0.979	1.043	0.985	1.023	0.986	1.022	0.975

Example 3**Five-Span Bridge, Span Lengths 120 ft, 140 ft, 140 ft, 140 ft, and 120 ft, Girder Spacing 11 ft-2 in.****Moment Comparison**

Table E3-M1

		Moment (kip-ft)								
		Span 1 - 0.4L	Pier 1	Span 2 - 0.5L	Pier 2	Span 3 - 0.5L	Pier 3	Span 4 - 0.5L	Pier 4	Span 5 - 0.6L
Unfactored DL moment (No Settlement)		2524	-4544	1807	-4213	1967	-4224	1822	-4522	2522
Unfactored LL moment	+ve	2369	432	2186	553	2231	542	2194	420	2357
	-ve	-610	-2629	-694	-2653	-710	-2653	-693	-2612	-591
Unfactored effect of 1 in. settlement at Abutment 1		-368	-920	-330	259	94	-72	-26	20	8
Unfactored effect of 1 in. settlement at Pier 1		585	1462	332	-797	-287	222	80	-62	-25
Unfactored effect of 1 in. settlement at Pier 2		-277	-691	192	1075	194	-687	-248	192	77
Unfactored effect of 1 in. settlement at Pier 3		77	194	-246	-689	195	1077	196	-684	-274
Unfactored effect of 1 in. settlement at Pier 4		-25	-62	82	225	-287	-799	334	1468	587
Unfactored effect of 1 in. settlement at Abutment 2		8	22	-26	-73	94	260	-337	-933	-373

Predicted Unfactored Total Settlements, S_t

Use appropriate method. Schmertmann method is assumed for this example.

Table E3-M2

Predicted Unfactored Total Settlements, S_t (in.)					
Abutment 1	Pier 1	Pier 2	Pier 3	Pier 4	Abutment 2
0.90	1.50	1.80	1.00	2.30	1.40

Estimated Unfactored Relevant Settlements, S_{tr} Should be calculated based on the site-specific soil conditions and loads at different stages of the bridge. Assumed as 50% of S_t for this example.

Table E3-M3

Estimated Unfactored Relevant Settlements, S_{tr} (in.)					
Abutment 1	Pier 1	Pier 2	Pier 3	Pier 4	Abutment 2
0.45	0.75	0.90	0.50	1.15	0.70

Factored Relevant Settlements, S_f For $\beta = 0.50$ and Schmertmann method, the load factor $\gamma_{SE} = 1.25$

Table E3-M4

Factored Relevant Settlements, S_f (in.)					
Abutment 1	Pier 1	Pier 2	Pier 3	Pier 4	Abutment 2
0.56	0.94	1.13	0.63	1.44	0.88

		Moment (kip-ft)								
		Span 1 - 0.4L	Pier 1	Span 2 - 0.5L	Pier 2	Span 3 - 0.5L	Pier 3	Span 4 - 0.5L	Pier 4	Span 5 - 0.6L
Unfactored DL moment (No Settlement)		2524	-4544	1807	-4213	1967	-4224	1822	-4522	2522
Unfactored LL moment	+ve	2369	432	2186	553	2231	542	2194	420	2357
	-ve	-610	-2629	-694	-2653	-710	-2653	-693	-2612	-591
Effect of unfactored S_{tr} at Abutment 1		-166	-414	-149	117	42	-32	-12	9	4
Effect of unfactored S_{tr} at Pier 1		439	1097	249	-598	-215	167	60	-47	-19
Effect of unfactored S_{tr} at Pier 2		-249	-622	173	968	175	-618	-223	173	69
Effect of unfactored S_{tr} at Pier 3		39	97	-123	-345	98	539	98	-342	-137
Effect of unfactored S_{tr} at Pier 4		-29	-71	94	259	-330	-919	384	1688	675
Effect of unfactored S_{tr} at Abutment 2		6	15	-18	-51	66	182	-236	-653	-261
Total unfactored effect of S_{tr} at all supports	+ve	483	1209	516	1343	380	887	542	1870	748
	-ve	-444	-1107	-290	-993	-545	-1570	-471	-1042	-417
Total factored effect of settlement using $\gamma_{SE} = 1.00$ and S_t	+ve	966	2418	1032	2686	760	1774	1084	3740	1496
	-ve	-887	-2214	-579	-1987	-1091	-3139	-942	-2083	-834
Total factored effect of settlement using $\gamma_{SE} = 1.25$ and S_{tr}	+ve	604	1511	645	1679	475	1109	678	2338	935
	-ve	-555	-1384	-362	-1242	-682	-1962	-589	-1302	-521

		Moment (kip-ft)								
		Span 1 - 0.4L	Pier 1	Span 2 - 0.5L	Pier 2	Span 3 - 0.5L	Pier 3	Span 4 - 0.5L	Pier 4	Span 5 - 0.6L
Case 1: 1.0 DL + 1.0 LL without SE	Max	4893	-4112	3993	-3660	4198	-3682	4016	-4102	4879
	Min	1914	-7173	1113	-6866	1257	-6877	1129	-7134	1931
Case 2: 1.0 DL + 1.0 LL + γ_{SE} SE (use $\gamma_{SE} = 1.00$ and S_t)	Max	5859	-1694	5025	-974	4958	-1908	5100	-362	6375
	Min	1027	-9387	534	-8853	166	-10016	187	-9217	1097
Case 3: 1.0 DL + 1.0 LL + γ_{SE} SE (use $\gamma_{SE} = 1.25$ and S_{tr})	Max	5497	-2601	4638	-1982	4673	-2573	4694	-1765	5814
	Min	1359	-8557	751	-8108	575	-8839	541	-8436	1410
Ratio of Case 3 to Case 1	Max	1.123	0.633	1.162	0.541	1.113	0.699	1.169	0.430	1.192
	Min	0.710	1.193	0.675	1.181	0.458	1.285	0.479	1.183	0.730
Ratio of Case 3 to Case 2	Max	0.938	1.535	0.923	2.034	0.942	1.349	0.920	4.874	0.912
	Min	1.324	0.912	1.407	0.916	3.458	0.882	2.884	0.915	1.285

		Moment (kip-ft)								
		Span 1 - 0.4L	Pier 1	Span 2 - 0.5L	Pier 2	Span 3 - 0.5L	Pier 3	Span 4 - 0.5L	Pier 4	Span 5 - 0.6L
Case 1: 1.25 DL + 1.75 LL without SE	Max	7301	-4924	6084	-4299	6363	-4332	6117	-4918	7277
	Min	2088	-10281	1044	-9909	1216	-9923	1065	-10224	2118
Case 2: 1.25 DL + 1.75 LL + γ_{SE} SE (use $\gamma_{SE} = 1.00$ and S_t)	Max	8266	-2506	7116	-1613	7123	-2558	7201	-1178	8773
	Min	1200	-12495	465	-11896	126	-13062	123	-12307	1285
Case 3: 1.25 DL + 1.75 LL + γ_{SE} SE (use $\gamma_{SE} = 1.25$ and S_{tr})	Max	7904	-3413	6729	-2620	6838	-3223	6795	-2580	8212
	Min	1533	-11665	682	-11151	535	-11885	476	-11526	1597
Ratio of Case 3 to Case 1	Max	1.083	0.693	1.106	0.610	1.075	0.744	1.111	0.525	1.128
	Min	0.734	1.135	0.653	1.125	0.440	1.198	0.447	1.127	0.754
Ratio of Case 3 to Case 2	Max	0.956	1.362	0.946	1.624	0.960	1.260	0.944	2.191	0.936
	Min	1.277	0.934	1.467	0.937	4.255	0.910	3.867	0.937	1.243

Example 3

Five-Span Bridge, Span Lengths 120 ft, 140 ft, 140 ft, 140 ft, and 120 ft, Girder Spacing 11 ft-2 in.

Shear Comparison

Table E3-S1.2

		Shear (kip)									
		Right of Abutment 1	Left of Pier 1	Right of Pier 1	Left of Pier 2	Right of Pier 2	Left of Pier 3	Right of Pier 3	Left of Pier 4	Right of Pier 4	Left of Abutment 2
Unfactored DL shear (No settlement)		112.6	-190.3	180.6	-175.9	178.1	-178.3	175.5	-180.9	189.3	-112.6
Unfactored LL shear	+ve	125.0	4.6	147.1	18.3	149.4	19.0	148.3	17.6	145.4	15.8
	-ve	-16.3	-145.4	-18.0	-146.5	-19.4	-147.6	-18.5	-146.8	-4.5	-124.8
Unfactored effect of 1 in. settlement at Abutment 1		-7.7	-7.7	8.4	8.4	-2.4	-2.4	0.7	0.7	-0.2	-0.2
Unfactored effect of 1 in. settlement at Pier 1		12.2	12.2	-16.1	-16.1	7.3	7.3	-2.0	-2.0	0.5	0.5
Unfactored effect of 1 in. settlement at Pier 2		-5.8	-5.8	12.6	12.6	-12.6	-12.6	6.3	6.3	-1.6	-1.6
Unfactored effect of 1 in. settlement at Pier 3		1.6	1.6	-6.3	-6.3	12.6	12.6	-12.6	-12.6	5.7	5.7
Unfactored effect of 1 in. settlement at Pier 4		-0.5	-0.5	2.1	2.1	-7.3	-7.3	16.2	16.2	-12.2	-12.2
Unfactored effect of 1 in. settlement at Abutment 2		0.2	0.2	-0.7	-0.7	2.4	2.4	-8.5	-8.5	7.8	7.8

Predicted Unfactored Total Settlements, S_t

Use appropriate method. Schmertmann method is assumed for this example.

Table E3-S2

Predicted Unfactored Total Settlements, S_t (in.)					
Abutment 1	Pier 1	Pier 2	Pier 3	Pier 4	Abutment 2
0.90	1.50	1.80	1.00	2.30	1.40

Estimated Unfactored Relevant Settlements, S_{tr}

Should be calculated based on the site-specific soil conditions and loads at different stages of the bridge. Assumed as 50% of S_t for this example.

Table E3-S3

Estimated Unfactored Relevant Settlements, S_{tr} (in.)					
Abutment 1	Pier 1	Pier 2	Pier 3	Pier 4	Abutment 2
0.45	0.75	0.90	0.50	1.15	0.70

Factored Relevant Settlements, S_f

For $\beta = 0.50$ and Schmertmann method, the load factor $\gamma_{SE} = 1.25$

Table E3-S4

Factored Relevant Settlements, S_f (in.)					
Abutment 1	Pier 1	Pier 2	Pier 3	Pier 4	Abutment 2
0.56	0.94	1.13	0.63	1.44	0.88

Table E3-S5

		Shear (kip)									
		Right of Abutment 1	Left of Pier 1	Right of Pier 1	Left of Pier 2	Right of Pier 2	Left of Pier 3	Right of Pier 3	Left of Pier 4	Right of Pier 4	Left of Abutment 2
Unfactored DL shear (No settlement)		112.6	-190.3	180.6	-175.9	178.1	-178.3	175.5	-180.9	189.3	-112.6
Unfactored LL shear	+ve	125.0	4.6	147.1	18.3	149.4	19.0	148.3	17.6	145.4	15.8
	-ve	-16.3	-145.4	-18.0	-146.5	-19.4	-147.6	-18.5	-146.8	-4.5	-124.8
Effect of unfactored S_{tr} at Abutment 1		-3.5	-3.5	3.8	3.8	-1.1	-1.1	0.3	0.3	-0.1	-0.1
Effect of unfactored S_{tr} at Pier 1		9.1	9.1	-12.1	-12.1	5.5	5.5	-1.5	-1.5	0.4	0.4
Effect of unfactored S_{tr} at Pier 2		-5.2	-5.2	11.4	11.4	-11.3	-11.3	5.7	5.7	-1.4	-1.4
Effect of unfactored S_{tr} at Pier 3		0.8	0.8	-3.1	-3.1	6.3	6.3	-6.3	-6.3	2.8	2.9
Effect of unfactored S_{tr} at Pier 4		-0.6	-0.6	2.4	2.4	-8.4	-8.4	18.6	18.6	-14.1	-14.1
Effect of unfactored S_{tr} at Abutment 2		0.1	0.1	-0.5	-0.5	1.7	1.7	-6.0	-6.0	5.4	5.4
Total unfactored effect of S_{tr} at all supports	+ve	10	10	18	18	13	13	25	25	9	9
	-ve	-9	-9	-16	-16	-21	-21	-14	-14	-16	-16
Total factored effect of settlement using $\gamma_{SE} = 1.00$ and S_t	+ve	20	20	35	35	27	27	49	49	17	17
	-ve	-19	-19	-31	-31	-42	-42	-28	-28	-31	-31
Total factored effect of settlement using $\gamma_{SE} = 1.25$ and S_{tr}	+ve	13	13	22	22	17	17	31	31	11	11
	-ve	-12	-12	-20	-20	-26	-26	-17	-17	-19	-19

Table E3-S6

		Shear (kip)									
		Right of Abutment 1	Left of Pier 1	Right of Pier 1	Left of Pier 2	Right of Pier 2	Left of Pier 3	Right of Pier 3	Left of Pier 4	Right of Pier 4	Left of Abutment 2
Service I Comparison											
Case 1: 1.0 DL + 1.0 LL without SE	Max	238	-186	328	-158	328	-159	324	-163	335	-97
	Min	96	-336	163	-322	159	-326	157	-328	185	-237
Case 2: 1.0 DL + 1.0 LL + γ_{SE} SE (use $\gamma_{SE} = 1.00$ and S_t)	Max	258	-166	363	-123	354	-132	373	-114	352	-79
	Min	78	-354	131	-354	117	-367	129	-355	154	-269
Case 3: 1.0 DL + 1.0 LL + γ_{SE} SE (use $\gamma_{SE} = 1.25$ and S_{tr})	Max	250	-173	350	-136	344	-142	354	-133	346	-86
	Min	85	-347	143	-342	133	-352	140	-345	165	-257
Ratio of Case 3 to Case 1	Max	1.053	0.932	1.067	0.861	1.051	0.895	1.095	0.812	1.032	0.888
	Min	0.880	1.034	0.879	1.061	0.836	1.080	0.890	1.053	0.895	1.082
Ratio of Case 3 to Case 2	Max	0.971	1.046	0.964	1.107	0.972	1.076	0.951	1.161	0.981	1.082
	Min	1.089	0.980	1.090	0.967	1.133	0.958	1.080	0.971	1.076	0.957

Table E3-S7

		Shear (kip)									
		Right of Abutment 1	Left of Pier 1	Right of Pier 1	Left of Pier 2	Right of Pier 2	Left of Pier 3	Right of Pier 3	Left of Pier 4	Right of Pier 4	Left of Abutment 2
Strength I Comparison											
Case 1: 1.25 DL + 1.75 LL without SE	Max	360	-230	483	-188	484	-190	479	-195	491	-113
	Min	112	-492	194	-476	189	-481	187	-483	229	-359
Case 2: 1.25 DL + 1.75 LL + γ_{SE} SE (use $\gamma_{SE} = 1.00$ and S_t)	Max	380	-210	518	-153	511	-163	528	-146	508	-96
	Min	94	-511	163	-508	147	-523	159	-511	198	-390
Case 3: 1.25 DL + 1.75 LL + γ_{SE} SE (use $\gamma_{SE} = 1.25$ and S_{tr})	Max	372	-217	505	-166	501	-173	510	-165	502	-102
	Min	101	-504	175	-496	163	-507	170	-500	209	-379
Ratio of Case 3 to Case 1	Max	1.035	0.945	1.045	0.883	1.035	0.911	1.064	0.843	1.022	0.904
	Min	0.897	1.023	0.899	1.041	0.862	1.054	0.908	1.036	0.915	1.054
Ratio of Case 3 to Case 2	Max	0.980	1.036	0.975	1.086	0.980	1.062	0.965	1.126	0.987	1.068
	Min	1.074	0.986	1.072	0.977	1.106	0.970	1.065	0.980	1.059	0.970

Appendix D
Proposed Modifications to Section 3 of AASHTO LRFD Bridge
Design Specifications

δ_f = factored deformation (rad. or in.) (Appendix C3)
 η_i = load modifier specified in Article 1.3.2; wall face batter (3.4.1) (3.11.5.9)

-
-
-
-
-

3.4—LOAD FACTORS AND COMBINATIONS

3.4.1—Load Factors and Load Combinations

C3.4.1

The total factored force effect shall be taken as:

$$Q = \sum \eta_i \gamma_i Q_i \quad (3.4.1-1)$$

The background for the load factors specified herein, and the resistance factors specified in other Sections of these Specifications is developed in Nowak (1992).

-
-
-
-
-

The evaluation of overall stability of retained fills, as well as earth slopes with or without a shallow or deep foundation unit should be investigated at the service limit state based on the Service I Load Combination and an appropriate resistance factor as specified in Article 11.5.6 and Article 11.6.2.3.

The investigation of foundation settlement shall proceed using the provisions of Article 10.6.2.4 using the load factor, γ_{SE} , specified in Table 3.4.1-4.

For structural plate box structures complying with the provisions of Article 12.9, the live load factor for the vehicular live loads *LL* and *IM* shall be taken as 2.0.

Applying these criteria for the evaluation of the sliding resistance of walls:

- The vertical earth load on the rear of a cantilevered retaining wall would be multiplied by γ_{pmin} (1.00) and the weight of the structure would be multiplied by γ_{pmin} (0.90) because these forces result in an increase in the contact stress (and shear strength) at the base of the wall and foundation.

- The horizontal earth load on a cantilevered retaining wall would be multiplied by γ_{pmax} (1.50) for an active earth pressure distribution because the force results in a more critical sliding force at the base of the wall.

Similarly, the values of γ_{pmax} for structure weight (1.25), vertical earth load (1.35) and horizontal active earth pressure (1.50) would represent the critical load combination for an evaluation of foundation bearing resistance.

Water load and friction are included in all strength load combinations at their respective nominal values.

The load factor for temperature gradient, γ_{TG} , should be considered on a project-specific basis. In lieu of project-specific information to the contrary, γ_{TG} may be taken as:

- 0.0 at the strength and extreme event limit states,
- 1.0 at the service limit state when live load is not considered, and
- 0.50 at the service limit state when live load is considered.

The effects of the foundation deformation on the bridge superstructure, retaining walls, or other load bearing structures shall be evaluated at applicable strength and service limit states using the provisions of Article 10.5.2.2 and the settlement load factor (γ_{SE}) specified in Table 3.4.1-4. For all bridges, stiffness should be appropriate to the considered limit state. Similarly, the effects of continuity with the substructure should be considered. In assessing the structural implications of foundation deformations of concrete bridges, the determination of the stiffness of the bridge components should consider the effects of cracking, creep, and other inelastic responses.

~~The load factor for settlement, γ_{SE} , should be considered on a project-specific basis. In lieu of project-specific information to the contrary, γ_{SE} , may be taken as 1.0. Load combinations which include settlement shall also be applied without settlement. As specified in Article 3.12.6, subsets of the settlements shall be considered when determining extreme combinations of force effects.~~

For segmentally constructed bridges, the following combination shall be investigated at the service limit state:

$$DC + DW + EH + EV + ES + WA + CR + SH + TG + EL + PS \quad (3.4.1-2)$$

For creep and shrinkage, the specified nominal values should be used. For friction, settlement, and water loads, both minimum and maximum values need to be investigated to produce extreme load combinations.

The load factor for temperature gradient should be determined on the basis of the:

- Type of structure, and
- Limit state being investigated.

Open girder construction and multiple steel box girders have traditionally, but perhaps not necessarily correctly, been designed without consideration of temperature gradient, i.e., $\gamma_{TG} = 0.0$.

The values of γ_{SE} in Table 3.4.1-4 are based on a target reliability index of 0.50 which assume that the effect of irreversible foundation deformations on the bridge superstructure will be reversed by intervention, e.g., shimming, jacking, etc. If intervention to relieve the superstructure is not practical or desirable for a given bridge type, then larger values of γ_{SE} consistent with target reliability index of 1.00 or larger shall be considered based on Kulicki et al., (2015) and Samtani and Kulicki (2016).

An owner may choose to use a local method that provides better estimation of foundation movement for local geologic conditions compared to methods noted in Section 10. In such cases, the owner will have to calibrate the γ_{SE} value for the local method using the procedures described in Kulicki et al., (2015) and Samtani and Kulicki (2016).

The application of γ_{SE} is illustrated in the flowchart in Appendix C3. The recommended procedure is to factor the deformations and evaluate the effect on the structure using the factored deformations. For example, if a structural analysis of factored deformations is performed, the resulting forces effects are already factored and these results are used directly in the appropriate load combinations in Table 3.4.1-1. The γ_{SE} in Table 3.4.1-1 does not indicate a second application of γ_{SE} . Rather it indicates that the force effects from the factored deformations are to be used in the indicated load combinations.

The value of $\gamma_{SE}=1.00$ for consolidation (long-term settlement time-dependent) settlement assumes that the estimation of consolidation settlement is based on appropriate laboratory and field tests to determine parameters (rather than correlations with index properties of soils) in the consolidation settlement equations in Article 10.6.2.4.3.

Table 3.4.1-2—Load Factors for Permanent Loads, γ_p

Type of Load, Foundation Type, and Method Used to Calculate Downdrag		Load Factor	
		Maximum	Minimum
<i>DC</i> : Component and Attachments		1.25	0.90
<i>DC</i> : Strength IV only		1.50	0.90
<i>DD</i> : Downdrag	Piles, α Tomlinson Method	1.4	0.25
	Piles, λ Method	1.05	0.30
	Drilled shafts, O’Neill and Reese (1999) Method	1.25	0.35
<i>DW</i> : Wearing Surfaces and Utilities		1.50	0.65
<i>EH</i> : Horizontal Earth Pressure			
Active		1.50	0.90
At-Rest		1.35	0.90
<i>AEP</i> for anchored walls		1.35	N/A
<i>EL</i> : Locked-in Construction Stresses		1.00	1.00
<i>EV</i> : Vertical Earth Pressure			
Overall Stability		1.00	N/A
Retaining Walls and Abutments		1.35	1.00
Rigid Buried Structure		1.30	0.90
Rigid Frames		1.35	0.90
Flexible Buried Structures			
o Metal Box Culverts, Structural Plate Culverts with Deep Corrugations, and Fiberglass Culverts		1.5	0.9
o Thermoplastic Culverts		1.3	0.9
o All others		1.95	0.9
<i>ES</i> : Earth Surcharge		1.50	0.75

Table 3.4.1-3—Load Factors for Permanent Loads Due to Superimposed Deformations, γ_p

Bridge Component	<i>PS</i>	<i>CR, SH</i>
Superstructures—Segmental Concrete Substructures supporting Segmental Superstructures (see 3.12.4, 3.12.5)	1.0	See γ_p for <i>DC</i> , Table 3.4.1-2
Concrete Superstructures—non-segmental	1.0	1.0
Substructures supporting non-segmental Superstructures using I_g	0.5	0.5
using $I_{effective}$	1.0	1.0
Steel Substructures	1.0	1.0

Table 3.4.1-4—Load Factors for Permanent Loads Due to Foundation Deformations, γ_{SE}

<u>Foundation Deformation and Deformation Estimation Method</u>	<u>SE</u>
<u>Immediate Settlement</u>	
• <u>Hough method</u>	<u>1.00</u>
• <u>Schmertmann method</u>	<u>1.25</u>
• <u>Local method</u>	<u>*</u>
<u>Consolidation settlement</u>	<u>1.00</u>
<u>Lateral Deformation</u>	
• <u>Soil-structure interaction method (P-y or Strain Wedge)</u>	<u>1.00</u>
• <u>Local method</u>	<u>*</u>
<u>*To be determined by the owner based on local geologic conditions.</u>	

-
-
-
-
-

3.16—REFERENCES

-
-
-
-

Kulicki, J. M. and D. Mertz. 2006. “Evolution of Vehicular Live Load Models During the Interstate Design Era and Beyond, in: 50 Years of Interstate Structures: Past, Present and Future”, *Transportation Research Circular*, E-C104, Transportation Research Board, National Research Council, Washington, DC.

Kulicki, J., W. Wassef, D. Mertz, A. Nowak, N. Samtani, and H. Nassif. 2015. *Bridges for Service Life Beyond 100 Years: Service Limit State Design. SHRP 2 Report S2-R19B-RW-1, SHRP2 Renewal Research, Transportation Research Board, National Research Council, The National Academies, Washington, D.C.*

Larsen, D. D. 1983. “Ship Collision Risk Assessment for Bridges.” In Vol. 1, *International Association of Bridge and Structural Engineers Colloquium*. Copenhagen, Denmark, pp. 113–128.

-
-
-

Sabatini, P. J., D. G. Pass, and R. C. Bachus. 1999. *Geotechnical Engineering Circular No. 4—Ground Anchors and Anchored Systems*, Federal Highway Administration, Report No. FHWA-SA-99-015. NTIS, Springfield, VA.

Samtani, N. and J. Kulicki. 2016. *Incorporation of Foundation Deformations in AASHTO LRFD Bridge Design Process*. SHRP2 Solutions. American Association of State Highway and Transportation Officials. Washington, DC.

Saul, R. and H. Svensson. 1980. “On the Theory of Ship Collision Against Bridge Piers.” In *IABSE Proceedings*, February 1980, pp. 51–82.

-
-
-
-

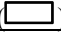
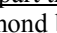
APPENDIX C3—CONSIDERATION OF FOUNDATION DEFORMATIONS IN BRIDGE DESIGN

Figure C3-1 shows a flow chart to consider foundation deformation in the bridge design process. The flow chart has two distinct parts, the left and right. The left part provides the outline of the process that a bridge designer may use without explicit consideration of foundation deformations other than what is required in the 7th Edition of *AASHTO LRFD*, i.e. without considering the method-specific load factor, γ_{SE} , the construction-point concept or the δ -0 concept. For convenience this will be called the “legacy loop”. The right part provides the recommended procedure to factor the deformations and evaluate the effect on the structure using the factored deformations. The sequence of activities in the deformation loop is based on the discussions in Samtani and Kulicki (2016) which includes the method-specific load factor, γ_{SE} , the construction-point concept or the δ -0 concept. For convenience this will be called the “refined (deformation) loop”. The flow chart applies to any type of foundation deformation and hence the symbol δ is used for deformations. If the flow chart is used for settlement, then symbol “S” may be substituted for δ .

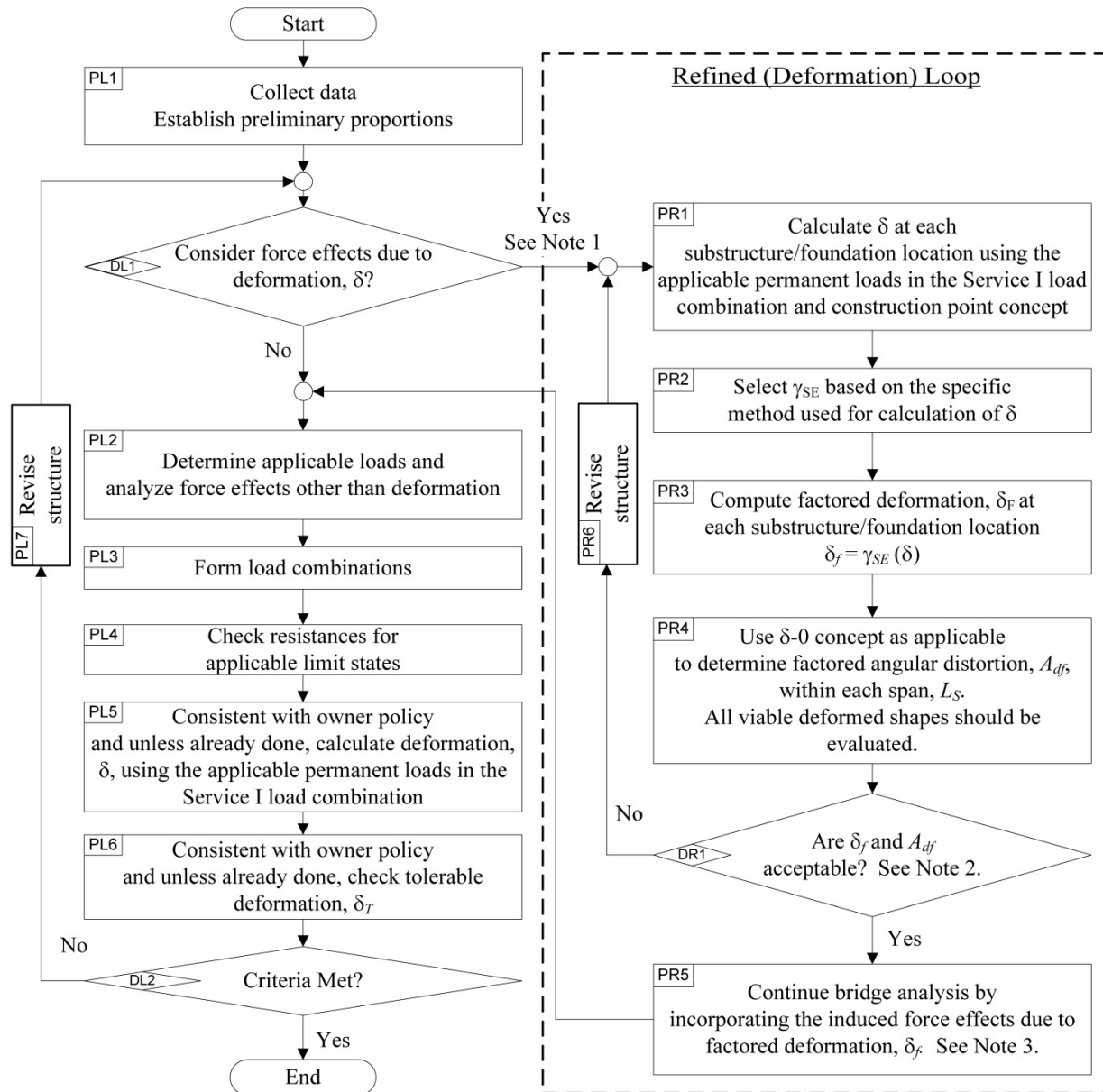
It is not the intention of the illustrated design process to universally require additional design effort beyond that required by the 7th edition of *AASHTO LRFD*, or approved owner policies that take advantage of well documented past geotechnical practice. For example, if the geomaterials at a site are well understood and past experience shows that a deep foundation is the best option or that a given service bearing pressure results in an acceptable foundation deformations with minimal structural or geometric consequences, then the decision to base a new design on legacy practices is a viable option. If, on the other hand, site conditions are not within past successful practice, there is a desire to consider possible economies of design that alter the experience base, or the structure requires more careful consideration of possible foundation deformations, then the additional provisions embodied in the refined (deformation) loop will result in a more thorough assessment of the implications of foundation deformations and the associated impact on the design and economy of the bridge.

Three notes are provided in the flow chart to include additional guidance for designer.

Some of the key points associated with the flow chart are as follows:

1. The process (“P”) related steps are indicated in rectangular boxes (). In the left (“L”) part there are six process boxes labeled PL1 to PL6. In the right (“R”) part there are five process boxes labeled PR1 to PR5.
2. The decision (“D”) related steps are indicated in diamond boxes (). In the left part there are two decision boxes labeled DL1 and DL2. The right part contains one decision box labeled DR1.
3. The left and right parts are connected at two levels. The first connection is established when a bridge designer decides to proceed with either the legacy or refined (deformation) loop in box DL1. The second connection is established after box PR5 once the designer has determined a favorable resolution of “Yes” to the decision in box DR1.
4. If the resolution to either box DL2 is “No,” then the structure is revised and the flow chart is re-entered at box DL1. Likewise, if the resolution at DR1 is “No” the structure is revised and the flowchart is re-entered at box PR1.
5. If the answer is “No” at box DL1, then the designer goes through the process provided in boxes PL2 to PL6 using the legacy approach as follows:
 - In box PL2 structural analysis proceeds without use of the construction-point or δ -0 concepts as they are not incorporated into the legacy approach. Consideration of foundation deformations is consistent with the owner’s implementation of the 7th edition of *AASHTO LRFD*.
 - Box PL3 indicates use of Table 3.4.1-1 as applicable to the situation at hand. Depending on the owner’s policies the values of γ_{SE} will effectively be zero or unity. In this case, the deformation may be evaluated based on past local experience with similar structures.
6. If the answer is “Yes” at box DL1, then the designer goes through the process provided in boxes PR1 to PR5, using the refined (deformation) approach. Note 1 is provided as guidance about entering the right side. The design proceeds as follows:
 - After the calculation of δ for the indicated loads in box PR1 and adjusting them for the construction-point concept they are scaled (factored) as indicated in box PR3 using the method-specific values of \square_{SE} determined in box PR2.
 - These factored deformations, δ_f , are used along with the δ -0 concept to calculate the factored angular distortions, A_{df} in box PR4.
 - In box DR1 the values of δ_f and A_{df} are compared to the applicable criteria. These criteria are geometric, not structural. Note 2 provides additional guidance.

- If the results are not acceptable the structure is revised and the design process returns to box PR1 to evaluate the modified structure.
 - If the results at box DR1 are acceptable the structural force effects from the factored deformations, δ_f , are calculated and are carried into the remaining steps of the legacy loop. Note 3 is vital to the correct formulation of load combinations using Table 3.4.1-1 in box PL5.
7. The “Criteria” in box DL2 can include any criteria related to bridge design such as deck grades, joint distress, crack control, moment and shear resistance.
 8. In boxes PL5 and PL6, the phrase “unless already done” acknowledges the possibility that the actions in these boxes may already have been performed by a designer who is entering these boxes after completing the right part of the flow chart.
 9. If all structural and geometric criteria are satisfied in box DL2 the design is satisfactory; if not, the structure is modified and the design process returns to box DL1.



Note 1: It may be efficient to run some early design iterations without including this loop until the proportions of the bridge are well developed, and then include this loop to consider the force effects from differential deformations.

Note 2: Compare A_{df} to permissible angular distortion criteria and δ_f to permissible values at abutment interfaces and within spans in terms of vertical clearance under bridge. Guidance in Article 10.5.2 may be used to establish permissible values. Owner may establish other permissible values.

Note 3: Note that the γ_{SE} is used to factor the deformations as shown in this flow chart. γ_{SE} also appears in Table 3.4.1-1 (Load Combinations and Load Factors). This does not imply a second application of γ_{SE} in the load combinations but rather it is an acknowledgement that the deformations have already been factored. Use of the factored deformations in a structural analysis program ensures that the output is factored value.

Figure C3-1—Foundation Deformation Procedure Flow Chart (Samtani and Kulicki, 2016)

Appendix E
Proposed Modifications to Section 10 of AASHTO LRFD
Bridge Design Specifications

Proposed Modifications to Section 10

TABLE OF CONTENTS

•
•
•
•
•
•

10.5—LIMIT STATES AND RESISTANCE FACTORS 10-xx
 10.5.1—General 10-xx
 10.5.2—Service Limit States..... 10-xx
 10.5.2.1—General 10-xx
 10.5.2.2—Tolerable Movements and Movement Criteria 10-xx
 10.5.2.2.1—General 10-xx
 10.5.2.2.2—Factored Relevant Total Settlement, S_f , and Factored Angular Distortion, A_{df} 10-xx
 10.5.2.3—Overall Stability 10-xx

•
•
•
•
•

10.6.2—Service Limit State Design	10-xx
10.6.2.1—General	10-xx
10.6.2.2—Tolerable Movements	10-xx
10.6.2.3—Loads	10-xx
10.6.2.4—Settlement Analyses	10-xx
10.6.2.4.1—General	10-xx
10.6.2.4.2—Settlement of Footings on Cohesionless Soils.....	10-xx
<u>10.6.2.4.2a—General</u>	<u>10-xx</u>
<u>10.6.2.4.2b— Elastic Half-space Method</u>	<u>10-xx</u>
<u>10.6.2.4.2c—Hough Method.....</u>	<u>10-xx</u>
<u>10.6.2.4.2d—Schmertmann Method</u>	<u>10-xx</u>
<u>10.6.2.4.2e—Local Method.....</u>	<u>10-xx</u>
10.6.2.4.3—Settlement of Footings on Cohesive Soils.....	10-xx

-
-
-
-
-

-
-
-
-
-
-

10.3—NOTATION

A_{ct}	=	cross-sectional area of steel casing considering reduction for threads (in. ²) (10.9.3.10.3a)
A_{df}	=	<u>factored angular distortion (10.5.2.2.2)</u>
A_g	=	cross-sectional area of grout within micropile (in. ²) (10.9.3.10.3a)
•		
•		
B	=	footing width; pile group width; pile diameter (ft) (10.6.1.3) (10.7.2.3.2) (10.7.2.4)
B_f	=	<u>least width of footing (10.6.2.4.2b)</u>
B'	=	effective footing width (ft) (10.6.1.3)
C_1	=	<u>correction factor to incorporate the effect of strain relief due to embedment (10.6.2.4.2b)</u>
C_2	=	<u>correction factor to incorporate time-dependent (creep) increase in settlement for t (years) after construction (10.6.2.4.2b)</u>
C_α	=	secondary compression index, void ratio definition (dim) (10.4.6.3)
•		
•		
d_q	=	correction factor to account for the shearing resistance along the failure surface passing through cohesionless material above the bearing elevation (dim) (10.6.3.1.2a)
E	=	modulus of elasticity of pile material (ksi) (10.7.3.8.2); <u>elastic modulus of layer i based on guidance provided in Table C10.4.6.3-1 (10.6.2.4.2b)</u>
E_d	=	developed hammer energy (ft-lb) (10.7.3.8.5)
•		
•		
I_w	=	weak axis moment of inertia for a pile (ft ⁴) (10.7.3.13.4)
I_z	=	<u>strain influence factor from Figure 10.6.2.4.2c-1a</u>
$i_\alpha, i_\phi, i_\gamma$	=	load inclination factors (dim) (10.6.3.1.2a)
•		
•		
L_b	=	micropile bonded length (ft) (10.9.3.5.2)
L_f	=	<u>length of footing (10.6.2.4.2b)</u>
L_i	=	depth to middle of length interval at the point considered (ft) (10.7.3.8.6g)
L_p	=	micropile casing plunge length (ft) (10.9.3.10.4)
L_s	=	<u>bridge span length over which A_{df} is computed (10.5.2.2.2)</u>
•		
•		
S_e	=	elastic settlement (ft) (10.6.2.4.1)
S_f	=	<u>foundation relevant total settlement (ft) (10.5.2.2.2)</u>
S_s	=	secondary settlement (ft) (10.6.2.4.1)
S_t	=	total settlement (ft) (10.6.2.4.1)

- S_{fa} = total foundation settlement using permanent loads in the Service I load combination (ft) (10.5.2)
- S_{fp} = total foundation settlement using permanent loads prior to construction of bridge superstructure in the Service I load combination (ft) (10.5.2.2.2)
- S_{fr} = relevant total foundation settlement defined as $S_{fa} - S_{fp}$ (10.5.2.2.2)
- S_u = undrained shear strength (ksf) (10.4.6.2.2)
-
-
- T = time factor (dim) (10.6.2.4.3)
- t = time for a given percentage of one-dimensional consolidation settlement to occur (yr) (10.6.2.4.3); time t from completion of construction to date under consideration for evaluation of C_2 (yrs) (10.6.2.4.2b)
- t_1, t_2 = arbitrary time intervals for determination of secondary settlement, S_s (yr) (10.6.2.4.3)
-
-
- W_{TI} = vertical movement at the head of the drilled shaft (in.) (C10.8.3.5.4d)
- X = width or smallest dimension of pile group (ft) (10.7.3.9); a factor used to determine the value of elastic modulus (10.6.2.4.2b)
- Y = length of pile group (ft) (10.7.3.9)
-
-
- γ_p = load factor for downdrag (C10.7.3.7)
- γ_{SE} = load factor for settlement (10.5.2.2.2)
- ΔH_i = elastic settlement of layer i (ft) (10.6.2.4.2)
- Δ = differential settlement between two bridge support elements spaced at a distance of L_s (ft) (10.5.2.2)
- Δ_f = factored differential settlement (10.5.2.2.2)
- Δp = net uniform applied stress (load intensity) at the foundation depth (Figure 10.6.2.4.2c-1b)

-
-
-
-
-

-
-
-
-
-
-

10.5—LIMIT STATES AND RESISTANCE FACTORS

10.5.1—General

The limit states shall be as specified in Article 1.3.2; foundation-specific provisions are contained in this Section.

Foundations shall be proportioned so that the factored resistance is not less than the effects of the factored loads specified in Section 3.

10.5.2—Service Limit States

10.5.2.1—General

Foundation design at the service limit state shall include:

- Settlements,
- Horizontal movements,
- Overall stability, and
- Scour at the design flood.

Consideration of foundation movements shall be based upon structure tolerance to total and differential movements, rideability and economy. Foundation movements shall include all movement from settlement, horizontal movement, and rotation.

Bearing resistance estimated using the presumptive allowable bearing pressure for spread footings, if used, shall be applied only to address the service limit state.

C10.5.2.1

In bridges where the superstructure and substructure are not integrated, settlement corrections can be made by jacking and shimming bearings. Article 2.5.2.3 requires jacking provisions for these bridges.

The cost of limiting foundation movements should be compared with the cost of designing the superstructure so that it can tolerate larger movements or of correcting the consequences of movements through maintenance to determine minimum lifetime cost. The Owner may establish more stringent criteria.

The foundation movements should be translated to the deck elevation to evaluate the effect of such movements on the superstructure. In this process, deformations of the substructure, i.e., elements between foundation and superstructure, should be added to foundation deformations as appropriate.

The design flood for scour is defined in Article 2.6.4.4.2, and is specified in Article 3.7.5 as applicable at the service limit state.

Presumptive bearing pressures were developed for use with working stress design. These values may be used for preliminary sizing of foundations, but should generally not be used for final design. If used for final design, presumptive values are only applicable at service limit states.

10.5.2.2—Tolerable Movements and Movement Criteria

10.5.2.2.1—General

Foundation movement criteria shall be consistent with the function and type of structure, anticipated service life, and consequences of unacceptable movements on structure performance. Foundation movement shall include vertical, horizontal, and rotational movements. The tolerable movement criteria shall be established by either empirical procedures or structural analyses, or by consideration of both.

Foundation settlement shall be investigated using all applicable loads in the Service I Load Combination specified in Table 3.4.1-1. Transient loads may be omitted from settlement analyses for foundations bearing on or in cohesive soil deposits that are subject to time-dependent consolidation settlements.

All applicable service limit state load combinations in Table 3.4.1-1 shall be used for evaluating horizontal movement and rotation of foundations.

Horizontal movement criteria should be established at the top of the foundation based on the tolerance of the structure to lateral movement, with consideration of the column length and stiffness.

10.5.2.2.2—Factored Relevant Total Settlement, S_f , and Factored Angular Distortion, A_{df}

In lieu of owner supplied provisions, the following steps should be followed to estimate and use practical values of factored settlement, S_f , and factored angular distortion, A_{df} , in the bridge design process as shown in Appendix C3 of Section 3:

1. At each support element, compute factored relevant total foundation settlement for the assumed foundation type (e.g., spread footings, driven piles, drilled shafts, etc.) as follows:
 - a. Determine the total foundation settlement, S_{fa} , using all applicable permanent loads in the Service I load combination.

C10.5.2.2.1

Experience has shown that bridges can and often do accommodate more movement and/or rotation than traditionally allowed or anticipated in design. Creep, relaxation, and redistribution of force effects accommodate these movements. Some studies have been made to synthesize apparent response. These studies indicate that angular distortions between adjacent foundations greater than 0.008 radians in simple spans and 0.004 radians in continuous spans should not be permitted in settlement criteria (Moulton et al., 1985; DiMillio, 1982; Barker et al., 1991; Samtani et al. 2010). Other angular distortion limits may be appropriate after consideration of:

- cost of mitigation through larger foundations, realignment or surcharge,
- rideability,
- vertical clearance.
- tolerable limits of deformation of other structures associated with a bridge, e.g., approach slabs, wingwalls, pavement structures, drainage grades, utilities on the bridge, etc.
- roadway drainage.
- aesthetics, and
- safety.

Rotation movements should be evaluated at the top of the substructure unit in plan location and at the deck elevation.

Tolerance of the superstructure to lateral movement will depend on bridge seat or joint widths, bearing type(s), structure type, and load distribution effects.

C10.5.2.2.2

Determination of relevant total settlement should include consideration of how and when settlement occurs during construction process and uncertainty of the settlement itself. These two factors are addressed by the construction-point concept and $S_f=0$ concept in this article, respectively.

Foundation deformations should not be estimated as if a weightless bridge structure is instantaneously set into place and all the loads are applied at the same time. In reality, loads are applied gradually as construction proceeds. Consequently, foundation deformations also occur gradually as construction proceeds. There are several critical construction points or stages during construction that should be evaluated separately by the

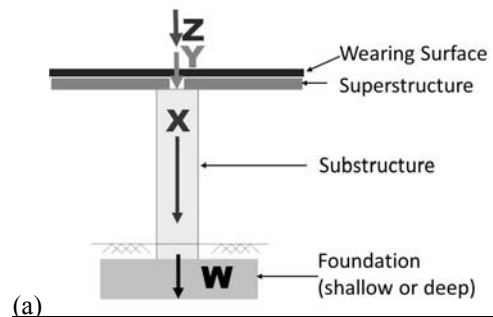
- b. Determine the total foundation settlement, S_{fp} , prior to construction of bridge superstructure. This settlement would generally be as a result of all applicable substructure loads computed in accordance with permanent loads in the Service I load combination.
- c. Determine relevant total settlement, S_{rr} , as $S_{rr} = S_{fa} - S_{fp}$.
- d. Determine the factored relevant total settlement, S_f , using Eq. 10.5.2.2.2-1

$$S_f = \gamma_{SE}(S_{rr}) \quad (10.5.2.2.2-1)$$

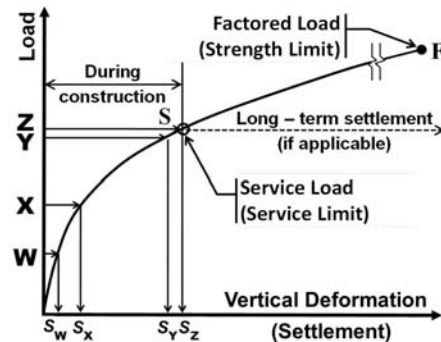
where:

γ_{SE} = SE load factor value selected from Table 3.4.1-4 based on the method used to estimate the settlement.

designer. Figure C10.5.2.2-1 shows the critical construction stages (W, X, Y, and Z) and their associated load-settlement behavior for the case of a pier and vertical loads. The settlements that occur before placement of the superstructure may not be relevant to the design of the superstructure. Thus, the settlements between application of loads X and Z are the most relevant. Formulation of settlements in a manner shown in Figure C10.5.2.2-1b permits an assessment of settlements up to that point that can affect the bridge superstructure. Although Figure C10.5.2.2-1 illustrates the construction-point concept for the case of a pier, vertical loads and settlements (vertical deformation), the concepts apply to other elements of bridge structure (e.g., abutments), load types (shears, moments, etc.) and deformation types (lateral movements, rotations, etc.).



(a)



(b)

Figure C10.5.2.2-1. Construction-point concept for a bridge pier. (a) Identification of critical construction points, (b) conceptual load-deformation pattern for a given foundation (Kulicki, et. al, 2015; Samtani and Kulicki, 2016).

Long-term settlements as shown by the horizontal dashed line corresponding to the total construction load (Z) in Figure C10.5.2.2-1 shall be included as appropriate.

The contribution of deformations in the substructure columns to the angular distortions at the deck elevation should be considered.

2. Compute the factored angular distortion within each span using the S_f -0 concept. At a given support element assume that the actual settlement could be as large as the factored relevant total settlement calculated by the chosen method, S_{f_i} . At the same time, assume that an adjacent support element does not settle at all. Thus, the factored differential settlement, Δ_{f_i} within a given bridge span is equal to the larger of the factored relevant total settlement at each of two supports of a bridge span. Compute factored angular distortion, A_{df_i} as the ratio of the factored differential settlement, Δ_{f_i} to the span length, L_{S_i} . Express A_{df} value in radians.

All viable deformation shapes should be evaluated.

While the angular distortion is generally applied in the longitudinal direction of a bridge, similar analyses should be performed in transverse direction based on consideration of bridge width and stiffness. If the distance between support elements in the transverse direction is less than one-half of the bridge width at that line of support elements then the angular distortion may be computed based on the difference between the factored relevant settlement between the support points rather than the S_f -0 approach.

While all analytical methods for estimating settlements have some degree of uncertainty, the uncertainty of the calculated differential settlement is larger than the uncertainty of the calculated total settlement at each of the two support elements used to calculate that differential settlement, e.g., between an abutment and a pier, or between two adjacent piers. The S-0 concept is used to account for this uncertainty.

A hypothetical 4-span bridge structure with span lengths, L_{S1} , L_{S2} , L_{S3} and L_{S4} is shown in Figure C10.5.2.2-2 to illustrate the application of S_f -0 concept and computation of factored angular distortion. The factored relevant total settlement, S_{f_i} is computed at each support element and the profile of S_{f_i} along the bridge is shown by the solid line. In this figure, $S_{f-A1} < S_{f-P1} > S_{f-P2} < S_{f-P3} < S_{f-A2}$. As shown, two viable modes of deformation shapes, Mode 1 and Mode 2, are possible. For each of these two modes, the S_{f_i} profile assumed for computation of the factored angular distortion, A_{df_i} for each span is represented by the dashed lines. The factored angular distortion within each span is computed as shown for each viable mode as shown in Figure C10.5.2.2-2. The symbols are in accordance with $\Delta_{f(i-j)}$ and $A_{df(i-j)}$ where i represents the span number (1 to 4) and j represents the mode (1 and 2).

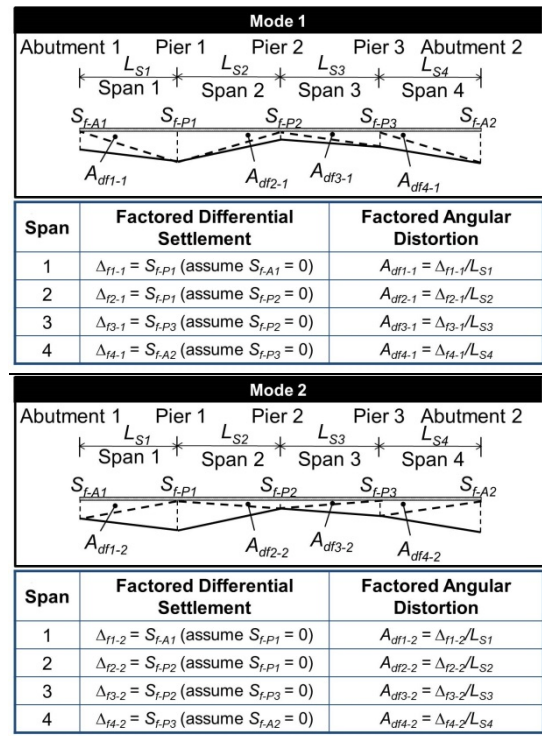


Figure C10.5.2.2-2—Computing Factored Angular Distortion, A_{df} , Based on S_f -0 Concept for a hypothetical 4-span Bridge (Samtani and Kulicki, 2016).

If γ_{SE} has already been applied in computation of factored settlement, S_f , as indicated in Step 1d, it should not be applied again during computation of differential settlement or angular distortion.

3. Compare the value of A_{df} within each span and value of S_f at each support element with owner specified total settlement and angular distortion criteria.

If owner specified angular distortion criteria are not available then use limiting angular distortion criteria noted in C10.5.2.2.1.

The value of S_f should be evaluated with respect to the various factors listed in C10.5.2.2.2.

4. Incorporate S_f and A_{df} in the bridge design process.

The flow chart in Appendix C3 illustrates a typical design process. Note that the flow chart in Appendix C3 uses the symbol δ that is general and applies to any type of deformation. When the flow chart is used for settlement, δ can be substituted with S.

10.5.2.3—Overall Stability

The evaluation of overall stability of earth slopes with or without a foundation unit shall be investigated at the service limit state as specified in Article 11.6.2.3.

10.5.2.4—Abutment Transitions

Vertical and horizontal movements caused by embankment loads behind bridge abutments shall be investigated.

C10.5.2.4

Settlement of foundation soils induced by embankment loads can result in excessive movements of substructure elements. Both short and long term settlement potential should be considered.

Settlement of improperly placed or compacted backfill behind abutments can cause poor rideability and a possibly dangerous bump at the end of the bridge. Guidance for proper detailing and material requirements for abutment backfill is provided in Cheney and Chassie Samtani and Nowatzki (2000).

Lateral earth pressure behind and/or lateral squeeze below abutments can also contribute to lateral movement of abutments and should be investigated, if applicable.

-
-
-
-
-
-
-

10.6.2.4—Settlement Analyses

10.6.2.4.1—General

Foundation settlements should be estimated using computational methods based on the results of laboratory or insitu testing, or both. The soil parameters used in the computations should be chosen to reflect the loading history of the ground, the construction sequence, and the effects of soil layering.

Both total and differential settlements, including time dependant effects, shall be considered.

Total settlement, including elastic, consolidation, and secondary components may be taken as:

$$S_t = S_e + S_c + S_s \quad (10.6.2.4.1-1)$$

where:

S_e = elastic settlement (ft)

S_c = primary consolidation settlement (ft)

S_s = secondary settlement (ft)

C10.6.2.4.1

Elastic, or immediate, settlement is the instantaneous deformation of the soil mass that occurs as the soil is loaded. The magnitude of elastic settlement is estimated as a function of the applied stress beneath a footing or embankment. Elastic settlement is usually small and neglected in design, but where settlement is critical, it is the most important deformation consideration in cohesionless soil deposits and for footings bearing on rock. For footings located on over-consolidated clays, the magnitude of elastic settlement is not necessarily small and should be checked.

In a nearly saturated or saturated cohesive soil, the pore water pressure initially carries the applied stress. As pore water is forced from the voids in the soil by the applied load, the load is transferred to the soil skeleton. Consolidation settlement is the gradual compression of the soil skeleton as the pore water is forced from the voids in the soil. Consolidation settlement is the most important deformation consideration in cohesive soil deposits that possess sufficient strength to safely support a spread footing. While consolidation settlement can occur in saturated cohesionless soils, the consolidation occurs quickly and is normally not distinguishable from the elastic settlement.

Secondary settlement, or creep, occurs as a result of the plastic deformation of the soil skeleton under a constant effective stress. Secondary settlement is of

principal concern in highly plastic or organic soil deposits. Such deposits are normally so obviously weak and soft as to preclude consideration of bearing a spread footing on such materials.

The principal deformation component for footings on rock is elastic settlement, unless the rock or included discontinuities exhibit noticeable time-dependent behavior.

To avoid overestimation, relevant settlements should be evaluated using the construction-point concept noted in Samtani and Kulicki (2016). The effect of settlement on superstructure shall be evaluated based on Article 10.5.2.2.

The effects of the zone of stress influence, or vertical stress distribution, beneath a footing shall be considered in estimating the settlement of the footing.

Spread footings bearing on a layered profile consisting of a combination of cohesive soil, cohesionless soil and/or rock shall be evaluated using an appropriate settlement estimation procedure for each layer within the zone of influence of induced stress beneath the footing.

The distribution of vertical stress increase below circular or square and long rectangular footings, i.e., where $L > 5B$, may be estimated using Figure 10.6.2.4.1-1.

For guidance on vertical stress distribution for complex footing geometries, see Poulos and Davis (1974) or Lambe and Whitman (1969).

Some methods used for estimating settlement of footings on sand include an integral method to account for the effects of vertical stress increase variations. For guidance regarding application of these procedures, see Gifford et al. (1987).

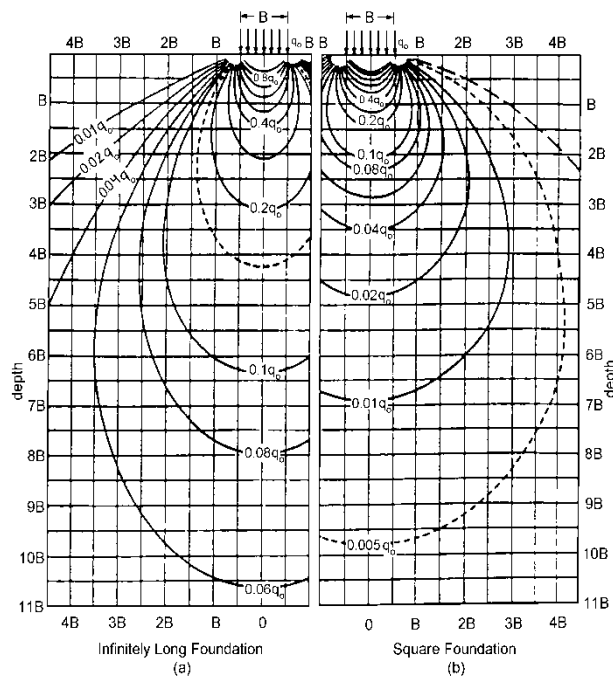


Figure 10.6.2.4.1-1—Boussinesq Vertical Stress Contours for Continuous and Square Footings Modified after Sowers (1979)

10.6.2.4.2—Settlement of Footings on Cohesionless Soils

10.6.2.4.2a—General

The settlement of spread footings bearing on cohesionless soil deposits shall be estimated as a function of effective footing width and shall consider the effects of footing geometry and soil and rock layering with depth.

Settlements of footings on cohesionless soils shall be estimated using elastic theory or empirical procedures.

10.6.2.4.2b—Elastic Half-space Method

The elastic half-space method assumes the footing is flexible and is supported on a homogeneous soil of infinite depth. The elastic settlement of spread footings, in feet, by the elastic half-space method shall be estimated as:

C10.6.2.4.2a

Although methods are recommended for the determination of settlement of cohesionless soils, experience has indicated that settlements can vary considerably in a construction site, and this variation may not be predicted by conventional calculations.

Settlements of cohesionless soils occur rapidly, essentially as soon as the foundation is loaded. Therefore, the total settlement under the service loads may not be as important as the incremental settlement between intermediate load stages. For example, the total and differential settlement due to loads applied by columns and cross beams is generally less important than the total and differential settlements due to girder placement and casting of continuous concrete decks.

Generally conservative settlement estimates may be obtained using the elastic half-space procedure or the empirical method by Hough. Additional information regarding the accuracy of the methods described herein is provided in Gifford et al. (1987), ~~and~~ Kimmerling (2002) and Samtani and Notwazki (2006). This information, in combination with local experience and engineering judgment, should be used when determining the estimated settlement for a structure foundation, as there may be cases, such as attempting to build a structure grade high to account for the estimated settlement, when overestimating the settlement magnitude could be problematic.

Details of other procedures can be found in textbooks and engineering manuals, including:

- Terzaghi and Peck (1967)
- Sowers (1979)
- U.S. Department of the Navy (1982)
- D'Appolonia (Gifford et al., 1987)—This method includes consideration for over-consolidated sands.
- Tomlinson (1986)
- Gifford et al. (1987)

C10.6.2.4.2b

For general guidance regarding the estimation of elastic settlement of footings on sand, see Gifford et al. (1987), ~~and~~ Kimmerling (2002), and Samtani and Notwazki (2006).

The stress distributions used to calculate elastic settlement assume the footing is flexible and supported

$$S_e = \frac{\left[q_o (1 - \nu^2) \sqrt{A'} \right]}{144 E_s \beta_z} \quad (10.6.2.4.2b-1)$$

where:

q_o = applied vertical stress (ksf)

A' = effective area of footing (ft²)

E_s = Young's modulus of soil taken as specified in Article 10.4.6.3 if direct measurements of E_s are not available from the results of in situ or laboratory tests (ksi)

β_z = shape factor taken as specified in Table 10.6.2.4.2b-1 (dim)

ν = Poisson's Ratio, taken as specified in Article 10.4.6.3 if direct measurements of ν are not available from the results of in situ or laboratory tests (dim)

Unless E_s varies significantly with depth, E_s should be determined at a depth of about 1/2 to 2/3 of B below the footing, where B is the footing width. If the soil modulus varies significantly with depth, a weighted average value of E_s should be used.

Table 10.6.2.4.2b-1—Elastic Shape and Rigidity Factors, EPRI (1983)

L/B	Flexible, β_z (average)	β_z Rigid
Circular	1.04	1.13
1	1.06	1.08
2	1.09	1.10
3	1.13	1.15
5	1.22	1.24
10	1.41	1.41

10.6.2.4.2c—Hough Method

Estimation of spread footing settlement on cohesionless soils by the empirical Hough method shall be determined using Eqs. 10.6.2.4.2c-2 and 10.6.2.4.2c-3. *SPT* blow counts shall be corrected as specified in Article 10.4.6.2.4 for depth, i.e. overburden stress, before correlating the *SPT* blow counts to the bearing capacity index, C' .

on a homogeneous soil of infinite depth. The settlement below a flexible footing varies from a maximum near the center to a minimum at the edge equal to about 50 percent and 64 percent of the maximum for rectangular and circular footings, respectively. The settlement profile for rigid footings is assumed to be uniform across the width of the footing.

Spread footings of the dimensions normally used for bridges are generally assumed to be rigid, although the actual performance will be somewhere between perfectly rigid and perfectly flexible, even for relatively thick concrete footings, due to stress redistribution and concrete creep.

The accuracy of settlement estimates using elastic theory are strongly affected by the selection of soil modulus and the inherent assumptions of infinite elastic half space. Accurate estimates of soil moduli are difficult to obtain because the analyses are based on only a single value of soil modulus, and Young's modulus varies with depth as a function of overburden stress. Therefore, in selecting an appropriate value for soil modulus, consideration should be given to the influence of soil layering, bedrock at a shallow depth, and adjacent footings.

For footings with eccentric loads, the area, A' , should be computed based on reduced footing dimensions as specified in Article 10.6.1.3.

C10.6.2.4.2c

The Hough method was developed for normally consolidated cohesionless soils.

The Hough method has several advantages over other methods used to estimate settlement in cohesionless soil deposits, including express consideration of soil layering and the zone of stress influence beneath a footing of finite size.

The subsurface soil profile should be subdivided into layers based on stratigraphy to a depth of about

$$S_e = \sum_{i=1}^n \Delta H_i \quad (10.6.2.4.2c-1)$$

in which:

$$\Delta H_i = H_c \frac{1}{C'} \log \left(\frac{\sigma'_o + \Delta \sigma_v}{\sigma'_o} \right) \quad (10.6.2.4.2c-2)$$

where:

n = number of soil layers within zone of stress influence of the footing

ΔH_i = elastic settlement of layer i (ft)

H_c = initial height of layer i (ft)

C' = bearing capacity index from Figure 10.6.2.4.2c-1 (dim)

σ'_o = initial vertical effective stress at the midpoint of layer i (ksf)

$\Delta \sigma_v$ = increase in vertical stress at the midpoint of layer i (ksf)

In Figure 10.6.2.4.2-1, N_1 shall be taken as N_{160} , Standard Penetration Resistance, N (blows/ft), corrected for overburden pressure as specified in Article 10.4.6.2.4..

three times the footing width. The maximum layer thickness should be about 10 ft.

While ~~Cheney and Chassie (2000)~~, and Hough (1959), did not specifically state that the SPT N values should be corrected for hammer energy in addition to overburden pressure, due to the vintage of the original work, hammers that typically have an efficiency of approximately 60 percent were in general used to develop the empirical correlations contained in the method. If using SPT hammers with efficiencies that differ significantly from this 60 percent value, the N values should also be corrected for hammer energy, in effect requiring that N_{160} be used (Samtani and Nowatzki, 2006).

Studies conducted by Gifford et al. (1987) and Samtani and Nowatzki (2006) indicate that Hough's procedure is conservative. Such conservatism may be acceptable for the evaluation of the settlement of embankments. However, in the case of shallow foundations such conservatism may lead to unnecessary use of costlier deep foundations in cases where shallow foundations may be viable.

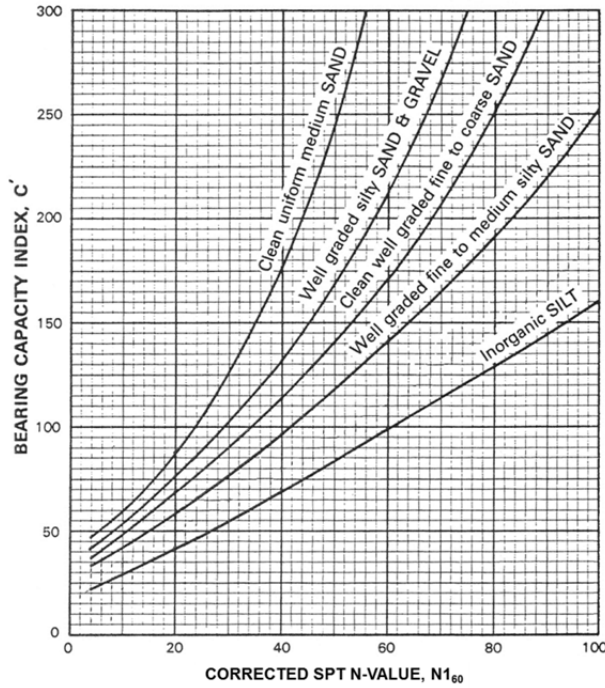


Figure 10.6.2.4.2c-1—Bearing Capacity Index versus Corrected SPT (Samtani and Nowatzki, 2006, after Hough, 1959)

The Hough method is applicable to cohesionless soil deposits. The “Inorganic Silt” curve should generally not be applied to soils that exhibit plasticity because N-values in such soils are unreliable. The settlement characteristics of cohesive soils that exhibit plasticity should be investigated using undisturbed samples and laboratory consolidation tests as prescribed in Article 10.6.2.4.3.

10.6.2.4.2d—Schmertmann Method

Estimation of spread footing immediate settlement, S_i , on cohesionless soils by the empirical Schmertmann method shall be made using Eq. 10.6.2.4.2d-1.

$$S_i = C_1 C_2 \Delta p \sum_{i=1}^n \Delta H_i \quad (10.6.2.4.2d-1)$$

in which:

$$\Delta H_i = H_c \left(\frac{I_z}{144XE} \right) \quad (10.6.2.4.2d-2)$$

$$C_1 = 1 - 0.5 \left(\frac{p_o}{\Delta p} \right) \geq 0.5 \quad (10.6.2.4.2d-3)$$

$$C_2 = 1 + 0.2 \log_{10} \left(\frac{t}{0.1} \right) \quad (10.6.2.4.2d-4)$$

where:

C10.6.2.4.2d

Background information for Schmertmann, *et al.* (1978) in the format as presented here can be found in Samtani and Nowatzki (2006).

For C_2 correction factor the time duration, t , in Eq. 10.6.2.4.2d-4 is set to 0.1 years to evaluate the settlement immediately after construction, i.e., $C_2 = 1$. If long-term creep deformation of the soil is suspected then an appropriate time duration, t , should be used in the computation of C_2 . Creep deformation is not the same as consolidation settlement. This factor can have an important influence on the reported settlement since it is included in Eq. 10.6.2.4.2d-1 as a multiplier. For example, the C_2 factor for time durations of 0.1 yrs, 1 yr, 10 yrs and 50 yrs are 1.0, 1.2, 1.4 and 1.54, respectively. In cohesionless soils and unsaturated fine-grained cohesive soils with low plasticity, time durations of 0.1 yr and 1 yr, respectively, are generally appropriate and sufficient for cases of static loads.

ΔH_i = elastic settlement of layer i (ft)

H_c = height of compressible soil layer i (ft)

I_z = strain influence factor from Figure 10.6.2.4.2d-1a. The dimension B_f represents the least lateral dimension of the footing after correction for eccentricities, i.e. use least lateral effective footing dimension. The strain influence factor is a function of depth and is obtained from the strain influence diagram. The strain influence diagram is constructed for the axisymmetric case ($L_f/B_f = 1$) and the plane strain case ($L_f/B_f \geq 10$) as shown in Figure 10.6.2.4.2d-1a. The strain influence diagram for intermediate conditions should be determined by simple linear interpolation.

n = number of soil layers within the zone of strain influence (strain influence diagram).

Δp = net uniform applied stress (load intensity) at the foundation depth (see Figure 10.6.2.4.2d-1b) (ksf).

E = elastic modulus of layer i based on guidance provided in Table C10.4.6.3-1 (ksi).

X = a factor used to determine the value of elastic modulus. If the value of elastic modulus is based on correlations with N_{60} -values or q_c from Table C10.4.6.3-1, then values of X shall be taken as follows:

$X = 1.25$ for axisymmetric case ($L_f/B_f = 1$)

$X = 1.75$ for plane strain case ($L_f/B_f \geq 10$)

Use interpolation for footings with values of L_f/B_f between 1 and 10.

If the value of elastic modulus is estimated based on the range of elastic moduli in Table C10.4.6.3-1 or other sources, use $X = 1.0$.

C_l = correction factor to incorporate the effect of strain relief due to embedment

p_o = effective in-situ overburden stress at the foundation depth and Δp is the net foundation pressure as shown in Figure 10.6.2.4.2d-1b

(ksf).

C_2 = correction factor to incorporate time-dependent (creep) increase in settlement for time t after construction

t = time t from completion of construction to date under consideration for evaluation of C_2 (yrs)

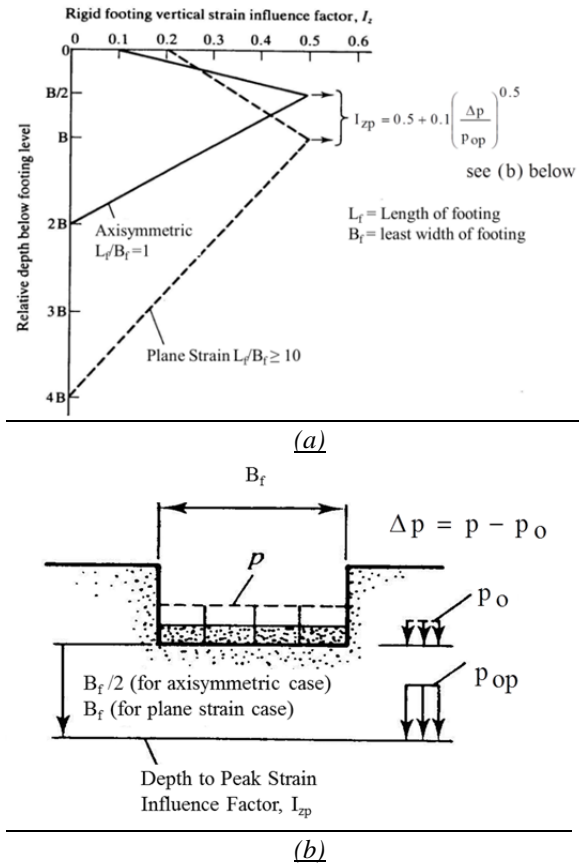


Figure 10.6.2.4.2d-1—(a) Simplified vertical strain influence factor distributions, (b) Explanation of pressure terms in equation for I_{zp} (Samtani and Notatzki, 2006, after Schmertmann, et al., 1978).

The C_2 parameter shall not be used to estimate time-dependent consolidation settlements. Where consolidation settlement can occur within the depth of the strain distribution diagram, the magnitude of the consolidation settlement shall be estimated as per Article 10.6.2.4.3 and added to the immediate settlement of other layers within the strain distribution diagram where consolidation settlement may not occur.

10.6.2.4.2e—Local Method

Use of methods based on local geologic conditions and calibration shall be used subject to approval from the Owner.

C10.6.2.4.2e

Calibration of local methods should be based on processes as described in SHRP 2 R19B program report (Kulicki et al., 2015) and Samtani and Kulicki (2016)

10.10—REFERENCES

-
-
-

Kulhawy, F.H. and Y-R Chen. 2007. “Discussion of ‘Drilled Shaft Side Resistance in Gravelly Soils’ by Kyle M. Rollins, Robert J. Clayton, Rodney C. Mikesell, and Bradford C. Blaise,” *Journal of Geotechnical and Geoenvironmental Engineering*, ASCE, Vol. 133, No. 10, pp. 1325–1328.

Kulicki, J., W. Wassef, D. Mertz, A. Nowak, N. Samtani, and H. Nassif. 2015. “Bridges for Service Life Beyond 100 Years: Service Limit State Design.” SHRP 2 Report S2-R19B-RW-1, SHRP2 Renewal Research, Transportation Research Board. National Research Council, The National Academies, Washington, D.C.

Kyfor, Z. G., A. R. Schnore, T. A. Carlo, and P. F. Bailey. 1992. *Static Testing of Deep Foundations*, FHWA-SA-91-042, Federal Highway Administration, Office of Technology Applications, U. S. Department of Transportation, Washington D. C., p. 174.

-
-
-

Sabatini, P. J., R. C. Bachus, P. W. Mayne, J. A. Schneider, and T. E. Zettler. 2002. *Geotechnical Engineering Circular 5 (GEC5)—Evaluation of Soil and Rock Properties*, FHWA-IF-02-034. Federal Highway Administration, U.S. Department of Transportation, Washington, DC.

Samtani, N. C., and Nowatzki, E. A. 2006. *Soils and Foundations*, FHWA NHI-06-088 and FHWA NHI 06-089, Federal Highway Administration, U.S. Department of Transportation, Washington, DC.

Samtani, N. C., Nowatzki, E. A., and Mertz, D.R. 2010. *Selection of Spread Footings on Soils to Support Highway Bridge Structures*, FHWA-RC/TD-10-001, Federal Highway Administration, Resource Center, Matteson, IL

Samtani, N. and J. Kulicki. 2016. *Incorporation of Foundation Deformations in AASHTO LRFD Bridge Design Process*. SHRP2 Solutions. American Association of State Highway and Transportation Officials. Washington, DC.

Schmertmann, J. H., Hartman, J. P., and Brown, P. R. 1978. "Improved Strain Influence Factor Diagrams." American Society of Civil Engineers, *Journal of the Geotechnical Engineering Division*, 104 (No. GT8), 1131-1135.

Seed, R. B. and L. F. Harder. 1990. SPT-Based Analysis of Pore Pressure Generation and Undrained Residual Strength. In *Proc., H. B. Seed Memorial Symposium*, Berkeley, CA, May 1990. BiTech Ltd., Vancouver, BC, Canada, Vol. 2, pp. 351–376.